Faculty of Mathematical, Natural and Physical Sciences
Department of Biology and Biotechnology “Charles Darwin”
Ph. D. course in Cell and Developmental Biology
XXXIII cycle

Cell wall DAMPs (damage-associated molecular patterns) and their oxidation in the Arabidopsis seed coat development and grafting

Ph.D. Student:
Sara Costantini

Supervisors:
Prof. Benedetta Mattei
Prof. Giulia De Lorenzo

Coordinator:
Prof. Giulia De Lorenzo

A.A. 2019/2020

Index

Synopsis 5

Section I 7

General Introduction and Aims of the work 7

I.1. The DAMPs (damage-associated molecular patterns) 7

I.1.1 THE OLIGOGALACTURONIDES 9

I.1.2 CELLODEXTRINS 9

I.1.3 THE HOMEOSTASIS OF OGs AND CDs CONTROLLED BY OLIGOSACCHARIDE OXIDASES 10

I.2 The seed coat development 13

I.3. Plant grafting 17

I.4. Aims of the work 20

Section II 22

Identification and characterization of CELLOX2, a berberine-bridge enzyme-like oxidase 22

Summary 22

Introduction 23

RESULTS 25

Bioinformatics analyses on the gene encoding a putative CELLOX 25

Heterologous expression in *Pichia pastoris* shows that At5g44360/BBE23 is a cellodextrin oxidase (CELLOX2) 28

Transient expressions of GFP- and RFP-tagged CELLOX2 in *N. tabacum* suggests an extracellular localization 32

CELLOX2 is expressed during seed development but not in seedlings or upon elicitor treatment 33

Unlike CELLOX1, CELLOX2 is not involved in immunity 37

Both *CELLOX1* and *CELLOX2* play a role in seed coat formation and characteristics 39

DISCUSSION 47

MATERIALS AND METHODS 50

Section III 64

Damage-Associated Molecular Patterns during plant graft formation 64

Summary 64
INTRODUCTION 65
RESULTS AND DISCUSSION 68
Cellotriose has a dual action on early auxin-regulated gene expression 68
OGs, CDs and their oxidation influence the phloem reconnection and vascular formation. 70
MATERIALS AND METHODS 75
Section IV 78
References 78

Synopsis

Plants have an innate immune system to respond to biotic stresses. The plant immunity relies on the recognition of pathogens through the pathogen/microbe-associated molecular patterns (PAMPs/MAMPs), microbial structures or compounds that activate the defense responses. Defense responses can be also triggered by endogenous elicitors, which are plant compounds that are released upon pathogen infection of mechanical injury and are indicated as DAMPs. Some DAMPs derive from the degradation of the cell wall polysaccharides, like the oligogalacturonides (OGs) from the homogalacturonan and cellodextrins (CDs) from cellulose. A possible mechanism to maintain the homeostasis of OGs and CDs has been recently identified in the laboratory where I performed my thesis. OGs and CDs are inactivated by specific oxidases, namely OGOX1-4 and CELLOX1, respectively, belonging to the Berberine-Bridge Enzyme-like (BBE-like) family.

The work of my thesis has been divided into two different parts.

The first part deals with the identification and characterization of a new member of the BBE-like family in *Arabidopsis thaliana,* encoded by the gene *At5g44360*/*BBE23.* This gene was chosen because is the member more closely related to CELLOX1, previously characterized. I investigated whether BBE23 is also a polysaccharide oxidase and possibly an oxidase of DAMPs, and determined its biochemical characteristics, its activity and its specific substrates and products. My results show that the enzymatic activity of BBE23, hereon named CELLOX2, is very similar to that of CELLOX1. Interestingly, the mixed-linked β-1,3/1,4-glucans (MLGs), also capable of acting as DAMPs, have been uncovered as substrates for both CELLOX1 and CELLOX2. Moreover, I also investigated the physiological role of both the paralogues CELLOX1 and CELLOX2 to assess if their action may somehow affect the plant cell wall structure. I used knockout mutants (CELLOX1 KO and CELLOX2 KO), and CELLOX1 (CELLOX1 OE) overexpressing plants. CELLOX2 is mainly expressed in the seed coat.

The second part of the work aimed at addressing the possible role of OGs and CDs and their oxidases during the process of grafting. Plant grafting is characterized by

tissue fusion and vascular reconnection and involves responses to wounding, which in part overlap with responses to pathogens. The molecular mechanisms of graft formation remain unknown. The elucidation of the grafting process includes the study of response to the wound itself, a process in which OGs have been already implicated by previous studies. It also includes the study of tissue regeneration and vascular reconnection, which involves a complex cross-talk among different signals including hormones, especially auxin and cytokinin. Transcriptional profiling has revealed that some defense-related genes, including the genes encoding OGOX1 and CELLOX, are differentially expressed at the graft junction, suggesting a role during the grafting process. It is known that OGs antagonize the action of auxin. In my thesis work I found that CDs, like OGs, inhibit auxin responses. However, whereas OGs block the expression of the auxin-regulated DR5::GUS gene in the root meristem, CDs activate its expression. I also found that OGs and CDs influence the grafting process, at the level of the vascular tissue formation and differentiation. Taken together, albeit preliminary, my results are very promising, as they suggest a role of OGs and CDs in the grafting process and may lead to a possible biotechnological optimization of the grafting process and vascular development.

Section I

General Introduction and Aims of the work

I.1. The DAMPs (damage-associated molecular patterns)

Plants have an innate immune system through which they respond to abiotic stresses, wounding and infections by microbes, nematodes and insects. Because plants are sessile organisms, an efficient system for recognition and decoding external or endogenous signals to danger in an optimal way is essential for survival (Jones & Dangl, 2006). For example, a pathogen attack is recognized through conserved pathogen/microbe-associated molecular patterns (PAMPs/MAMPs) and plant-derived damage-associated molecular patterns (DAMPs). PAMPs/MAMPs are microbial structures or compounds that activate the defense responses, also indicated as exogenous elicitors (Jones & Dangl, 2006; Zipfel & Felix, 2005). Among these elicitors there are, for example, the lipopolysaccharides, peptidoglycans, chitin from the cell wall of the fungal/ oomycete pathogens, proteins like the bacterial flagellin and the elongation factor EF-Tu (Boller & Felix, 2009; Gust et al., 2007; Kaku et al., 2006; Liu et al., 2012) or the most recently identified MLG43, a mixed-linked (β-1→3, β-1→4) glucan trisaccharide present in the cell wall of phytopathogens (Rebaque et al., 2021). DAMPs, also referred to as endogenous elicitors, are plant compounds released upon pathogen infection. Among these, there are fragments originating from cell wall polysaccharides, such as the oligogalacturonides (OGs) (De Lorenzo et al., 2018; Ferrari et al., 2013), cellodextrins (CDs), xyloglucans (Claverie et al., 2018), mannanoligosaccharides (Zang et al., 2019) and arabinoxylans (Mélida et al., 2020). Both PAMPs and DAMPs are recognized by specialized transmembrane proteins indicated as PRRs (pattern recognition receptors) (Zipfel, 2014).

The interaction between PAMPs/DAMPs and PRRs leads to the activation of the so-called pattern-triggered immunity (PTI), which is considered as a first layer of immunity (Boller & Felix, 2009). PTI includes the increase of cytosolic Ca^{2+} levels, MAP kinase activation and production of reactive oxygen species (ROS), the expression of pathogenesis-related (PR) genes, the production of antimicrobial compounds (phytoalexins), nitric oxide, and cell wall reinforcement like callose deposition. Propagation of ROS waves to stimulate and amplify the danger signal at a systemic level is also part of the PTI (Figure I.1.). Many pathogens have evolved the capability of successfully infecting a plant species through the acquisition of specialized effectors that may trigger the so-called ETI (effector-triggered immunity). PTI is an accelerated, amplified and genotype-specific response that in most cases results in a disease resistance characterized by a hypersensitive cell death response (HR) at the infection site. The evolution of PTI and ETI is illustrated in the zigzag model (Jones & Dangl, 2006).

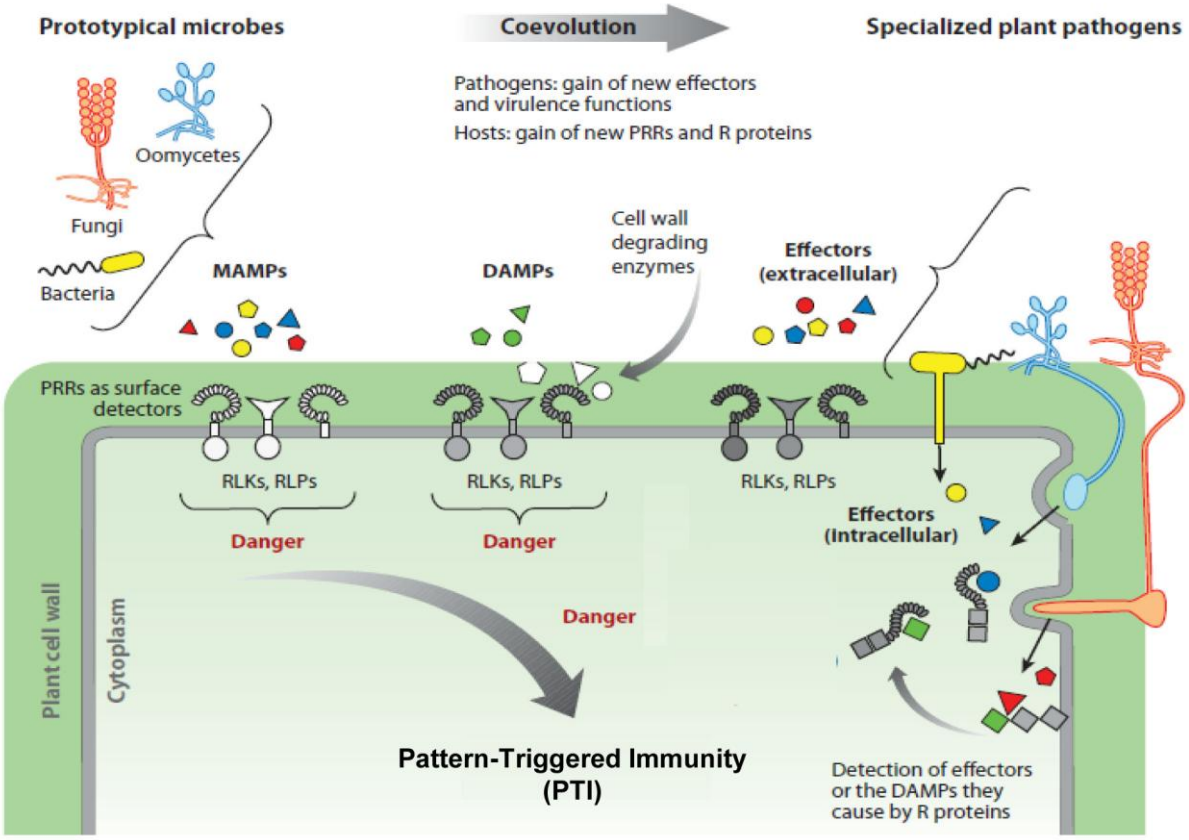

Figure I.1. The plant immune system is of the innate type. Overview of perception of microbe-associated molecular patterns (MAMPs) and damage-associated molecular patterns (DAMPs) through pattern recognition receptors (PRRs). Perception activates a signaling cascade that culminates in the Pattern–Triggered Immunity (PTI), the first level of plant immunity. RLK, receptor-like kinase; RLP, receptor-like protein. Adapted from Boller and Felix (2009).

I.1.1 THE OLIGOGALACTURONIDES

The oligogalacturonides (OGs) are oligomers of 1,4-linked-α-D-galacturonosyl residues that are released from the degradation of homogalacturonan, a major component of pectin in plant cell wall, by the action of endogenous polygalacturonase (PGs) and other pectic enzymes upon wounding and mechanical damage, or of pathogen-encoded PGs and other pectic enzymes during infection (De Lorenzo et al., 2018). Accumulation of OGs is favored by the interaction of PGs with plant-derived PG-inhibiting proteins (PGIPs) (Cervone et al., 1989; Kalunke et al., 2015), which are leucine-rich repeat (LRR) proteins capable of retarding the plant wall degradation and reducing the fungal invasion (De Lorenzo & Ferrari, 2002).

The activity of OGs as DAMPs capable of increasing the defense and protection against the pathogens is well documented (Aziz et al., 2004; Ferrari et al., 2007). OGs are recognized by the extracellular domain of the wall-associated receptor kinase1 WAK1 (Brutus et al., 2010). The activation of WAK1 triggers, in Arabidopsis, complex downstream responses, typical of PTI, including calcium increase, oxidative burst, synthesis of phytoalexins, deposition of callose (Aziz et al., 2007; Bellincampi et al., 2000; Broekaert & Pneumas, 1988; Davis et al., 1986; Davis & Hahlbrock, 1987; Galletti et al., 2008; Gramegna et al., 2016; Rasul et al., 2012), phosphorylation of Mitogen-Activated Protein Kinases (MAPKs), in particular MPK6 and MPK3 (Galletti et al., 2011; Gravino et al., 2017; Gravino et al., 2015; Mattei et al., 2016; Savatin, Gigli-Bisceglia, et al., 2014), and upregulation of defense-related genes in the cell wall (Denoux et al., 2008; Souza et al., 2017).

I.1.2 CELLODEXTRINS

Besides OGs, other oligosaccharides released from the cell wall have been recently shown to behave as DAMPs. Cellodextrins (CDs), linear oligomers of 1,4-linked β-D-glucosyl residues in a range of DP 3 to 9, are derived from cellulose. CDs and OGs likely have a different perception system and use different pathway of signaling (Aziz et al., 2007). Elicitation with CDs leads to induction of a rapid release of H_2O_2, and an increase in calcium level in grapevine (Aziz et al., 2007). CDs up-regulate the expression of defense–related genes like *PHENYLALANINE AMMONIA LYASE* (*PAL)* and *STILBENE SYNTHASE* (*STS)* and induce the accumulation of chitinases, β-1,3 glucanase (β-Glu1), PGIPs and serine-protease inhibitor (PIN) (Aziz et al., 2007).

Cellobiose, cellotriose (CD3) and cellotetraose (CD4) in *Arabidopsis thaliana* have been shown to be responsible for the strong activation of the defense-related gene

WRKY30 in seedling roots and shoots (Souza et al., 2017). Moreover, cellobiose has been described to lead to early activation of MPK3 and MPK6, up-regulation of some defense-related genes such as SAG101, PAD5 (associated with salicylic acid signaling), ACS7 (related with ethylene synthesis), LOX3 and LOX4 (linked with jasmonic acid production). Unlike other PAMP/DAMPs, cellobiose does not increase the production of ROS but, nevertheless, increases resistance to *Pseudomonas syringae* pv. *tomato* DC3000. In contrast with the trade-off theory, it has shown that seedlings grown with high levels of cellobiose increase the fresh weight in comparison with those grown in absence or low concentration of it. The gene BGLU27, a β - glucosidase, is highly induced exclusively by cellobiose, this may suggest that this enzyme provides glucose availability from cellobiose disruption, useful for growth (Souza et al., 2017). The elicitor activity of CD3 and CD4 but not of cellobiose has been confirmed in a more recent paper (Locci et al., 2019).

CD3 extracted from the cell wall of the endophytic fungus *Piriformospora indica* also behaves as an elicitor (Johnson et al.). CD3 induces defense responses in *Arabidopsis* and in tobacco roots, including the increase of cytosolic calcium level, the production of H_2O_2 mediated by the NADH oxidase RBOHD, also in synergy with chitin treatments, and the upregulation of the expression of *RBOHD* itself. Moreover, early defense response marker genes such as *MAPK3* and *ZAT12* are up-regulated by CD3. The hormone response marker genes *NPR1* and *LOX1* as well as genes involved in growth and root development also respond to CD3 (Johnson et al., 2018a).

I.1.3 THE HOMEOSTASIS OF OGs AND CDs CONTROLLED BY OLIGOSACCHARIDE OXIDASES

It has been shown that elevated levels of OGs reduce plant growth (Benedetti et al., 2015) likely due to their auxin antagonistic activity (Bellincampi et al., 1993; Ferrari et al., 2013; Savatin et al., 2011), suggesting that OGs play a role in the growth-defense trade-off (Pontiggia et al., 2020). Moreover, at very high level, the release of OGs is deleterious and becomes lethal (hyper-immunity) (Benedetti et al., 2015). This effect suggests that mechanisms likely exist for controlling the homeostasis of OGs and preventing dangerous consequences. Recently a possible mechanism by which the homeostasis of OGs activity can be maintained has been discovered, represented by specific oligogalacturonide oxidases (OGOXs) that nearly abolish the elicitor activity of OGs. OGOXs belong to the so-called Berberine-Bridge Enzyme-like (BBE-like) family (Figure I.2.) (Benedetti et al., 2018; Daniel et al., 2017). At least four members of this family, which comprises a total of 27 members all predicted to bind FAD, are

OG oxidases (Benedetti et al., 2018). OGOX1-4 oxidize the residue at the reducing end of OGs to galactaric acid and are inhibited by sulphites. The maximal activity of OGOX1 is on OGs with a degree of polymerization greater than 4.
A role of OGOXs in immunity has been demonstrated (Benedetti et al., 2018). Plants overexpressing OGOX1 are more resistant to the necrotrophic fungus *Botrytis cinerea*, although they do not show a higher activation of defense responses. The increased resistance against this fungus is likely due to the difficult digestion of the oxidized OG dimer by the *Botrytis* polygalacturonases in the OGOX1 overexpressing plants. Indeed, a high accumulation of oxidized di-galacturonic acid has been detected in Arabidopsis infected with *B. cinerea* at a late stage of infection (Voxeur et al., 2019).

Notably, an oxidase of CDs has also been found among the members of the BBEl-family. Locci et al. (2019) showed that *At4g20860*/*CELLOX1*, which upon biotic stresses shows an expression profile remarkably similar to that of *OGOX1*, is a cellodextrins oxidase (*CELLOX1*) with maximal activity against CD3, the most active cellodextrin. Expression of high levels of CELLOX1 in transgenic *Arabidopsis* plant leads to an increased resistance against *B. cinerea* infection (Locci et al., 2019), likely by hampering the digestion of cellulose fragment by the fungus.

Likely oxidases function to attenuate the continuous DAMP elicitor activity once the danger has ceased. Oxidation of elicitors protects against hyper-immunity and avoids pathogen dissemination, also making them difficult to be metabolized (Benedetti et al., 2018; Locci et al., 2019). With their capability to oxidize and inactivate oligosaccharide DAMPs, DAMP oxidases can be considered as "DAMP suppressors" able to avoid an harmful un-balanced level of signals in plants, acting as a sort of human –SAMPs (Suppressing DAMPs, (Land, 2020). The discovery and characterization of plant DAMP-suppressors may leads to biotechnological applications to overcome the growth/defense trade-off limitations and the deleterious effects of hyper-immunity (Li et al., 2020; Pontiggia et al., 2020).

Notably, oxidation of OGs and CDs is accompanied by the formation of H_2O_2 (Benedetti et al., 2018; Locci et al., 2019). H_2O_2 plays an important role in defense, directly by participating as cell wall strengthening factor (cross-linking of structural protein and lignin polymers), repairing plant tissues (Farvardin et al., 2020) and being toxic against pathogens. Indirectly, H_2O_2 may act as a second messenger in signaling and in wound repair (Huang et al., 2019; Mhamdi & Van Breusegem, 2018; Sies & Jones, 2020), for example at the sites of cell-wall ruptures and micro-lesions during plant growth and development (Benedetti et al., 2018; Galletti et al., 2008;

Levine et al., 1994). It is suggested that enzymatic oxidation of oligosaccharides derived from cell wall might represent a mechanism to localize a limited production of H_2O_2, useful for example as a short range signal communication. Moreover the oxidation of wall polysaccharides might be crucial for cell expansion hampering the trans-glycosylation, and thus contributing to the growth-defense trade off (Franková & Fry, 2020; Pontiggia et al., 2020).

Besides a well-known role in immunity, DAMPs, and as a consequence their respective oxidases, might play a role in cell wall remodeling during development (Haas et al., 2020; Zhang & Zhang, 2020), growth (Leon et al., 2001; Tucker et al., 2018), wound signaling (Bergey et al., 1999; Savatin, Gramegna, et al., 2014) and tissue healing, including the sealing of the graft junction (Ferrari et al., 2013; Pontiggia et al., 2020; Sala et al., 2019).

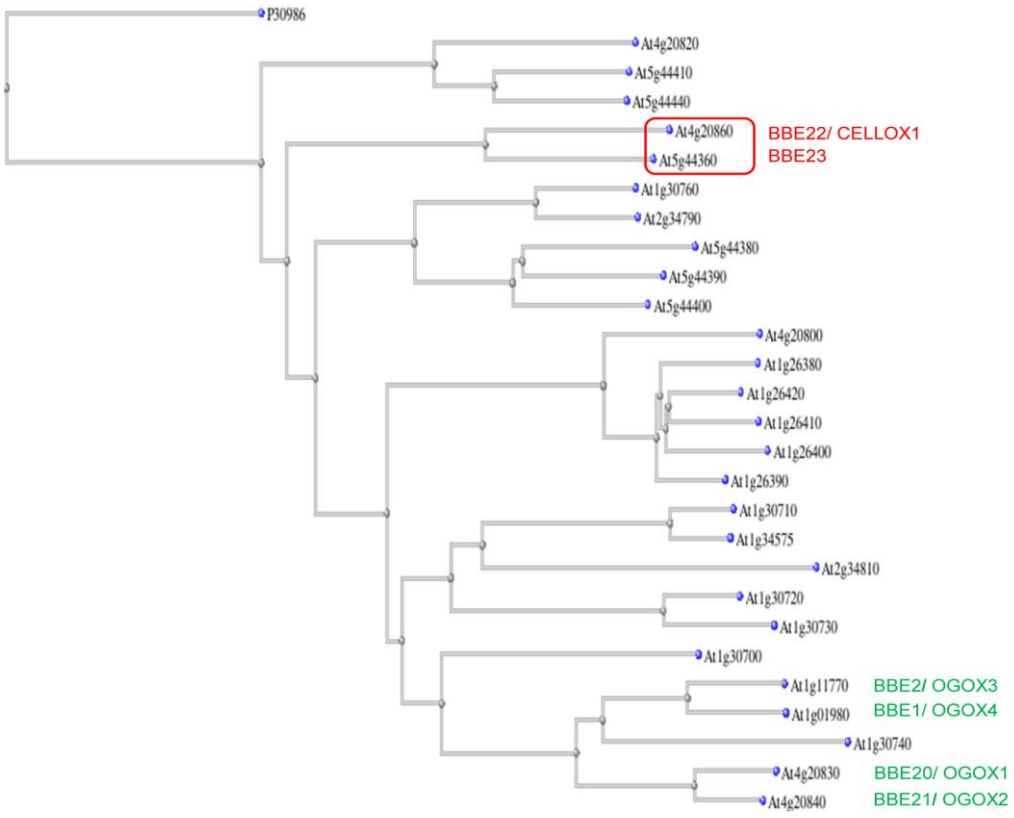

Figure I.2. Homology tree of the BBE-like protein family showing the characterized oligosaccharide oxidases. As an outgroup, a true Berberine Bridge Enzyme, P30986, has been included in the analysis (Locci et al., 2019). The closest paralogue of CELLOX1 (At5g44360), still uncharacterized, is also shown.

I.2 The seed coat development

The seed coat, also known as testa, derived from maternal ovule integuments, surrounds the embryo throughout its development and dormancy, providing protection from mechanical damage and pathogens, and regulating germination, dispersal and seed viability in hostile environments (Ben-Tov et al., 2015a; Haughn & Chaudhury, 2005; Huang et al., 2008; Yang et al., 2011). In a process called myxospermy, some plant species, including Arabidopsis, accumulate in the apoplast of seed coat epidermal cells a large quantity of a polysaccharidic, mostly pectinaceous, mucilage that is extruded upon seed imbibition forming a gel-like capsule around the seed (Western et al., 2000; Windsor et al., 2000).The role of seed mucilage is not totally defined, but it includes seed hydration for the germination, seed dispersal, protection and interaction with microorganisms(Ben-Tov et al., 2015a; Engelbrecht & García-Fayos, 2012; Penfield et al., 2001; Saez-Aguayo et al., 2014; Western, 2012; Yang et al., 2013).

The seed coat, widely studied in Arabidopsis, is originated from the seed coat epidermis (SCE), the outermost layer in developing seeds, and in particular by the so-called Mucilage Secretory Cells (MSC) (Figure I.3.). These are polygonal cells displaying a primary and two distinct secondary walls. The sequential deposition of these walls is shown in Figure I.4. MSC, after an initial phase of cell expansion, synthesize polysaccharides that are accumulated into the apoplast in a polarized way, between the radial and outer tangential cell walls (Figure I.4A.). The deposition of a thick ring of pectin-rich mucilage leads to the formation of a volcano-shaped cytoplasmic column, which is gradually displaced by the deposition of a cellulose-rich secondary wall named *columella*. The volcano-shaped columella is connected to the radial cell walls in the polygonal MSC cells. Later, the MSC reaches maturity, undergo a programmed cell death and desiccate (Voiniciuc, Yang, et al., 2015).

Upon seed hydration, mucilage expands and breaks the radial primary cell wall, permitting the release of mucilage externally around the seed (Figure I.4B.). The breakage involves the anticlinal wall boundaries, but not necessarily the outer periclinal walls, which can remain intact. At this point mucilage is organized in a denser inner layer tightly attached to the seed surface, called adherent mucilage, and an outer, water soluble and diffuse layer, called not-adherent soluble mucilage (Figure I.4B.). Both the adherent and not-adherent soluble mucilage are composed mainly (>80%) of un-branched rhamnogalacturonan 1 (RG-I), a polymer made of alternating repeats of (1,4)-α-galacturonic acid and (1,2)-α-l-rhamnose units. The

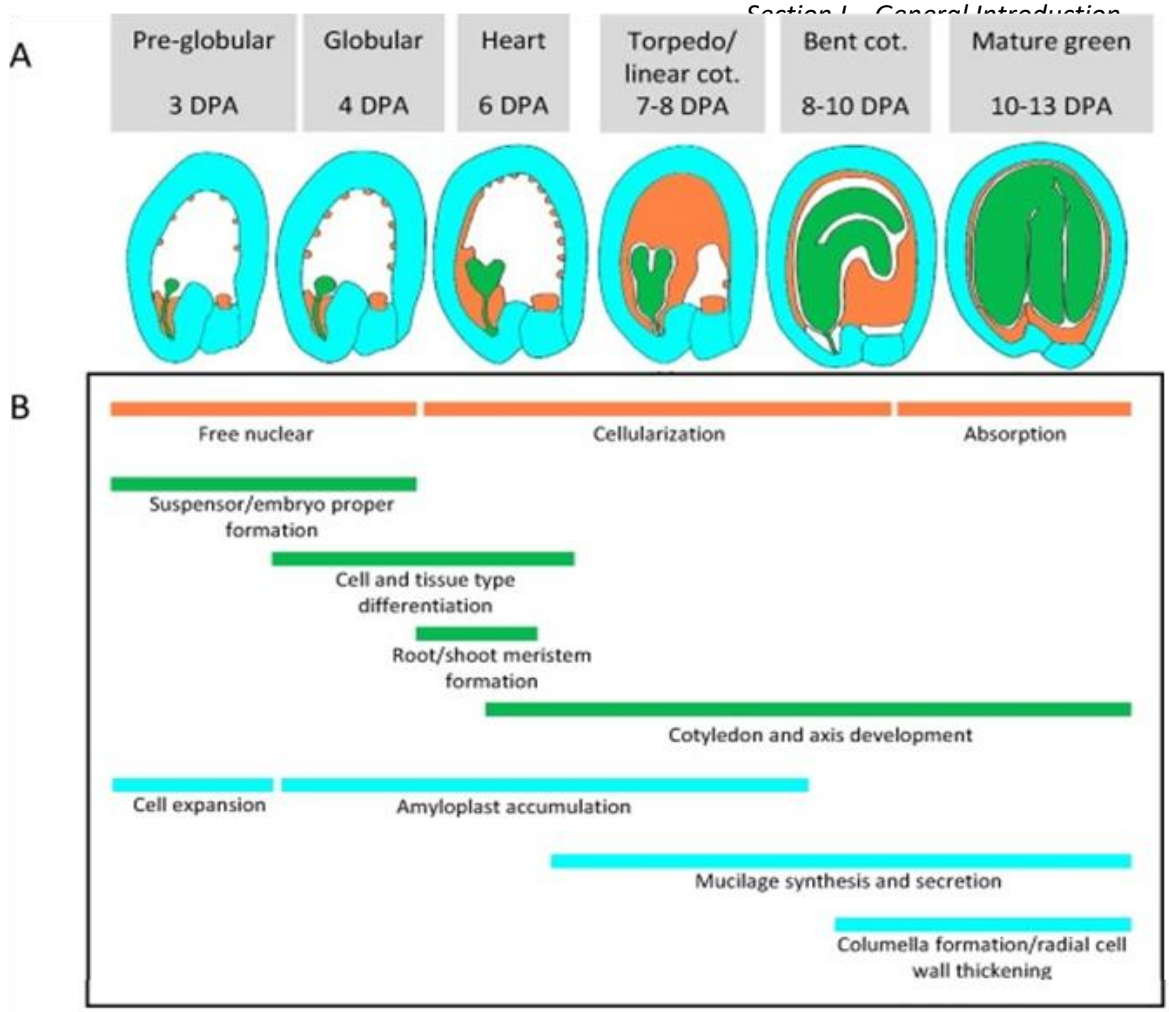

Figure I.3. Seed development stages in Arabidopsis. (A) Seed development stages from pre-globular to mature green with approximate days post anthesis (DPA) for each stage indicated. The maternal seed coat is showed in cyan, the endosperm is in orange and the developing embryo is in green. (B) Major physiological events occurring during seed development. Colors refer to the corresponding tissue shown in the figure. Images have been adapted from Golz et al, 2018.

soluble mucilage contains also traces of arabinose, xylose, mannose, galactose, and glucose (Ralet et al., 2016).

The adherent mucilage is constituted of 12-19 % cellulose, found as dense "rays" departing from the top of columella; cellulose is also present as a less dense layer among the rays. The adherent mucilage is in turn divided in two layers as shown by changes in mucilage staining density with ruthenium red surrounding the cellulosic rays. In particular, an inner layer is closely adjacent to the seed surface and includes, besides RG-I, a small amount of branched RG-I, cellulose, galactans (Macquet et al., 2007; Western et al., 2004; Willats et al., 2001). The more external zone of the adherent mucilage contains RG I, highly- methylated homogalacturonan (HG), galactans, and arabinans (Arsovski et al., 2009; Macquet et al., 2007; Willats et al., 2001). Whether the inner adherent mucilage also contains arabinans and highly methyl-esterified and de-esterified HG is not clear.

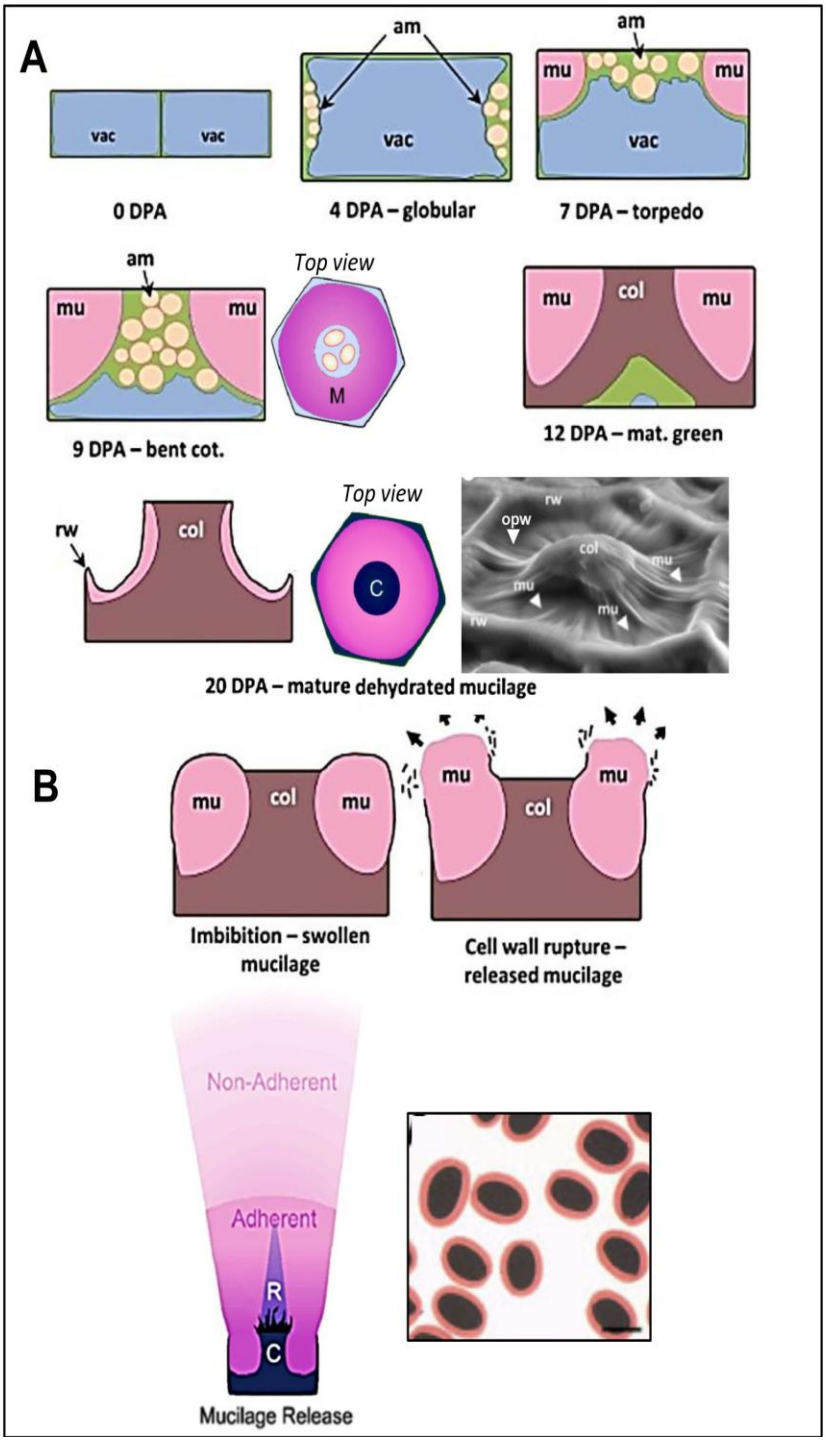

Figure I.4. **Models of seed wall deposition and extruded mucilage structure**. A) By 4 days post-anthesis (DPA), SCE cells have fully expanded and contain amyloplasts (am), which partially displace the central vacuole (vac). From 5 to 8 DPA, mucilaginous polysaccharides synthesis occurs. Mucilage (mu) is secreted between the radial and outer tangential cell walls, forming a thick ring of it. This results in the formation of a volcano-shaped cytoplasmic column (C), the top view of which is shown. From 9 to 13 DPA, the cytoplasmic column is gradually displaced by the deposition of a secondary wall known as the columella (col). By 18 DPA, the SCE cells reach maturity and are fully desiccated. Desiccated mucilage (mu) is located in the apoplastic space beneath the outer cell wall. On the right, scanning electron micrographs of mature Arabidopsis seed surface showing a hexagonal MSC with radial cell walls (rw; or anticlinal wall; perpendicular to seed surface), outer periclinal wall (opw; parallel to seed surface) and central columella (col). B) Hydration of dry seed makes the mucilage burst out, rupturing the primary wall and forming a two-layered capsule and a ray-like structure (R). The two layers adherent and non adherent are showed in the drawing at left bottom (C columella; R, ray). At right bottom, the top view of *Arabidopsis* seeds stained with Ruthenium Red that highlight in red the mucilage around the seed (Adapted and combined from Voiniciuc et al, 2015, and Golz et al, 2018).

In the adherent layer xylans, xyloglucan, heteromannans like glucomannans and galactoglucomannans have also been found, likely involved in structuring the mucilage interacting with cellulose, despite their low abundance (Voiniciuc, Schmidt, et al., 2015; Voiniciuc, Yang, et al., 2015; Walker et al., 2011; Yu et al., 2014). Recently it has been shown that cellulose and pectin interact with each other (Du et al., 2020; Palacio-Lopez et al., 2020) and that cellulose microfibers and HG nanofilaments form a single cohesive network (Haas et al., 2020; Zhang & Zhang, 2020). Moreover, branched RG-I contains xylans that, through non-covalent interactions, contribute to maintain cellulose soluble (Sullivan et al., 2011). Callose is present only in the *columella* (Macquet et al., 2007). A number of mutants affected in seed coat structure and mucilage production have been identified. For example, mutants defective in mucilage release and /or composition are *mum1-3,5* and *mum4*, defective in the biosynthetic enzyme UDP-rhamnose synthase (Macquet et al., 2007; Oka et al., 2007; Usadel et al., 2004; Western et al., 2001; Western et al., 2004). Mutants associated with changes in the columella structure are *myb5* (Gonzalez et al., 2009), *ttg2* (Johnson et al., 2002) and *myb61* (Penfield et al., 2001). The APETALA2 mutants (*ap2*) are the most severely affected, in both mucilage and columella (Jofuku et al., 1994). Moreover, mutants affected in seed coat structure and mucilage production are those with defective cellulose synthases (CESA3 CESA5, CESA10) and with a reduced cellulose production (FEI2, SOS5) (Griffiths et al., 2014; Harpaz-Saad et al., 2011; Mendu et al., 2011; Sullivan et al., 2011), the *csla2* mutants, affected in the biosynthesis of glucomannan (Yu et al., 2014) and a putative galactose oxidase mutant, *ruby* (Šola et al., 2019).

It has to be considered also that secreted pectins represent a target for bacterial and fungal enzymes (Willats et al., 2001) and the composition of these pectin components, in particular those of the outer layer of mucilage, can influence and condition the rhyzosphere in preparation of seedling germination (Macquet et al., 2007) and the interactions among microorganism and the seed.

Given the rich content of polysaccharides, the seed coat represents an interesting and useful system to study the cell wall structure and to identify genes involved in the cell wall modification (Arsovski et al., 2010; Dean et al., 2007; Haughn & Western, 2012). Knowledge of the seed coat and cell wall physiology through the study of enzymes involved in the modification of polysaccharides could have a broad spectrum of applications. For example, it could be important for improving seed viability and resistance of agricultural crops, but also for modifying the seed content in relation to food security, as well as for the production of sustainable biomass and biodegradable materials.

I.3. Plant grafting

Plant grafting is a process known since ancient times and widely used in agriculture. It consists of physically joining the upper portion of a plant, which is usually the shoot or the bud of a donor plant and is indicated as the scion, and the lower part that receives the scion, which comprises the roots system, indicated as the rootstock (Figure I.5.) (Melnyk & Meyerowitz, 2015; Mudge et al., 2009). Even if it is an ancient technique, the molecular mechanism of grafting and what determines the compatibility among plants is not well known (Gaut et al., 2019).

Grafting includes several processes like wounding, cell de-differentiation, tissue regeneration, healing and vascular reconnection (Melnyk, 2017d). When grafting occurs, the intact cells of the joined scion and rootstock interdigitate among them and strengthen their connection with time. Then, enrichment in polysaccharides such as pectin occurs at the level of the graft junction and, at the same time, a callus of stem cells is produced. Pluripotent cells of the callus will differentiate in plant vascular tissue, the phloem and subsequently the xylem. The process includes also the formation of plasmodesmata between adjacent cells at the level of the graft junction that will guarantee nutrient and signals exchanges among the two parts of the new chimeric organism. Vascular connection develops only in the compatible and successful grafts (Ikeuchi et al., 2019; Ikeuchi, 2013; Melnyk & Meyerowitz, 2015; Melnyk et al., 2015).

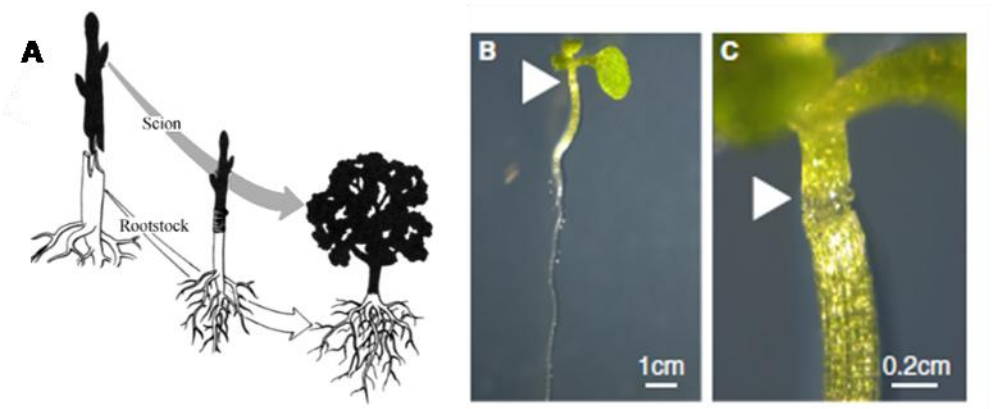

Figure I.5. Grafted plants consist of an upper part from a plant donor, the scion, and a lower portion, the rootstock. A) the scion will constitute the shoot system of the grafted plant, while the rootstock will constitute the root system. B) a grafted Arabidopsis seedling, used as a model to study the grafting process. C) magnification of the graft junction showed by the arrow. Images adapted from Mudge et al., 2009 and Melnyk and Meyerowitz, 2015.

Phytohormones are involved in the plant development and also in the processes of wound healing and grafting (Melnyk, 2017d; Nanda & Melnyk, 2018). In particular it is known that auxin biosynthesis is induced by grafting (Matsuoka et al., 2016; Melnyk et al., 2015; Wang et al., 2014; Yin et al., 2012) and the reunion of hypocotyls is inhibited when cotyledons, which are an important source of auxin, are cut or treated with auxin inhibitors (Matsuoka et al., 2016; Procko et al., 2014). Auxin induces the formation of vascular tissues (Aloni, 1980, 1987; Petrásek & Friml, 2009; Sachs, 1991; Sieburth, 1999) and, indeed, secondary xylem and phloem cells increase with high level of auxin in petunia (Klee et al., 1987), while low auxin levels decrease the number of xylem cells in tobacco and in general lead to de-differentiation of phloem in callus (Aloni, 1980; Romano et al., 1991). Cytokinins applied together with auxin seem to promote vascular reconnection during grafting (Nanda & Melnyk, 2018; Parkinson & Yeoman, 1982). Jasmonate (JA) and ethylene biosynthesis genes are activated at the graft junction, but it is not clear if this is due to wound response or if they play a role during grafting (Liu et al., 2016; Nanda & Melnyk, 2018; Yin et al., 2012). Recently, Wang et al. (2020) showed that the levels of JA undergo a different accumulation at the top and bottom of the initial wounding and then change from asymmetrical to symmetrical distribution at both sides after grafting. Expression of genes related to JA synthesis also became symmetric after grafting (Wang et al., 2020).

Cytokinins along with auxins are known to trigger the proliferation and development of cambium, which is considered as a key factor for a successful grafting (Melnyk, 2017a, 2017d; Melnyk et al., 2015; Notaguchi et al., 2020). Cambium differentiation is intense at the graft site, and genes involved with cambium, phloem and xylem formation are suddenly activated after grafting (Elo et al., 2009; Melnyk et al., 2018; Sharma & Zheng, 2019).

In addition to plant hormones, also in the case of sugars and sugar metabolism, both having a role in vascular reconnection (Melnyk et al., 2018), evidence indicates that the top and bottom of the cut do not behave similarly. The expression of many genes differs between the two grafted parts (asymmetric expression) and the difference does not merely depend on the difference of induction by wounding in the separated (not grafted) parts.

This is particularly evident early upon grafting. A study of the genome-wide temporal and spatial gene expression changes during grafting indicates that genes involved in response to sugar are expressed asymmetrically and mainly above the junction, which correlates with the accumulation of starch. Instead, genes associated

with cell division and vascular formation as well as auxin responsiveness are induced simmetrically. Such gene expression dynamics leads to a unique physiological condition that promotes wound healing (Melnyk et al., 2018).

Once the scion and rootstock are connected, movement of nuclear and plastid DNA (Stegemann & Bock, 2009; Stegemann et al., 2012; Taller et al., 1998), messenger RNA (Notaguchi et al., 2015; Yang et al., 2015), small interfering RNA (Chitwood & Timmermans, 2010; Melnyk et al., 2011) and proteins (Paultre et al., 2016; Spiegelman et al., 2015; Xoconostle-Cázares et al., 1999) occur across the graft junction. Exchanges of these molecules could regulate physiological and developmental processes that help to seal the two parts (Sharma & Zheng, 2019). Interestingly, genes encoding cell wall modifying enzymes such as β-1,4 glucanase, β -1,3-glucanase, xyloglucan hydrolase and proteins such as expansin are up-regulated after grafting particularly in proliferated cambial cells or pith region at the graft boundary, both in *Nicotiana* interfamily grafting and *Arabidopsis,* soybean and morning glory intrafamily grafting. These cell-wall enzymes and proteins seem to be important for cell wall reconstruction after the cut. In particular β-1,4-glucanase of the GH9B family seem to facilitate the adhesion of the facing cells at the graft cut and the graft success (Notaguchi et al., 2020). Notably, abundant unmethylated or poorly methyl-esterified homogalacturonan (HG) and extensins have been detected in the extracellular material on graft union site (Sala et al., 2019). Probably HG is an important constituent of the pectin gel necessary for cell wall stiffening and cell adhesion as well as for limiting cell division and confining proliferating cells in a predetermined volume. Moreover, the increase of extensins outside the callus cells in the adhesion zone and in the intercellular spaces seems to be involved in regulating cell wall growth, stabilization and hydration. Extensins through the strengthening of cell wall are important also for plant defense responses after damage (Sala et al., 2019). Studying grafting and shading a light on its molecular mechanism should be important to improve crop yield, resistance to pathogen and abiotic stresses, but also it can be used as model technique to study bimolecular systemic transport, signal trafficking, plant tissue differentiation and development. Transcriptional analysis revealed that genes involved in immune responses are highly differentially expressed, especially shortly after grafting and mostly in the root grafted bottom (Melnyk et al., 2018).

I.4. Aims of the work

This research aims at investigating how the control of immunity triggered by cell wall- derived DAMPs, such as oligogalacturonides (OGs) and cellodextrins (CDs), may prevent deleterious effects on the plant growth and whether the same molecules that act as DAMPs play also a role as signals in development.
The work has been divided into two different parts. The first part deals with the identification and characterization of a new member of the BBE-like family in *Arabidopsis thaliana,* encoded by the gene *At5g44360/BBE23.* This gene was chosen because is the member more closely related to CELLOX1, previously characterized. I investigated whether BBE23 is a also polysaccharide oxidase and possibly an oxidase of DAMPs, and determined its biochemical characteristics, its activity and its specific substrates and products. I also investigated the physiological role of both the paralogues CELLOX1 and BBE23 to assess if their action may somehow affect the plant cell wall structure. Knowledge acquired may be exploited to improve crops resistance to biotic stresses, associated with an optimization of plant development and growth.
The second part of the thesis, carried out thanks to a collaboration with Dr. Melnyk (SLU, Uppsala, Sweden), addresses the possible role of DAMPs such as OGs and CDs and their oxidases during the process of grafting, whose molecular mechanisms are still largely unknown. The elucidation of the grafting process includes the study of response to the wound itself, a process in which OGs have been already implicated by previous studies. It also includes the study of tissue regeneration and vascular reconnection. Transcriptional profiling has revealed that some defense-related genes, including the genes encoding OGOX1 and CELLOX, are differentially expressed at the graft junction, suggesting a role during the grafting process. My study aims at contributing to deepen our understanding of the signaling events during the graft formation. This knowledge may lead to the optimization of the grafting and eventually to overcome problems of compatibility among species. In particular, this second part of investigation includes also analyses on the cross-talk between DAMPs and the hormonal pathways since, while it is known that OGs are able to antagonize the action of auxin, nothing is known about the role of other DAMPs such as CDs.

This whole research may potentially be an interesting starting point for further studies that can open on to a wide range of applications. For example, knowledge

may be exploited to modulate immunity, improve plant resistance providing exogenous DAMPs or even through the use of transgenic resistant rootstock in agriculturally productive wild type crops, without compromising the physiological fitness and development of the plants. This could be particularly relevant to preserve biodiversity and to contrast emerging pathogens due to climate changes. Moreover, the study and the ability to modify plant cell wall structure and composition through the oxidation of its fragments could be important to modulate the fiber content and food nutritional composition, as well as to produce biomaterials with different uses.

Section II

Identification and characterization of CELLOX2, a berberine-bridge enzyme-like oxidase

Summary

Plants defense responses can be triggered by endogenous elicitors referred to as damage-associated molecular patterns (DAMPs), which are released upon pathogen infection or mechanical injury. Among the DAMPs, there are fragments originating from cell wall polysaccharides, such as the oligogalacturonides (OGs), derived from the homogalacturonan, and cellodextrins (CDs), derived from cellulose. The activity of OGs as DAMPs is well documented. Recently a possible mechanism by which the homeostasis of OGs and CDs is maintained by specific oxidases, namely OGOX1-4 and CELLOX1, respectively, has been identified in the laboratory where I performed my thesis. These enzymes belong to the berberine-bridge enzyme-like (BBE-like) family and their role in immunity has been demonstrated. In this part of the work, a new oxidase of CDs, named CELLOX2 (At5g44360/BBE23), which is the closest paralogue of CELLOX1, has been identified and its activity characterized. The activity is very similar to that of CELLOX1. Moreover, the mixed-linked β-1,3/1,4-glucans (MLGs), also capable of acting as DAMPs/MAMPs, have been uncovered as substrates for both CELLOX1 and CELLOX2. The physiological role of these oxidases has been investigated, using the knockout transgenic plant (CELLOX1 KO and CELLOX2 KO), and the overexpressing CELLOX1 (CELLOX1 OE), focusing on the seed coat, where CELLOX2 is shown here to be exclusively expressed. I show that both CELLOX1 and CELLOX2 are involved in cell wall cellulose/hemicelluloses modification in the seed coat, besides their potential in plant defense.

Introduction

Endogenous elicitors of plant defenses, referred to as damage-associated molecular patterns (DAMPs), include the fragments of wall polysaccharides such as oligogalacturonides (OGs), cellodextrins (CDs), xyloglucans (Claverie et al., 2018), mannan oligosaccharide (Zang et al., 2019) and arabinoxylans (AX) (Mélida et al., 2020; Pontiggia et al., 2020). DAMPs induce responses that are typical of PTI (Boller & Felix, 2009; Jones & Dangl, 2006) and are recognized by specific PRRs (Brutus et al., 2010; Zipfel, 2014).

Oxidases of oligosaccharides capable of dampening their DAMP activity have been recently discovered in *Arabidopsis*, in particular OG oxidases [OGOX1-4; (Benedetti et al., 2018)], and one CD oxidase [CELLOX1;(Locci et al., 2019; Pontiggia et al., 2020)]. These enzymes belong to the FAD-binding berberine-bridge enzyme-like (BBE-like) family (Daniel et al., 2017). Oligosaccharide oxidases are well represented not only in plants but also in microbes (Pontiggia et al., 2020), and the challenge is to understand their physiological role, their specific enzyme characteristics and their localization.

Arabidopsis CELLOX1 (BBE22/At4g20860) uses as substrates CDs, mainly with a DP higher than 2, with a higher activity on CD3 (cellotriose) (Locci et al., 2019). Notably CD3 is the most efficient elicitor-active CD (Locci et al., 2019). Oxidation by CELLOX1 occurs at the C1 of the residue at reducing end of a β-1,4–oligo or polysaccharide chain, producing gluconic acid and H_2O_2. CELLOX1 does not oxidize glucose, indicating that its enzymatic activity is different from that of two carbohydrate oxidases that have been isolated in sunflower and lettuce (*Helianthus annuus* carbohydrate oxidase Ha-CHOX and *Lactuca sativa* carbohydrate oxidase Ls-CHOX), also belonging to the BBE-like family (Custers et al., 2004).
CELLOX1, like OGOXs, is a putative apoplastic protein and displays a high pH optimum (Benedetti et al., 2018; Locci et al., 2019; Pontiggia et al., 2020). Like all the BBE-like proteins, CELLOX1 possesses the sites for the bicovalent linkage of the FAD isoalloxazine ring to a cysteine and histidine residue (H91 and C154), the presence of a relatively large active site of type IV (Daniel et al., 2016; Schall et al., 2020). CELLOX1 shows a denser distribution of negative charges around the active site as opposed to the positively charged region of OGOX1. CELLOX1 also maintains the oxygen gate-keeper valine (V157) and the surrounding residues (Locci et al., 2019).
Expression of high levels of the CELLOX1 in transgenic *Arabidopsis* plant leads to an increased resistance against *B. cinerea* infection (Locci et al., 2019), likely because, like in the case of OGOXs, it leads to a decreased digestibility of the oxidated cellulose fragments by the fungal enzymes.

CELLOX1 is present on chromosome 4, in the same cluster that includes *OGOX1* and *OGOX2*. *OGOX1* and *CELLOX1* show a remarkably similar expression profile during the immune response (Locci et al., 2019), suggesting that they might act in concert. The closest paralogue of *CELLOX1* is *At5g44360*/*BBE23.* Nothing is known about this gene and its encoded product.

In this work, the biochemical and physiological characterization of *At5g44360*/*BBE23* has been undertaken. I have characterized the activity of the encoded product, upon heterologous expression in *Pichia pastoris*, showing that it is a cellodextrin oxidase, thereby named CELLOX2. The *CELLOX2* gene is expressed only during the intermediate stages of seed development while *CELLOX1* is present both in seeds and seedling. Unlike *CELLOX1*, *CELLOX2* is not up-regulated during the immune response.

RESULTS

Bioinformatics analyses on the gene encoding a putative CELLOX

In *Arabidopsis thaliana*, the closest paralogue of the gene *CELLOX1*/*At4g20860* is *At5g44360* (also described as *BBE23*; 1906 bp; Figure II.1.), a gene whose product is still uncharacterized in terms of enzyme characteristics and physiological role. *At5g44360*/*BBE23* is localized on chromosome 5, in a gene cluster that includes other 5 paralogues (*At5g44380*/*BBE24*, *At5g44390*/*BBE25*, *At5g44400*/*BBE26*, *At5g44410*/*BBE27*, *At5g44440*/*BBE28*). The encoded product of *At5g44360*/*BBE23* shares 65.21 % of similarity with CELLOX1 by sequence alignment, being 532 amino acid (aa)-long, while CELLOX1 is 530 aa, with molecular masses of 60.49 kDa and 60.4 kDa, respectively. At5g44360/BBE23 shares with CELLOX1/At4g20860 the oxygen binding site motif PTVGVGG (Figure II.2.).

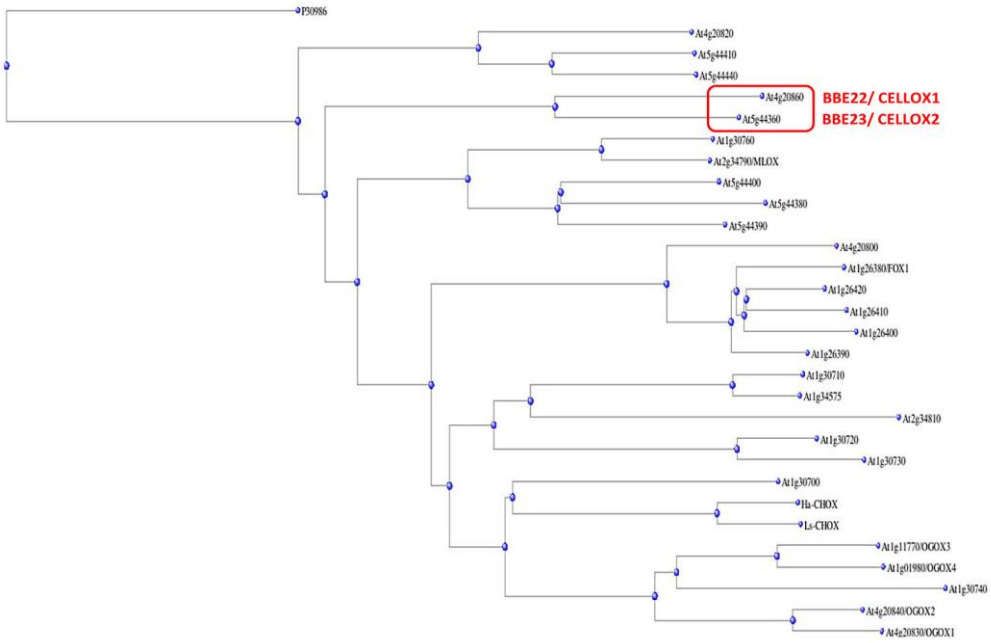

Figure II.1. Homology tree of the BBE-like family proteins. As an outgroup, a true Berberine Bridge Enzyme, P30986, has been included in the analysis (Locci et al., 2019).

Figure II.2. At5g44360 and CELLOX1/At4g20860 sequence alignment. At5g44360 is in the top line. The two proteins share an identity of 65.21%. In red, the reactive oxygen motif (PTVGVGG). Residues of the putative catalytic site (type IV) according to (Daniel *et al.*, 2016) are shown in blue. The conserved FAD-binding site is shown in green. The software used is DNAMAN (https://www.lynnon.com/).

A homology-based molecular modelling of its 3D structure was built by the server SWISS-MODEL (Waterhouse et al., 2018) and the software PyMOL (The PyMOL Molecular Graphics System, Version 2.0 Schrödinger, LLC.) using as template the crystallographic structure of the monolignol oxidase At2g34790/BBE15 (code 4UD8 in the Protein Data Bank, http://www.pdb.org). The monolignol oxidase shares with At5g44360/BBE23 an identity of 50.81% and catalyzes the oxidation of aromatic allylic alcohols, such as coumaryl-, sinapyl-, and coniferyl alcohol, to the corresponding aldehydes. At5g44360/BBE23 shares with CELLOX1 the residues of the putative type IV active site, also conserved in the cellobiose oxidase of *Physcomitrella patens* (PpCBOX). These are the cysteine and the histidine residues responsible for the FAD binding and the two tyrosine residue that are important for the proton abstraction (Figure II.3.) (Daniel et al., 2017; Daniel et al., 2016; Messenlehner et al., 2021; Toplak et al., 2018). CELLOX1 and At5g44360/BBE23 also

share residues negatively charged at physiological pH around the active site, suggesting they may have similar activity (Locci et al., 2019).

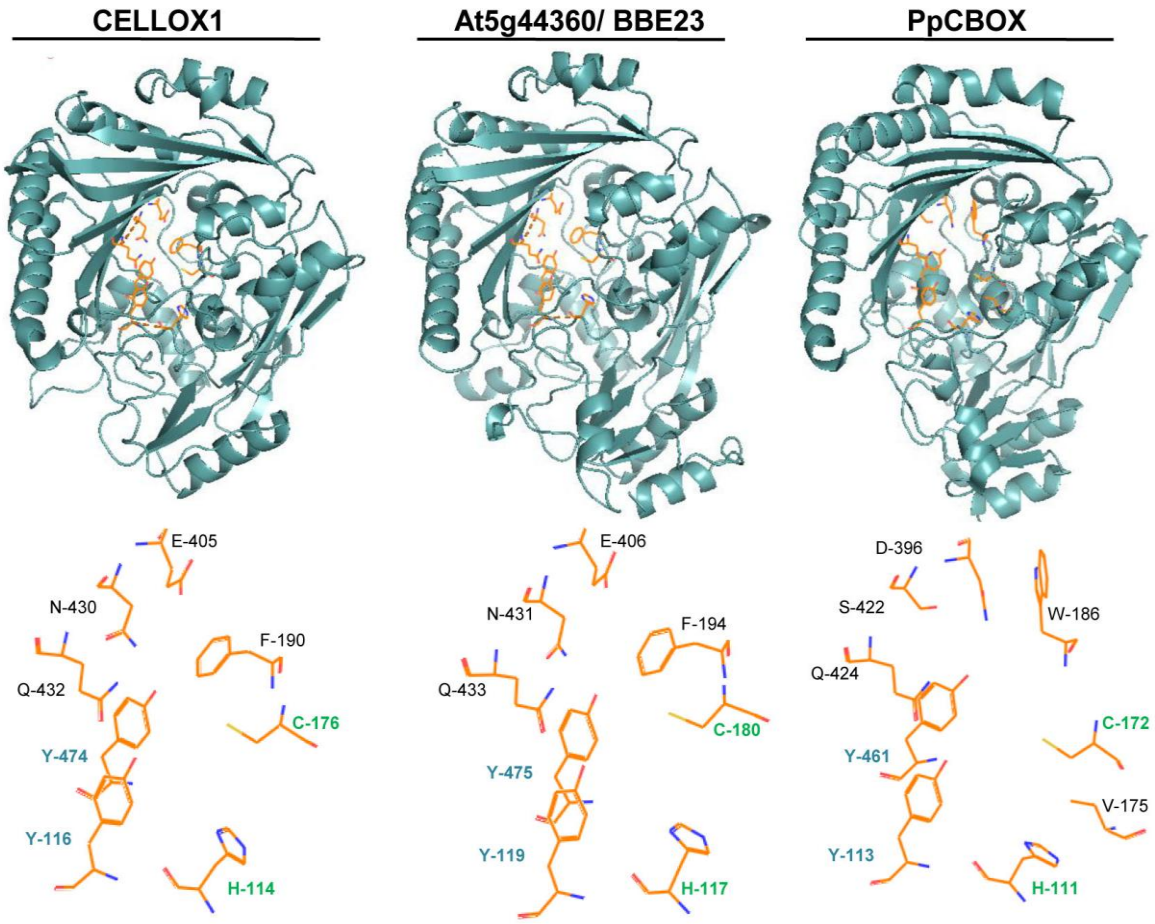

Figure II.3. The predicted model of *At5g44360/ BBE23* with a close-up view of the catalytic site type IV. Both the models of CELLOX1 and *At5g44360/ BBE23* were built using the homology with the already-characterized by X-ray crystallography monolignol oxidase (AtBBE15, At2g34790), with which *At5g44360/ BBE23* shares a sequence identity of 50.81%. CELLOX1 and the X-ray crystallography charcterized *P. patens* cellobiose oxidase (PpCBOX; Toplak et al., 2018) share the same catalytic site and they are showed as comparison with *At5g44360/ BBE23*. Type IV catalytic sites (Daniel et al., 2017) are highlighted in gold on the bottom. The two amino acids responsible for FAD bicovalent attachment are highlighted in green (Daniel et al., 2017; Toplak et al., 2018). In blue Tyrosine residues involved in proton abstraction (Messenlehner et al., 2021). The color of heteroatoms is according to a standard color scheme (red for oxygen, blue for nitrogen, yellow for sulfur). Amino Acids are shown as letter code, Glutamate (E), Phenylalanine (F), Cysteine (C), Histidine (H), Tyrosine (Y), Glutamine (Q), Asparagine (N), Aspartate (D), Tryptophan (W), Valine (V), Serine (S). PDB server and the software PyMOL were used for modeling (https://www.wwpdb.org/; https://pymol.org/2/)

Heterologous expression in *Pichia pastoris* shows that At5g44360/BBE23 is a cellodextrin oxidase (CELLOX2)

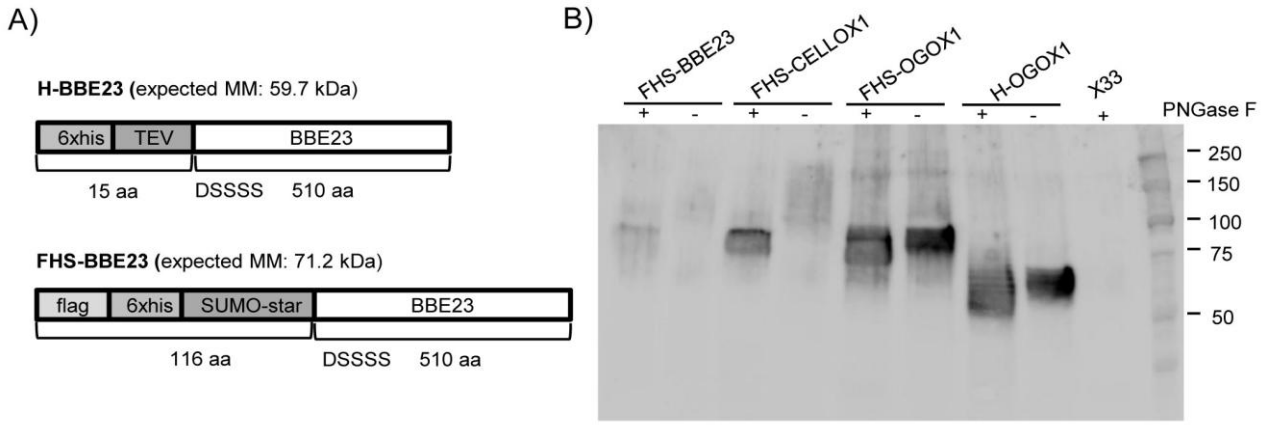

Figure II.4. Heterologous expression of BBE23 in ***P. pastoris.*** A) Schematic representation of his- (H-BBE23) and flag-his-SUMOstar- (FHS-BBE23)-tagged forms of BBE23. The mature BBE23 (starting with the amino acid sequence DSSS) was fused downstream of the his- and flag-his-SUMOstar tags, in turn placed downstream of the signal peptide of the α factor for translocation into the endoplasmic reticulum and secretion (not shown in the figure). B) Immuno-decoration of untreated (-) and deglycosylated PNGase F-treated (+) proteins in culture filtrates of Pichia expressing different BBE-l after a 48-h induction with methanol**.** AbHIS- HRP from rabbit was used as antibody**.** Pichia expressing H-OGOX1, FHS-OGOX1 and FHS-CELLOX1 were used as reference. Experiment in collaboration with Manuel Benedetti, Università dell'Aquila.

For characterization, the protein encoded by *At5g44360/BBE23*, tagged with the myc epitope at the C-terminus, was expressed in *Pichia pastoris*, as reported previously for the expression of other proteins belonging to the BBE-like enzyme family (Benedetti et al., 2018). Unfortunately, no protein was detected in the *Pichia* medium by western blot analysis, using the anti-myc antibody, also after an enrichment of the proteins by acetone precipitation.

Successful expression of At5g44360/BBE23 was obtained by optimizing the codon usage for expression in *Pichia* and utilizing the SUMOstar gene fusion technology (LifeSensorsInc.) in a collaboration with Dr. Manuel Benedetti [University of L'Aquila (Italy)]. In particular, the mature form of At5g44360/BBE23 was fused downstream of the his-tag (H-BBE23 fusion) or downstream of the flag-his-SUMOstar tag (FHS-BBE23 fusion). The SUMOstar system was used because it makes the recombinant products more stable resulting in a subsequent improvement of their purification (www.lifesensor.com) (Figure II.4.A.). Both fusions were placed downstream of the signal peptide of the α-factor for protein secretion and the promoter of alcohol oxidase (AOX1) to drive expression upon methanol induction. Due to the hyper-glycosylation performed by *Pichia,* de-glycosylation of both H-BBE23 and FSH-BBE23 protein fusions with a peptide-N-glycosidase (PNGase) was

necessary to reveal their presence in the culture filtrates by Western Blot (Figure II.4B.).

The expressed tagged protein FHS-BBE23 was purified and its enzymatic activity tested with different substrates, in an assay that measures the hydrogen peroxide produced in the reaction. Like CELLOX1, the protein encoded by *At5g44360*/*BBE23* acted on β-1,4-linked cellodextrins, in particular those with a degree of polymerization (DP) of 2-6, with a much lower relative activity on cellobiose (CD2) and the highest relative activity on cellotriose (CD3), cellotetraose (DP 4; CD4) and celloexaose (Figure II.5.). These results indicate that, similarly to CELLOX1, the protein encoded by *At5g44360*/*BBE23*, hereon named CELLOX2, is a cellodextrin oxidase.

Interestingly, FHS-CELLOX2 and the flag-his-SUMOstar tagged FHS-CELLOX1 both showed a slight activity also on β-D-cellobiosyl-(1→3)-β-D-glucose (O-BGTRIB hereon indicated as MLG43), β-D-glucosyl-(1→3)-β-D-cellobiose (O-BGTRIA, MLG34), and a mixture of β-D-cellobiosyl-(1→3)-β-D-cellobiose (80%) + β-D-

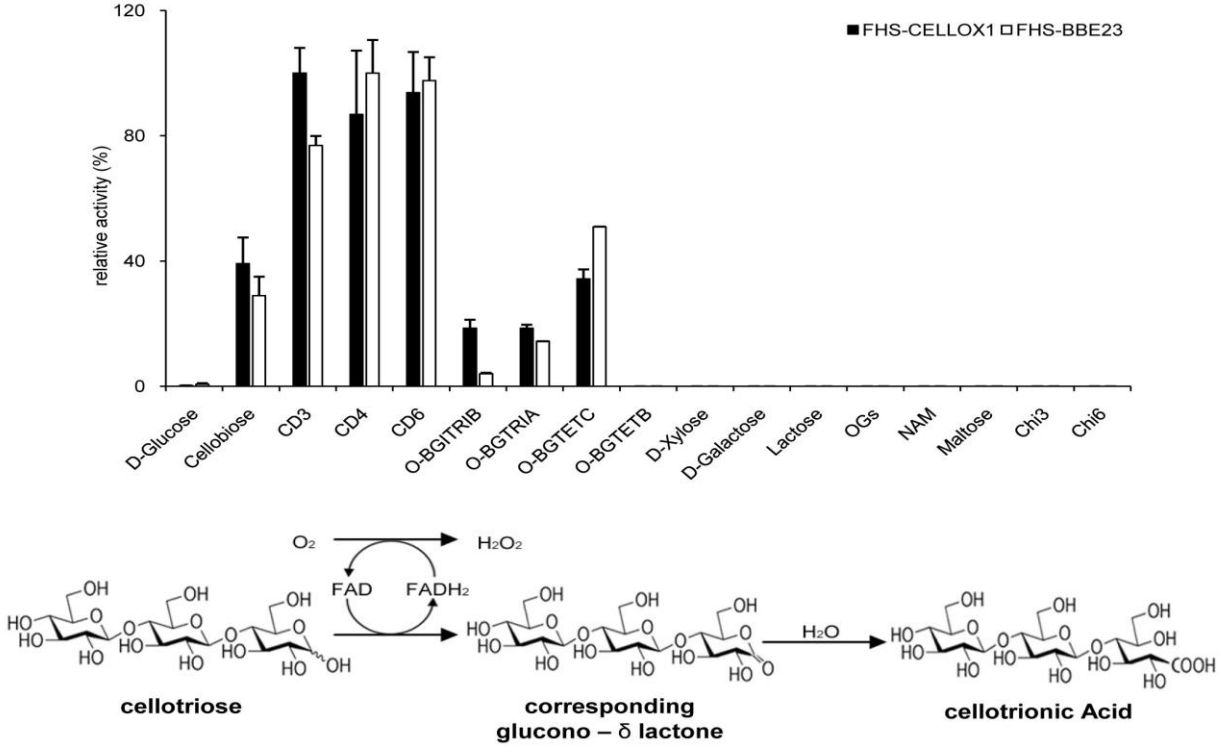

Figure II.5. Relative activity of FHS-BBE23 and FHS-CELLOX1 towards different substrates. The flag-his-SUMOstar- (FHS-BBE23)-tagged form of BBE23 was tested on different carbohydrate substrates (0.4 mM each) at pH 7.5 and 37°C. CD3: cellotriose, CD4: cellotetraose; CD6: cellohexaose, Chi3: chitotriose, Chi6: chitohexaose, O-BGTETB/MLG443: β-D-cellotriosyl-(1→3)-β-D-glucose, O-BGTETC/MLG434+344: a mix of β-D-cellobiosyl-(1→3)-β-D-cellobiose (80%) + β-D-glucosyl-(1→3)-β-D-cellotriose (20%), O-BGTRIA/MLG34: β-D-glucosyl-(1→3)-β-D-cellobiose, O-BGTRIB/MLG43: β-D-cellobiosyl-(1→3)-β-D-glucose, OGs: oligogalacturonides, NAM: N-acetyl-glucosamine. Experiments were performed in collaboration with Manuel Benedetti, Università dell'Aquila. At the bottom, a schematic of the reaction of oxidation of the last residue at the reducing end of cellotriose, a cellodextrin, showing the parallel reduction of FAD in FADH2 and the reduction of molecular oxygen to reconstitute the FAD, leading to the production of hydrogen peroxide as a secondary product.

glucosyl-(1→3)-β-D-cellotriose (20%) (O-BGTETC, MLG434+344). No activity was detected when glucose, xylose, lactose, galactose, maltose, N-acetyl-glucosamine (NAM), chitotriose (Chi3), chitohexaose (Chi6), OGs and β-D-cellotriosyl-(1→3)-β-D-glucose (O-BGTETB, MLG443) were used as substrates (Figure II.5.). Thus, both CELLOX1 and CELLOX2 catalyze the oxidation of the C1 of the β-1,4 glucose residue at the reducing end, forming the glucono–δ-lactone and then the gluconic acid, in a reaction that involves the simultaneous reduction of the associated coenzyme FAD to $FADH_2$. FAD is reconstituted through the reduction of molecular oxygen with the consequent production of hydrogen peroxide as a secondary product (Figure II.5.).

Like FHS-CELLOX1, FHS-CELLOX2 showed a relative activity (%) in a range of pH between 5 and 11 that increased at increasing pHs, with a maximum at pH 10 (Figure II.6A.). The predicted electrostatic potential on both CELLOX1 and CELLOX2 surfaces does not change much by changing from an acidic pH to a neutral and a basic pH. The distribution of charged groups of both CELLOX1 and CELLOX2 is not affected by a change in pH of the medium, and it may be assumed that there are not significative conformational changes at the level of the substrate binding site (Figure II.6B.).

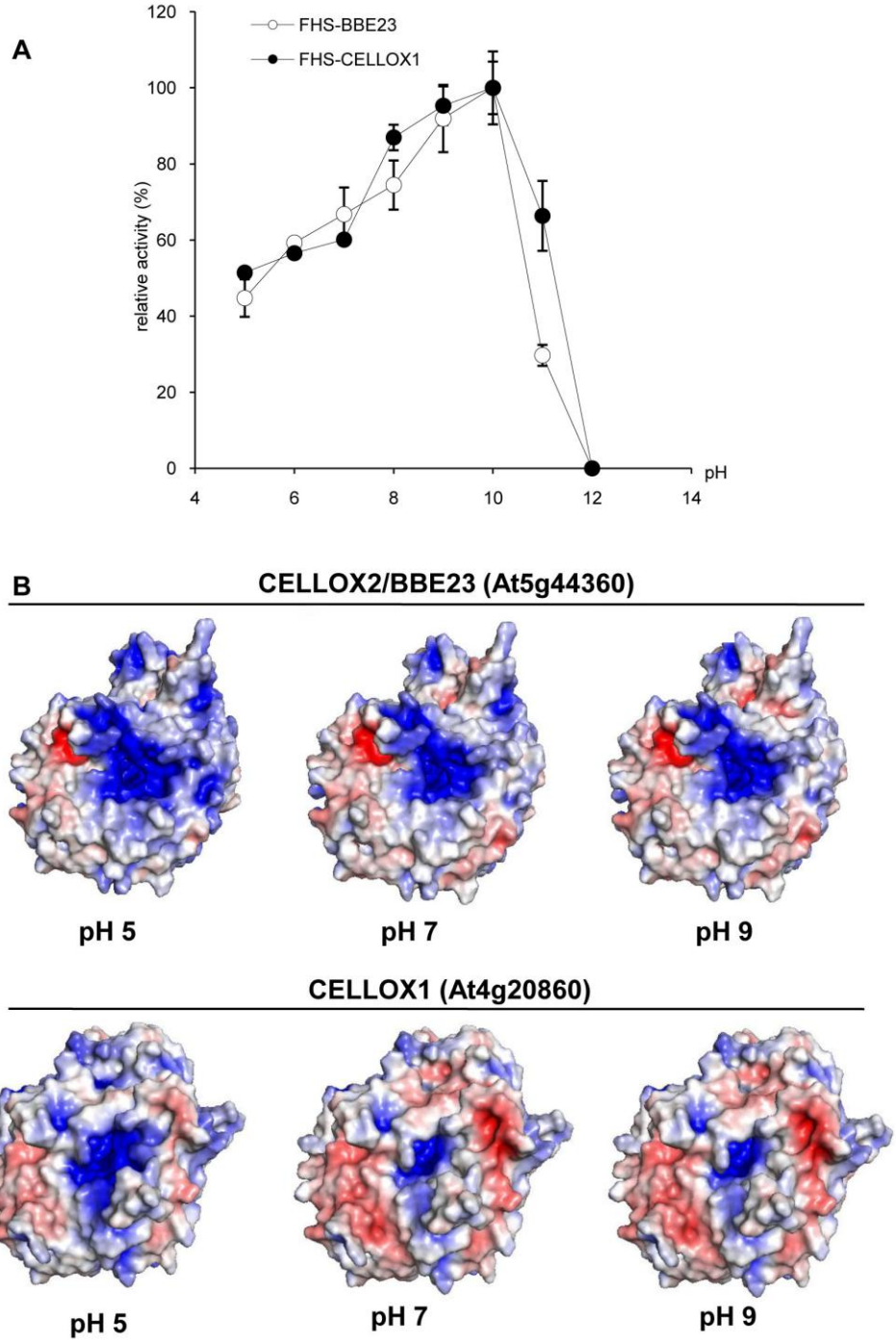

Figure II.6. Relative enzymatic activity (%) and predicted electrostatic potential surfaces of CELLOX1 and CELLOX2 at different pH. A) Both FHS-BBE23 and FHS-CELLOX1 relative activity (%) has a peak at pH 10, using 0.4 mM cellobiose as substrate. In collaboration with Manuel Benedetti, Università dell'Aquila. B) Distribution of charged groups in CELLOX1 and CELLOX1 at pH 5, 7 and 9 using APBS-PDB2PQR software (Dolinsky et al., 2004). Positive charges are shown in blu and negative charges are shown in red on the predicted protein surface. PDB server and the software PyMOL were used for modeling (https://www.wwpdb.org/; https://pymol.org/2/)

Transient expressions of GFP- and RFP-tagged CELLOX2 in *N. tabacum* suggests an extracellular localization

CELLOX2 is predicted to be extracellular according to SignalIP 4.1 (Petersen et al., 2011) and Uniprot (www.uniprot.org) (Figure II.7.).

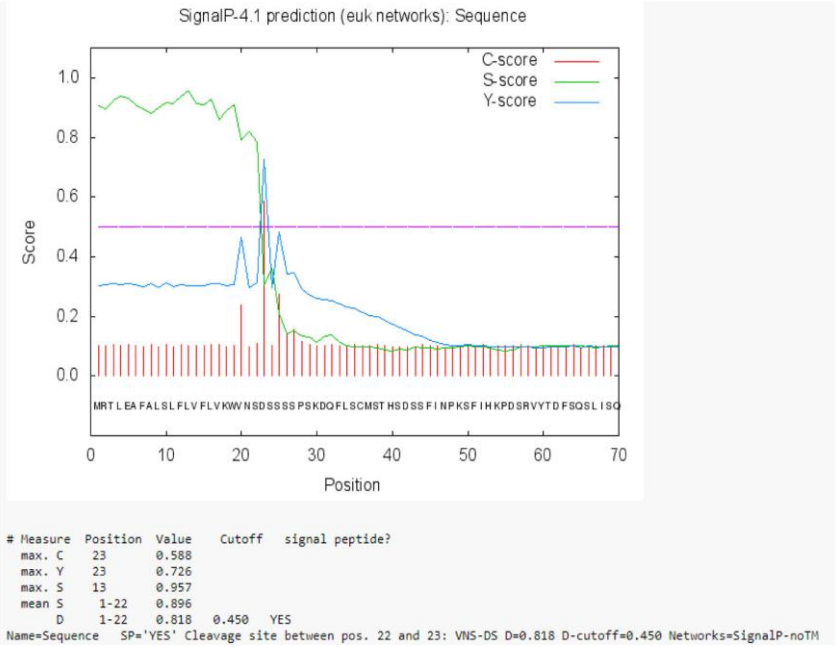

Figure II.7. Predicted signal peptide and membrane-spanning regions in At5g44360. At5g44360 is likely to be secreted according to the tool SignalIP 4.1 (http://www.cbs.dtu.dk/services/SignalP/).

In order to determine the localization of CELLOX2 *in planta*, the protein was expressed in both the native and fluorescent form under the constitutive strong promoter *CaMV35S*. Because it is reported that the GFP has the tendency to be degraded at the typical pH condition of the apoplast, the CELLOX2 protein was tagged not only with GFP but also with RFP. *N. tabacum* leaves were transiently transformed by agroinfiltration with the constructs expressing the fluorescent proteins. By confocal microscopy analysis, fluorescence was observed with both the GFP- and RFP-tagged form. With the GFP-tagged protein, a localization pattern was observed, characterized by fluorescence mainly in the cell periphery, which includes the apoplast and coherent with the prediction that CELLOX2 is a secreted protein. For the RFP-tagged form, signals were diffused and suggested artifacts that may be due to a defective expression of the protein fusion (Figure II.8.).

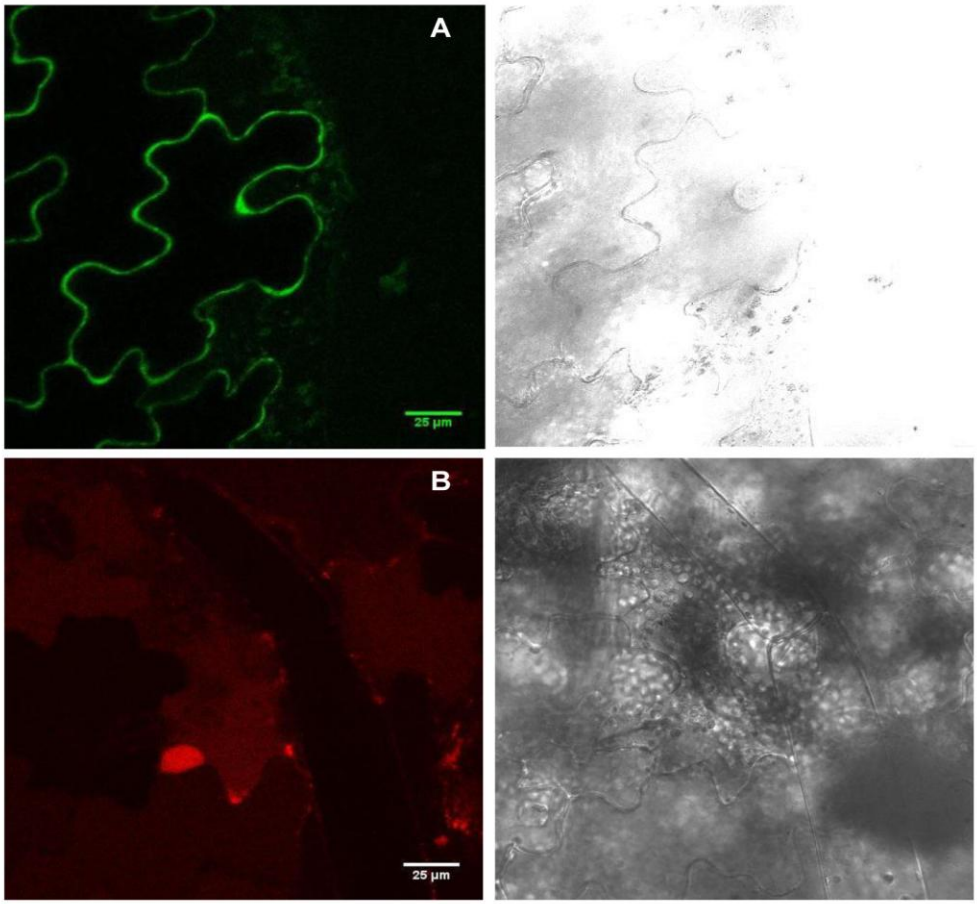

Figure II.8. Transient expression of 35S::*CELLOX2-GFP* (A) and *35S::CELLOX2-RFP* (B) in agro-infiltrated tobacco leaves. CELLOX2 may be localized in the apoplast as suggested by the distribution of fluorescence (CELLOX2- GFP). CELLOX2-RFP showed a more diffused signal. Confocal microscopy images.

Stable transformation of *Arabidopsis* seedlings, by floral dip, has been performed to obtain stable expression of the tagged protein and overexpression of the native one. T1 and T2 seeds have been collected and selection of the transformed seedlings in a selective media is in progress.

CELLOX2 is expressed during seed development but not in seedlings or upon elicitor treatment

In silico analysis of the spatial distribution of the expression of CELLOX2/*At5g44360* and *CELLOX1*/*At4g20860* was performed using the database eFP browser and Genevestigator (Hruz et al., 2008; Nakabayashi et al., 2005; Schmid et al., 2005). *CELLOX2* expression is absent in seedlings, adult leaves, stems and roots, whereas *CELLOX1* appears to be expressed in these organs (Figure II.9.).

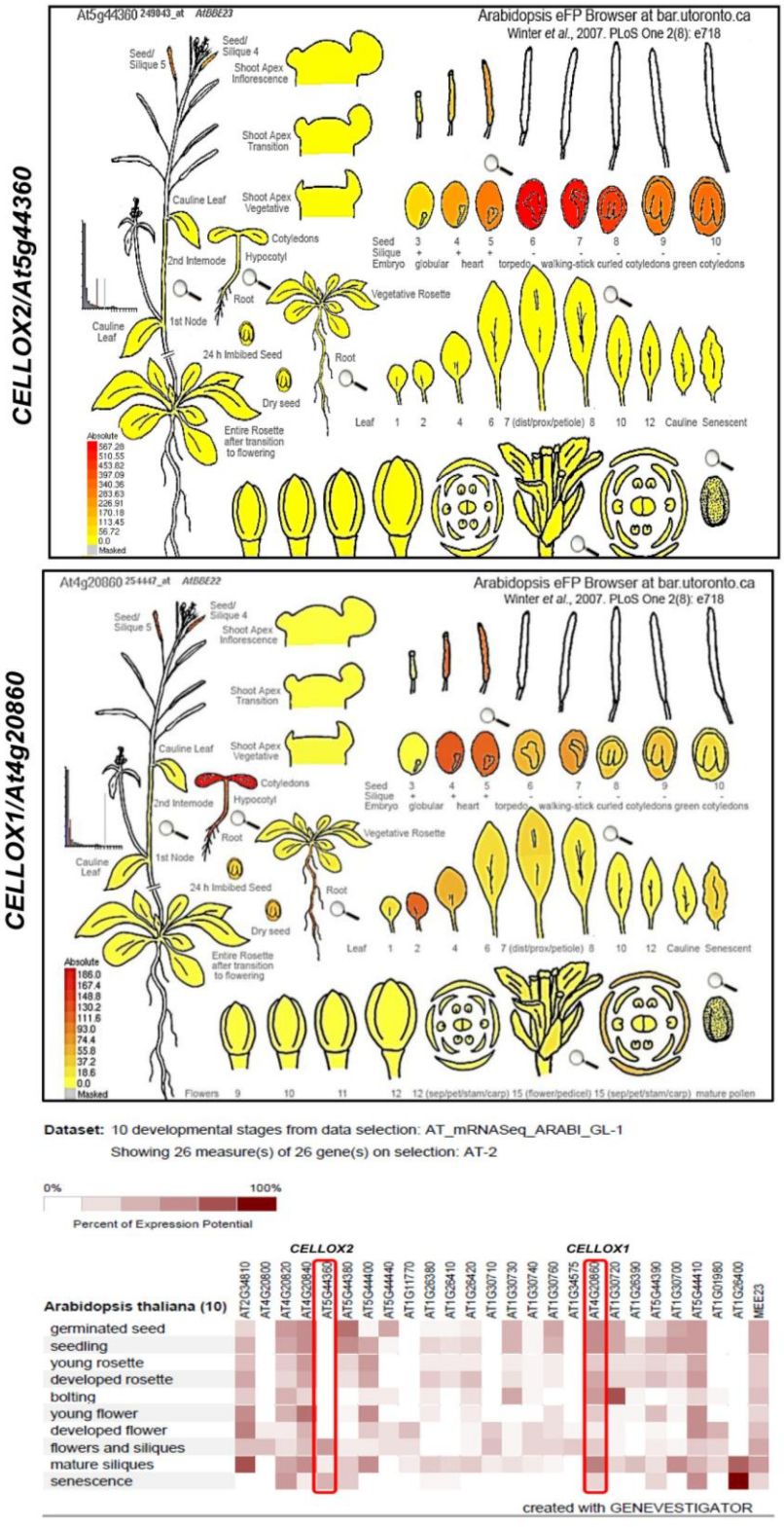

Figure II.9. Localization of the transcripts of *CELLOX2*/*At5g44360* and *CELLOX1*/*At4g20860* according to the database eFPbrowser and Genevestigator. The higher expression of *CELLOX2* is in the seed during development. *CELLOX1* is also expressed in the seed, with a different expression profile.

Both *CELLOXs* are expressed during seed development with a different temporal profile (Figure II.10.). Moreover, whereas the expression of *CELLOX1* is induced by *Pseudomonas syringae*, *Botrytis cinerea*, and elicitors such as flg22 and OGs (Locci et al., 2019), the expression of CELLOX2 is not predicted to be induced in infected

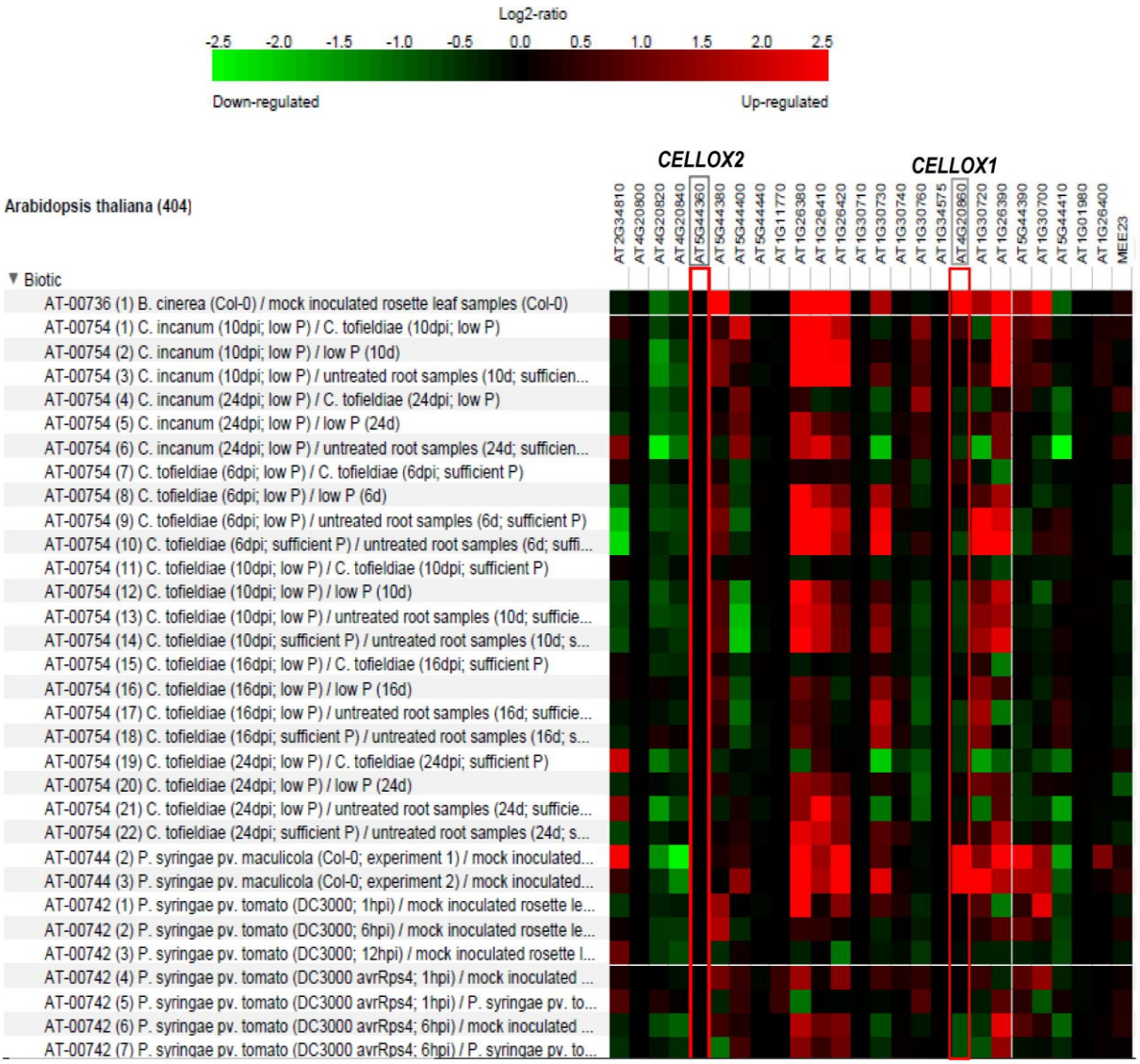

Figure II.10. Differential expression of BBE-like family genes against biotic pertubations. Differential expression of BBE-like members including *CELLOX2 and* and *CELLOX1* upon biotic stresses. Unlike *CELLOX1, CELLOX2* is not expressed upon pathogen infection. From *Arabidopsis* RNAseq data. Data were obtained using the software Genevestigator (Hrutz et al., 2008).

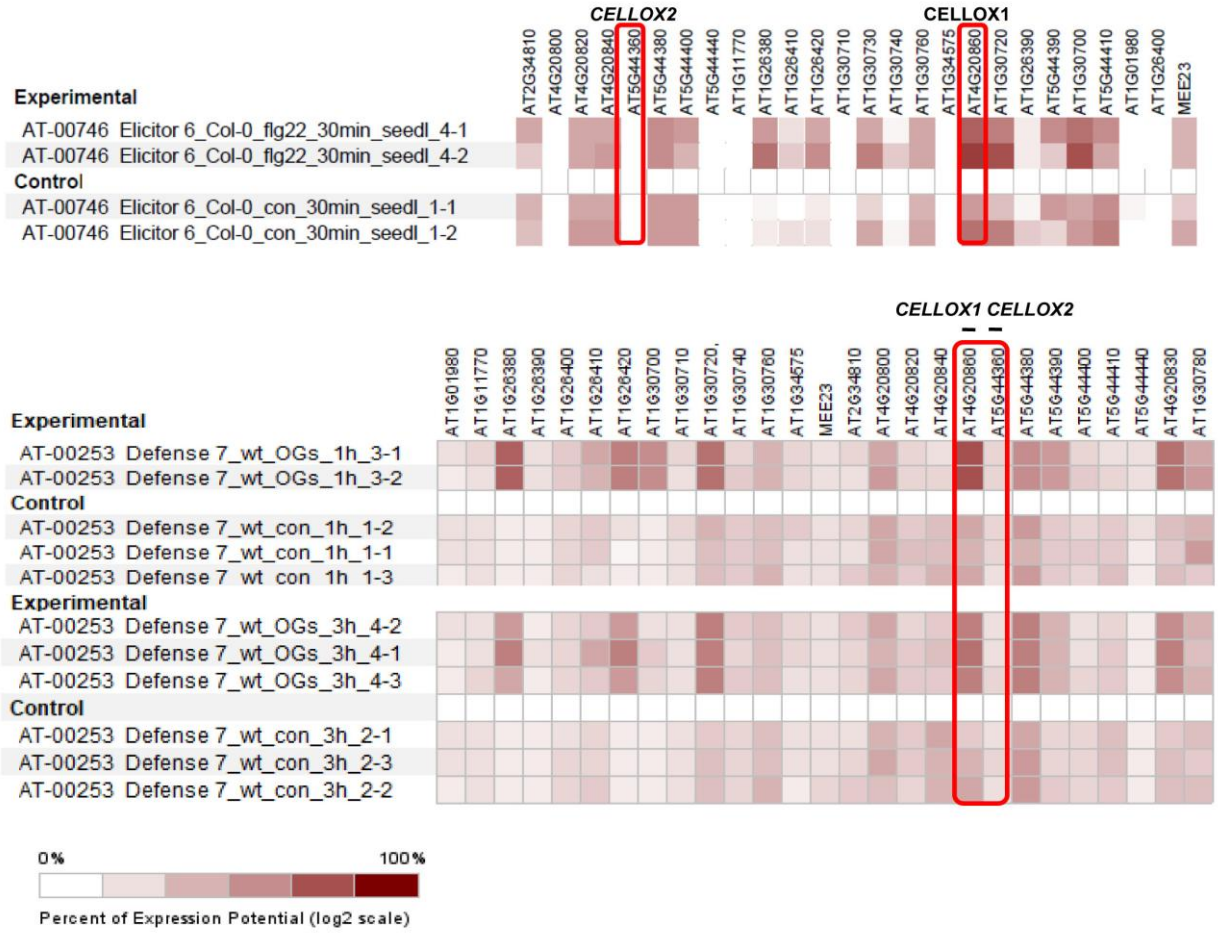

Figure II.11. Differential expression of BBE-like family genes against elicitation with flg22 and OGs. Differential expression of BBE-like members including *CELLOX2 and* and *CELLOX1.* Differential expression upon elicitation with flg22 for 30 min (top panel; from *Arabidopsis* RNAseq data) and OGs for 1 and 3 h (bottom panel; Affymetrix *Arabidopsis* ATH1 Genome Array). Both sets of data were obtained using the software Genevestigator (Hrutz et al., 2008).

seedlings and upon induction with flg22 and OGs [Genevestigator, (Hruz et al., 2008); Figure II.10. and II.11.].In agreement with the transcription data, I did not detect the transcripts of *CELLOX2* in seedlings (Col-0) under physiological conditions (Figure II.12.). Expression of *CELLOX2* was analyzed also in seedlings upon a 1-h treatment with the elicitors flg22, elf18, OGs, and CD3. No *CELLOX2* transcripts were detected also in this case (Figure II.12.), suggesting that this gene is not involved in the defense of the vegetative parts of the plant.

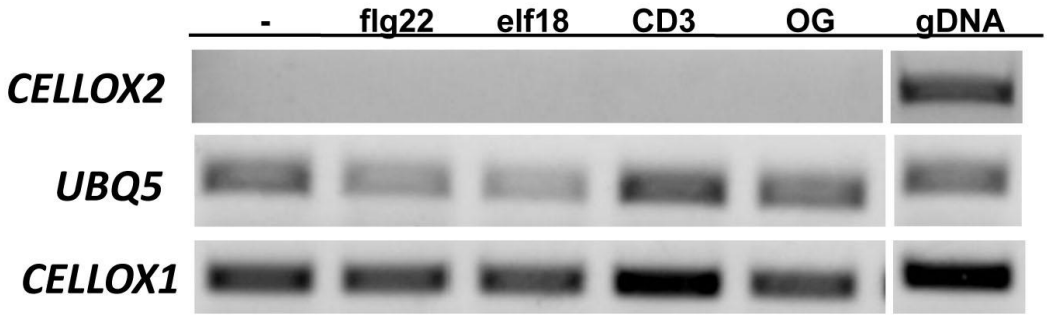

Figure II.12. Expression of *CELLOX2* compared to that of *CELLOX1* in Col-0. Expression was analyzed by semiquantitative RT-PCR under physiological conditions (-) and after elicitation with flg22, elf18, CD3 (cellotriose) and OGs. using UBIQUITIN 5 (UBQ5) transcripts as a reference. Genomic DNA (gDNA) was used as positive control in the same experiment.

Unlike CELLOX1, CELLOX2 is not involved in immunity

A reverse genetic approach was undertaken to study the physiological role of *CELLOX1* and *CELLOX2*. Commercially available seeds for T-DNA insertional mutants for both the genes CELLOX2/*At5g44360* (Col-2 background) and CELLOX1/At4g20860 (Col-0 background) were obtained. Insertions within the coding DNA sequence (CDS) were chosen to ensure disruption of these genes (Figure II.13.). Mutant lines were genotyped (Figure II.13.). Two allelic homozygous mutants were obtained for *CELLOX1,* respectively *cellox1-1*, and *cellox1-2*. Quantitative RT-PCR analyses revealed that *cellox1-1* is a knockdown mutant, because mRNA expression, albeit lower with respect to the wild type, is still detectable (Figure II.13.). The T-DNA insertion of *cellox1-1* is positioned at the end of the CDS, at the level of the 3'UTR, likely producing a truncated transcript but still expressed. The line *cellox1*-2 is instead a knockout mutant, as determined by semiquantitative RT-PCR analysis (sqRT-PCR; Figure II.13.), hereon named *CELLOX1* KO. For CELLOX2, a single homozygous mutant line was obtained (*cellox2-1*, in the col-2 background), carrying the insertion about in the middle of the CDS, and likely a knockout, here named *CELLOX2 KO* (Figure II.13.). Because normal expression of this gene is absent in seedlings, transcript analysis to demonstrate that the mutation is null likely has to be performed in seeds, where the gene is expected to be expressed. Since the T-DNA insertion of *CELLOX2* is on the Col-2 ecotype background, Col-2 was

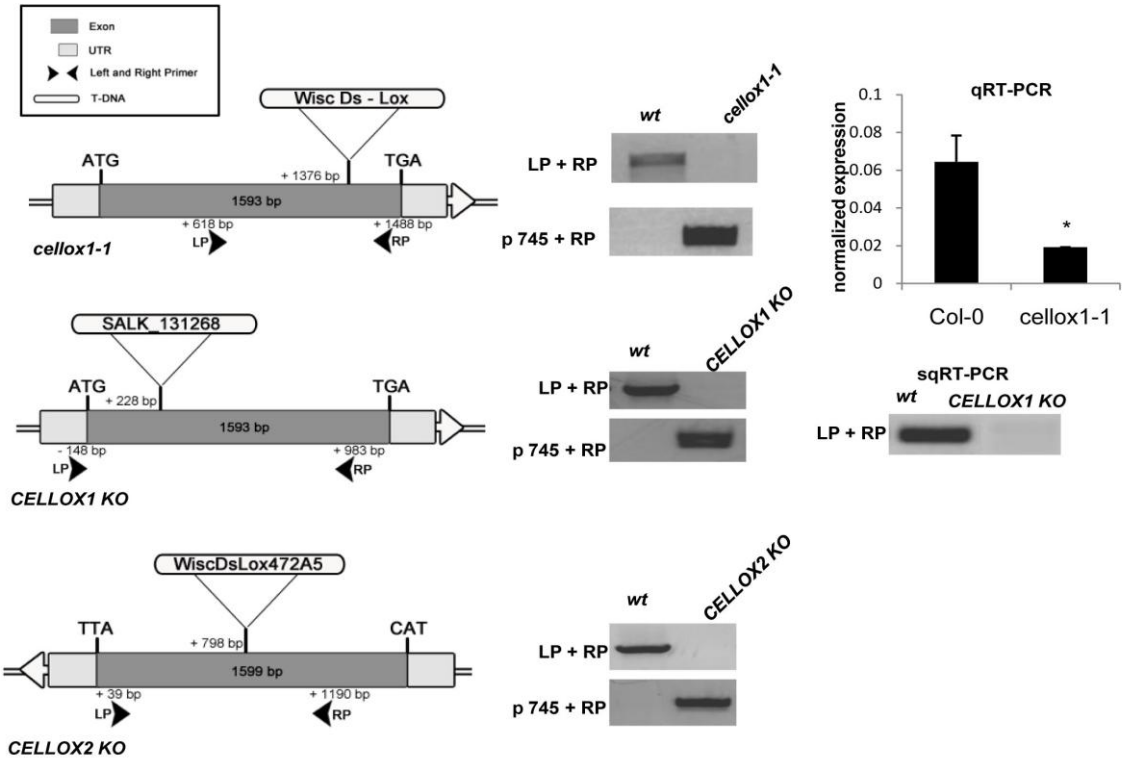

Figure II.13. Characterization of the T-DNA insertional mutants *cellox1-1*, CELLOX1 KO and CELLOX2 KO. Left panels, representation of T-DNA insertions in *cellox1-1, CELLOX1 KO and CELLOX2 KO.* Middle panels, PCR on genomic DNA showing that they are homozygous mutants. LP and RP are respectively Left Primer and Right primer, p745 indicates the T-DNA left border primer. Right panels, transcript analysis of *cellox1-1* by qRT-PCR (real time quantitative PCR) or sqRT-PCR (semiquantitative PCR) for *CELLOX1 KO* as indicated. Transcript levels were analyzed by qRT-PCR and normalized to UBQ5 expression. T-student * = p value < 0.05.

used as control for CELLOX2 KO analysis, while the Col-0 ecotype is the background of CELLOX1 KO and CELLOX1 OE mutants.

It has been shown that overexpression of *CELLOX1* increases resistance against *Botrytis cinerea* infection (Locci et al., 2019). To complete the study of the role of CELLOX1 in plant resistance against this fungus and to assess whether CELLOX2 plays a role in immunity, the corresponding knockout mutants were infected with *B. cinerea* and the area of the lesions at 48 h after inoculation (hpi) was measured. *CELLOX1 KO* showed a lesion area significantly greater than the wild type, in agreement with the data of Locci et al.(2019) reporting that the overexpressing plants are more resistant to the fungus (Figure II.14.). In the CELLOX2 KO mutant, lesion area was similar to that of the wild type, suggesting that *CELLOX2* does not play a role in the response to this fungus (Figure II.14.). It was concluded that, unlike *CELLOX1*, *CELLOX2* does not play a role in the resistance to *Botrytis cinerea*.

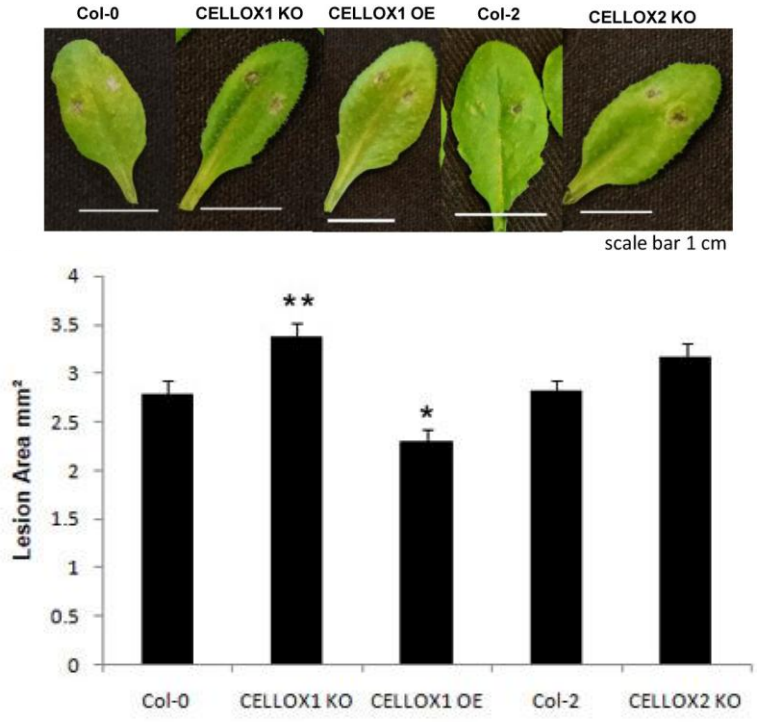

Figure II.14. Infection of CELLOXs mutants with *Botritis cinerea*. Lesion area (mm², average ± SE) of transgenic *Arabidopsis* knockout and overexpressing mutant (CELLOX1 KO, CELLOX2 KO and CELLOX1 OE) leaves 48 h after inoculation with *Botrytis cinerea* spores. T-test. **p<0.01, *p < 0.05

Both *CELLOX1* and *CELLOX2* play a role in seed coat formation and characteristics

CELLOX2 is mainly expressed in the seed coat during the seed development, in particular in the so-called heart stage, with a lower expression in the pre-globular, globular, and in the mature embryo stages. *CELLOX1*, instead, is mainly expressed at the level of the seed coat, only during the linear cotyledon stage, when instead *CELLOX2* is not expressed (Figure II.15.). During the maturation stage both the enzymes are predicted to be expressed at the same time with different localizations: *CELLOX2* is expressed in the mature embryo and peripheral endosperm and *CELLOX1* in the seed coat.

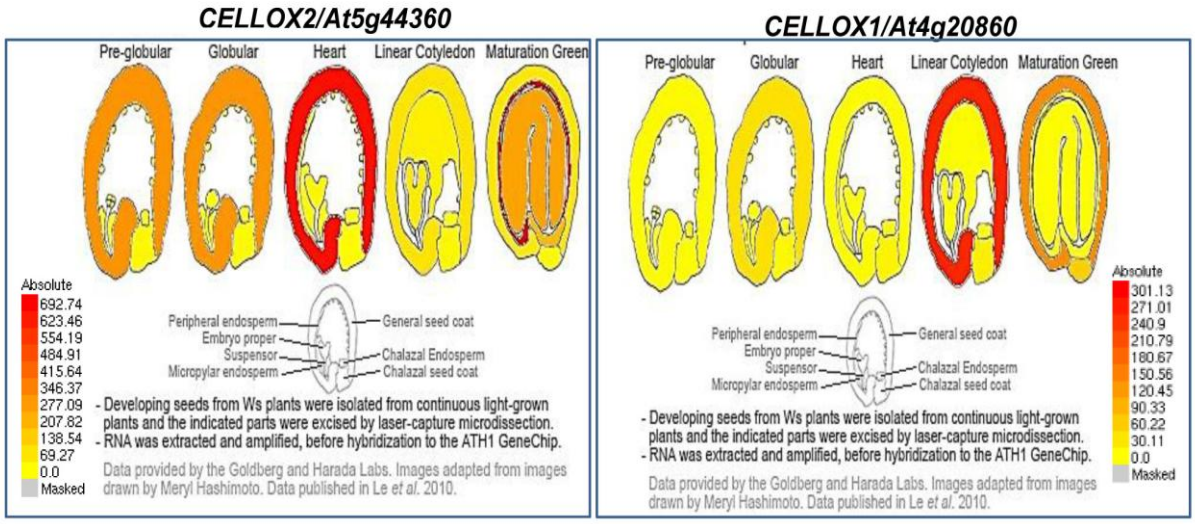

Figure II.15. Localization of the transcripts of *CELLOX2*/*At5g44360* and *CELLOX1*/*At4g20860* in the developing seed according to the database eFPbrowser. *CELLOX1* and *CELLOX2* are expressed in the seed during development, with a different expression profile.

Collectively, these data suggest a role of both *CELLOX1* and *CELLOX2* in seed development, while only *CELLOX1* is involved in immunity and may be involved in the regulation of defense responses in the seed (Dalling et al., 2020).

The KO mutants of CELLOX1 and CELLOX2 and the transgenic lines overexpressing CELLOX1 (CELLOX1 OE) were examined, in parallel with the wild-type ecotypes Col-2 and Col-0 (as controls for CELLOX2 KO and CELLOX1 KO respectively). First, the area of hydrated seeds, excluding the mucilage, was measured to determine whether alterations in the expression of CELLOXs lead to morphological differences. The seeds of the different genotypes were all collected at the same time from plants grown under the same conditions. Col-2 seed were significantly larger that Col-0 seeds, whereas no significant differences were detected between the CELLOX1 KO and CELLOX2 KO mutant seeds and the corresponding wild-type seeds (Col-0 and Col-2, respectively). On the contrary, CELLOX1-OE seeds showed a significatively increased area in comparison with Col-0 and the two CELLOX KO mutants. It is worth noting that the area of CELLOX1-OE seeds was similar to that of Col-2 seeds (Figure II.16B.). Dry seeds area of the same genotypes showed a very similar, albeit not significant, trend (Figure II.16B.).

Next, mucilage features were examined in the seeds of the mutant/transgenic genotypes. Mutations affecting mucilage formation are not lethal and are easily identified using histochemical stains, for example with Ruthenium Red, which

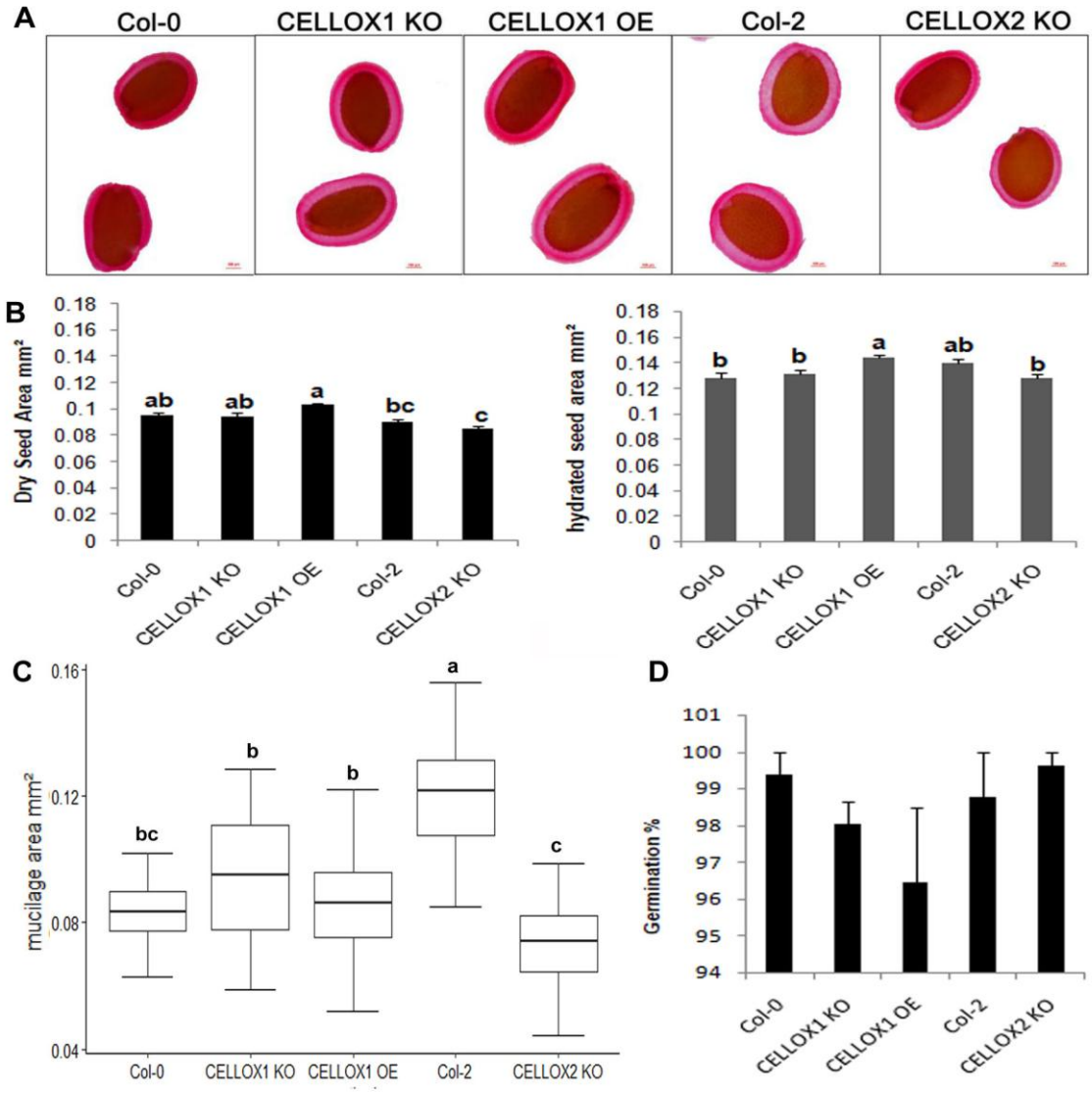

Figure II.16. Phenotypical characterization of seeds for each CELLOXs single mutant. A) Seed mucilage of each mutant is highlighted by Ruthenium Red staining. Images were taked at optical microscope 4 X, scale bar 100 µm. B) Seed area of dry seed (on the left) and seed area of hydrated seed (on the right) for each mutant. C) Box plot of adherent mucilage area (mm^2) of each mutant, measured after hydratation and Ruthenium Red staining. D) Percentage of germination for each mutant. Ecotypes Col-0 and Col-2 were used as controls. B, C, D) Average ± SE of at least three replicates; different letters indicate statistically significant differences according to ANOVA followed by post-hocTukey's HSD test ($P < 0.05$).

detects acid polysaccharides such as pectins (Hanke & Northcote, 1975). Seeds of *CELLOX2* KO, CELLOX1 KO, CELLOX1-OE, and in parallel those of the ecotypes Col-2 and Col-0 as controls, were stained with Ruthenium Red (Figure II.16A.). Col-2 showed the highest mucilage area. In comparison, CELLOX2 KO had a significatively decreased mucilage, which was reduced also in comparison to all the

other genotypes. No significant differences were detected in *CELLOX1* mutants with respect to the wild-type control (Figure II.16C.).

Since defects in mucilage could affect the germination of seeds (Western, 2012), and CELLOX2 KO mutants showed a decreased mucilage area, the germination rate of homozygous T3 progeny seeds of Col-0, CELLOX1 KO, CELLOX1 OE, Col-2 and CELLOX2 KO was measured. Seeds were collected and then sown under the same conditions. No difference was observed among the genotypes, suggesting that defects in CELLOXs single mutants do not affect the germination in the experimental conditions examined (Figure II.16D.).

In order to verify possible morphological differences, scanning electron microscopy (SEM) analysis was performed on dry seeds of CELLOX mutants, the transgenic OE line and the respective controls (Figure II.17A.). The micrographs revealed that both seeds of CELLOX1 OE and CELLOX1 KO had a significatively decreased area of the

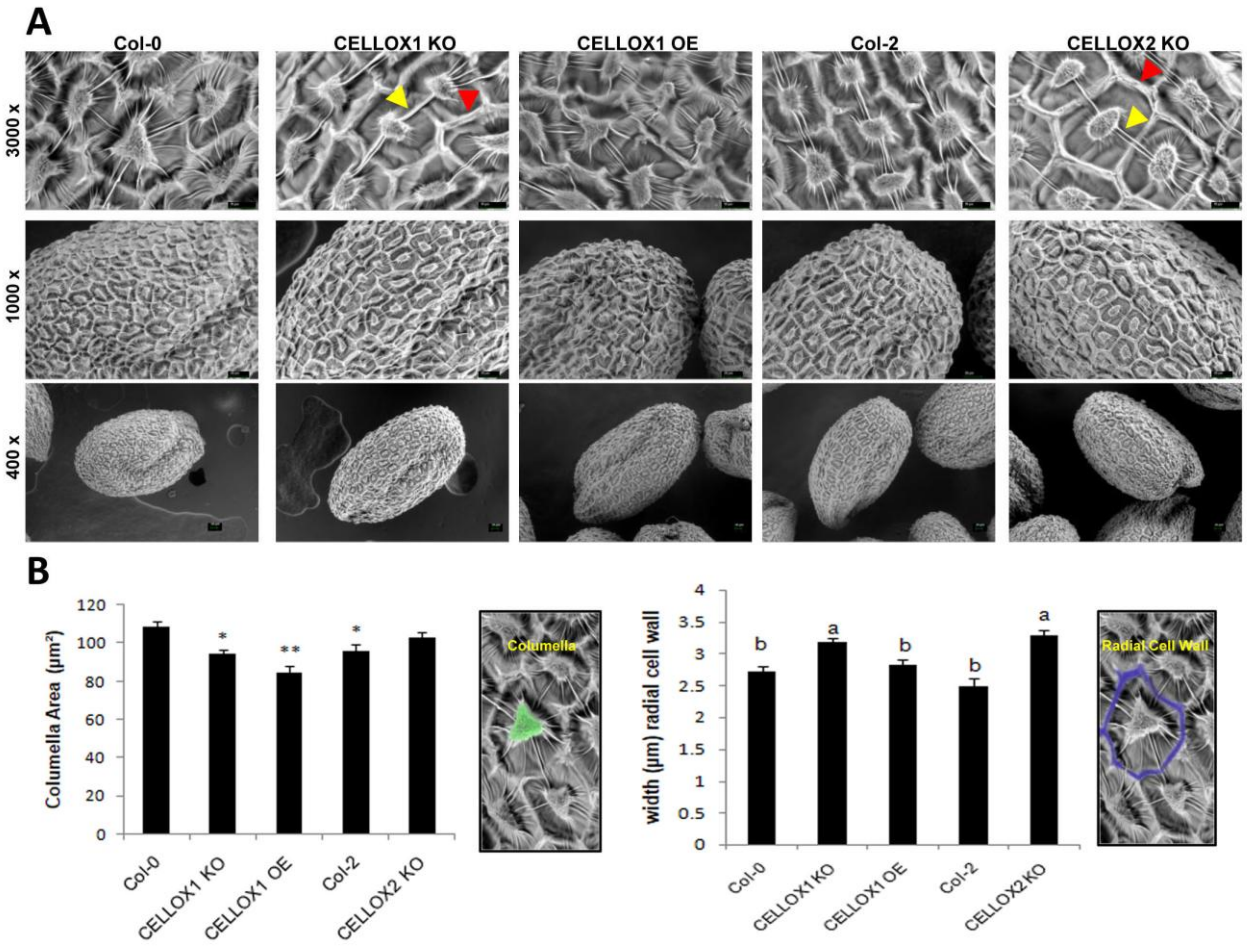

Figure II.17. Scanning electron microscopy of mature CELLOXs transgenic seeds. A) In the upper panel, close up view of epidermal cells with radial cell walls (red arrow) and connections from central *columella* to radial cell walls (yellow arrow) for each mutant. (3000 x). In the lower panels is possible to observe different magnifications at 1000 x and 400 x which show the entire shape of each mutant seed. B) The left plot shows the area (µm²; average ± SE) of columella for each CELLOXs transgenic seed, highlighted in green in the picture on the right. T.test **p < 0.001, *p < 0.05. Plot on the right shows the width of radial cell wall (um) for each mutant. Radial cell wall are highlighted in blue on the right. Col-0 and Col-2 were used as controls. Different letters indicate statistically significant differences according to ANOVA followed by post-hoc Tukey's HSD test (P < 0.05). Columella area and the width of radial cell wall were measured using Image J software. Experiment in collaboration with Dr. Moira Giovannoni, University of L'Aquila.

columella compared with their control Col-0. Col-2 showed a slightly reduced *columella* area (Figure II.17B.). Moreover, it was observed that radial connections from central *columella* and the radial cell wall are less represented in both CELLOXs knockout mutants compared to Col-0 and Col-2 (Figure II.17A.).

It was also possible to detect a significative thicker width of the radial cell wall of CELLOX1 KO and CELLOX2 KO epidermal cells compared to the other genotypes (Figure II.17B.). However, at the moment is not possible to discriminate whether the radial walls were actually thicker or the increased width is due to a main relaxation in the wall adherence of two adjacent epidermal cells.

Hydrated seeds of each genotype were also stained with the fluorescent dye Direct Red 23 (also referred to as pontamine fast scarlet, 4BS), which is specific for cellulose (Anderson et al., 2010; Harpaz-Saad et al., 2011; Mendu et al., 2011). In seed coat this dye highlights the cellulose rays that radially depart from the central *columellae* of epidermal cells, and it stains also the *columella* itself. Confocal images analyzed showed a lower fluorescence intensity at the level of seed coat rays and *columellae* in the CELLOX1 OE mutant seeds compared to all other mutants. No significative differences were detected in other CELLOX mutants and controls Col-0 and Col-2 (Figure II.18.). This observation suggests that cellulose may be less abundant in rays and *columellae* of seeds overexpressing CELLOX1.

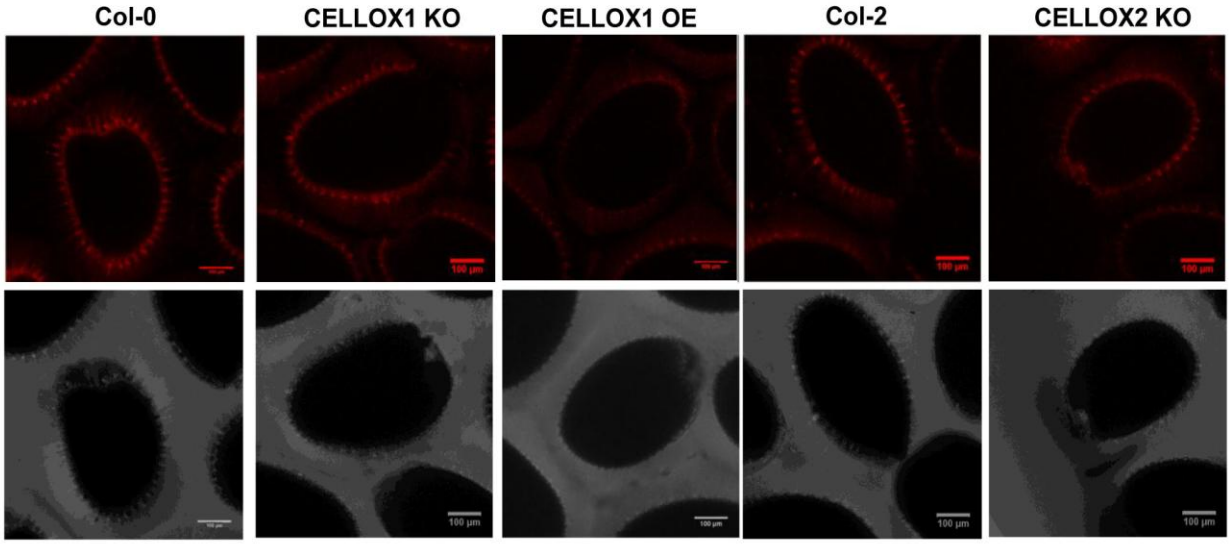

Figure II.18. Direct Red 23 staining of seeds for cellulose. Direct Red 23 or (pontamine fast scarlet 4BS) is a cellulose-specific fluorescent dye and highlights the cellulosic rays and the *columellae* in each mutant. CELLOX1 OE showed decreased DIrect Red fluorescence compared with other mutants and controls Col-0 and Col-2. Confocal images. Scale bar 100 μm.

On the other hand, hydrated seeds of CELLOX mutants and transgenic lines were labeled with the dye fluorescein isothiocyanate (FITC), capable of staining the dextran molecules (70 kDa). FITC surrounds each seed without the capacity to physically go through the mucilage adherent layer and the staining excludes partially the cellulose rays too (Voiniciuc, Schmidt, et al., 2015; Willats et al., 2001). This analysis was performed to study the porosity and the density of polysaccharides of the mucilage adherent layers. Images obtained at confocal microscope revealed a less dense mucilage layer in both the knockout mutants of CELLOX1 and CELLOX2. It was indeed possible to observe that the FITC penetrates through the mucilage, among the cellulose rays, reaching the most inner part of the seed coat surface. On

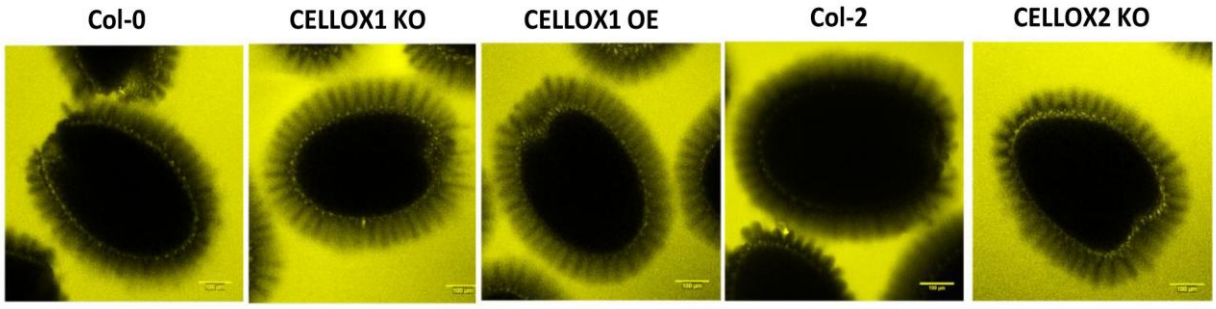

Figure II.19. Dextran molecules (70 kDa) labeled with fluorescein isothiocyanate (FITC) surrounding each mutant seed. FITC staining is used to examine mucilage porosity (Willats et al., 2001). Dextran 70 kDa does not normally penetrates in the mucilage adherent layer and is partially excluded from cellulose thin rays (Voiciniuc et al., 2015). As a consequence, it allows to observe how dense the mucilage in the adherent polysaccharides is. FITC dextran molecules are completely excluded from thin rays and from adherent layer of Col-0 and Col-2, indicating a dense layer, while they penetrated partially though mucilage of CELLOX1 OE, and mostly of CELLOX1 KO and CELLOX2 KO mutants. Scale bar 100 μm. Confocal images.

the contrary, the polysaccharide layer of controls Col-0 and Col-2 was denser and more compact compared to the KO mutants. CELLOX1 OE plants showed a slightly, but denser layer too (Figure II.19.). This could indirectly indicate defects in adherent mucilage consistency of the KO mutants.

The alteration of the structure of the coat observed upon microscopy analyses prompted to investigate the composition of the seed mucilage and coat. The total mucilage layer and Alcohol Insoluble Solids (AIS) fraction obtained from de-mucilaged seeds were analyzed by high-performance anion exchange chromatography (HPAEC) after acid hydrolysis to evaluate the monosaccharide composition in CELLOX1 and CELLOX2 mutants and transgenic plants compared to the corresponding wild-type plants. The total amount of sugars did not change significatively among the genotypes and respective controls in fractions of both total mucilage and AIS after treatment with TFA and/or H_2SO_4 (Figure II.20A.).

Total mucilage was subjected to TFA hydrolysis and analyzed. In the wild-type Col-0 and Col-2, Rha and GalA were the most represented monosaccharides, in agreement with the previously reported high RG-I presence in mucilage, with a small amount of Ara (Macquet et al., 2007). Traces of gluconic acid (OxGlc) were also detected in all samples (Figure II.20B.). No significant differences were observed in monosaccharide composition among the genotypes (Figure II.20B.).

The insoluble residue obtained from the TFA hydrolysis of the total mucilage was hydrolyzed with H_2SO_4 to evaluate the amount of cellulosic material. Also in this case, no differences between the genotypes were observed.

AIS fractions from de-mucilaged seeds were first subjected to TFA hydrolysis,

A

	Total sugars		
	TFA-hydrolyzed mucilage (nmol/ mg seed)	TFA - hydrolized AIS (nmol/ mg AIS)	H_2SO_4 - hydrolized AIS (nmol/ mg AIS)
Col-0	27.89 ± 1.18	322.08 ± 103	551.23 ± 72.35
CELLOX1 KO	36.97 ± 10.31	344.92 ± 47.65	508.50 ± 160.98
CELLOX1 OE	30.19 ± 0.75	509.01 ± 53.77	583.61 ± 103.96
Col-2	32.67 ± 9.37	245.05 ± 26.88	448.02 ± 1.60
CELLOX2 KO	30.98 ± 5.55	211.49 ± 2.05	545.29 ± 180.1

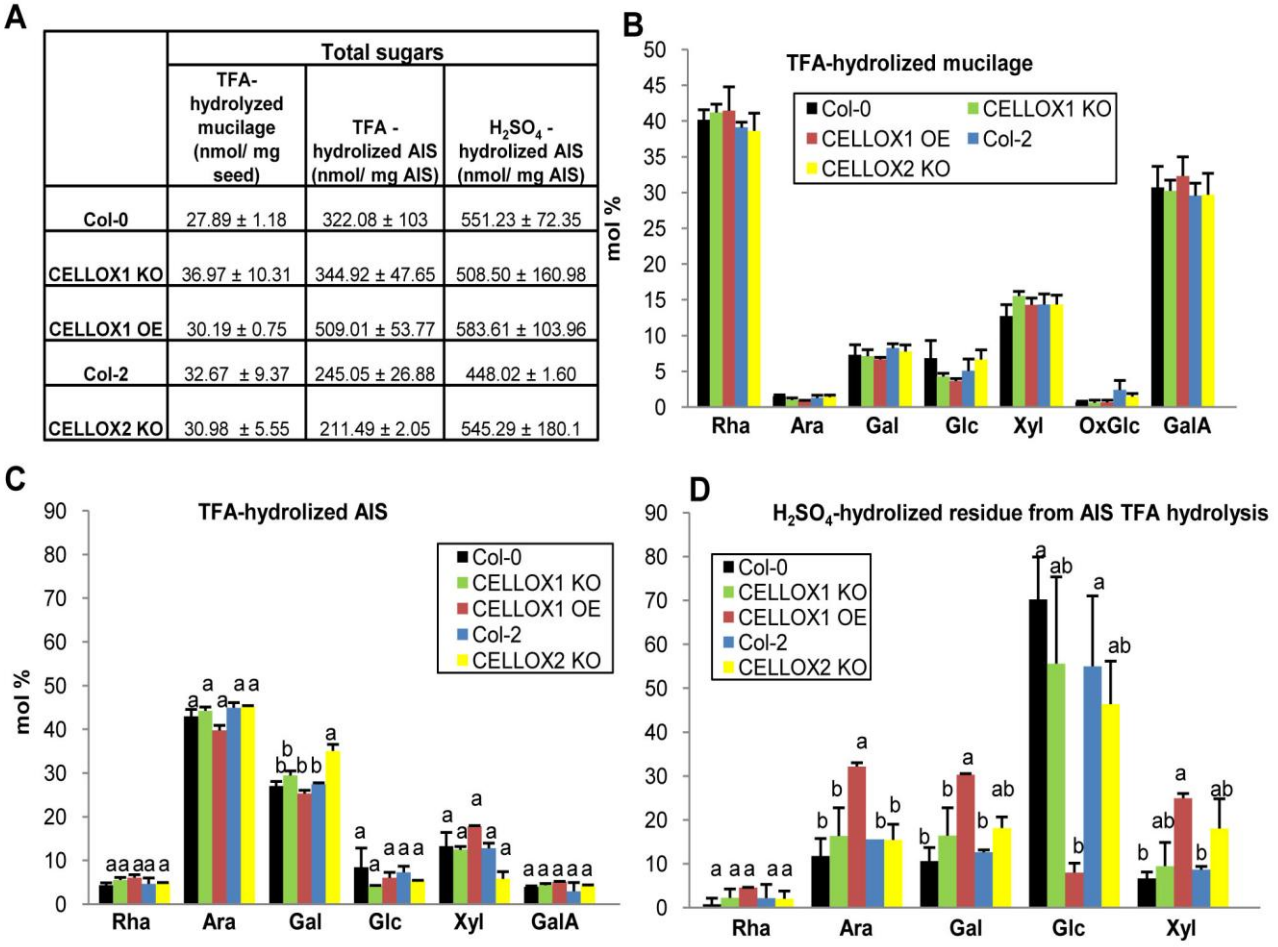

Figure II.20. Monosaccharide composition of total mucilage extracts and AIS fractions from de-mucilaged seeds. Total mucilage extracts were subjected to TFA hydrolysis. The AIS fraction obtained from demucilaged seed was first hydrolyzed with TFA and subsequently the residue was hydrolyzed with H_2SO_4. A) Total sugars of TFA-hydrolized mucilage (nmol/mg seed) and of TFA/H_2SO_4–hydrolyzed AIS (nmol/mg AIS). Values are means ± SD of at least two replicates per genotype. B) Relative monosaccharide composition (mol %) of TFA–hydrolyzed mucilage. C) Relative monosaccharide composition (mol %) of TFA-hydrolyzed AIS from de-mucilaged seeds. D) Relative monosaccharide composition (mol %) of the AIS residue of TFA hydrolysis in turn hydrolyzed with H_2SO_4. B, C, D) Data show means + SD of at least two replicates for genotype. Col-0 and Col-2 are used as controls of CELLOX1 and CELLOX2 mutants respectively. Sugars are indicated as Rhamnose (Rha), Arabinose (Ara), Galactose (Gal), Glucose (Glc), Xylose (Xyl), Galacturonic Acid (GalA), Glucuronic Acid (GlcA), Gluconic Acid (OxGlc). Different letters indicate statistically significant differences according to ANOVA followed by post-hocTukey's HSD test ($P < 0.05$).

followed by hydrolysis with H_2SO_4 of the TFA residue (Macquet et al., 2007; Seaman et al., 1996). TFA-hydrolyzed monosaccharides showed a similar profile in all the genotypes analyzed (Figure II.20C.). This fraction was characterized by a high amount of Ara (molar ratio of about 45 %) and Gal (about 27 %). With a molar ratio of about 35% Gal content was higher in the CELLOX2 KO mutant compared to the other genotypes (Figure II.20C.). Other sugars evenly detected in smaller quantity were Rha (~ 4.6 %), Glc (~ 5.8 %), Xyl (~ 13 %), and GalA (~ 3.6 %).

The fractions hydrolyzed with H_2SO_4 showed a very high amount of Glc (~56 %), with lower amounts of Ara (~14 %), Gal (~14 %), Xyl (~12 %) also present, as well as traces of Rha (Figure II.20D.). Interestingly, differences were observed in the fraction obtained from CELLOX1 OE plants compared to the control Col-0 and to the other genotypes (Figure II.20D.). In particular, there was a strong reduction of the Glc amount with a molar ratio of about 10% (a 85% reduction), which made this sugar the least represented one, together with Rha. Conversely, significantly higher levels of Ara, Gal and Xyl were observed in this mutant, with Ara and Gal representing the most abundant monosaccharides in this fraction, followed by Xyl (Figure II.20D.).

In order to understand whether defects in mucilage observed were due to a direct activity of the enzyme on the extruded mucilage or on the cellulose of the seed coat, or they were somehow a consequence of a previous process, total mucilage and Alcohol Insoluble solids (AIS) were extracted from Col-0 seeds and tested as substrate of both FHS-CELLOX2 and FHS-CELLOX1. The substrate cellotetraose (CD 4) was used as technical positive control. Hydrogen peroxide production was not revealed in any sample where mucilage or AIS was added in the reaction mixture. Indeed, the optic density (OD) was quite similar to the reaction mixture without substrates. While the OD was high in reaction mix with CD 4 confirming that the enzyme was active. This may suggest that CELLOX2, as well as CELLOX1 are involved in modifications that take place before the seed hydration and mucilage extrusion take place. Moreover, as seen before, these enzymes are predicted to be expressed during an intermediate phase of seed development, and not at the level of mature seed.

DISCUSSION

A new member of the BBE-like family, CELLOX2 (BBE23/At5g44360), has been identified and characterized in this work. CELLOX2 is similar by aminoacidic sequence to CELLOX1 (65.21 % similarity), and the two proteins share a type IV active site (Daniel et al., 2016). CELLOX2 is predicted to be localized in the apoplast and experimental evidence supports this prediction. Studies of biochemical characterization revealed that, similarly to CELLOX1, CELLOX2 is an oxidase of cellodextrins. Notably, a new insight from this work is that both CELLOX1 and CELLOX2 are able to oxidize also the mixed-linked β-1→3/ β-1→4-glucans (MLGs), newly identified as molecular patterns capable of activating the plant immune responses (Rebaque et al., 2021). MLGs are present in microbial cell walls, like fungi, oomycetes and bacteria (Fontaine et al., 2000; Lee & Hollingsworth, 1997; Pettolino et al., 2009; Pérez-Mendoza et al., 2015; Samar et al., 2015) and therefore may be considered as MAMPs. However, they are also present as component of hemicellulose (Burton & Fincher, 2009) in the cell wall of monocotyledons like plants from *Poaceae* family, or other species like *Equisetum*, bryophytes and *algae* (Fry et al., 2008; Popper & Fry, 2003; Salmeán et al., 2017; Sørensen et al., 2008; Trethewey et al., 2005). It is interesting that the type IV active site, characteristic of CELLOX1 and CELLOX2, is found in monocotyledons (Messenlehner et al., 2021), suggesting a sort of evolutionarily more ancestral derivation of these oxidases within the BBE-family. Notably, the fact that CELLOX substrates are recognized as cell wall-derived DAMPs/MAMPs leads to the hypothesis that at least part of the BBE-l family members are specialized in the regulation of the homeostasis of these signals.

As revealed by the enzymatic assays, both the enzymes CELLOX1 and CELLOX2 show a higher activity at basic pH condition. It is known that disease resistance lead in plant to an alkalinization of the apoplastic pH (Felle et al., 2005). Thus, at basic pH, the electrostatic potential surface of these molecules could become more negative at the level of the active site, possibly facilitating the interaction with the respective substrate.

CELLOX2 and CELLOX1 are expressed differently in tissues. In particular, CELLOX2 is not expressed at all in seedlings or in the adult plant and its transcripts are found only in seed coat, during the intermediate stages of seed development. CELLOX1 is also expressed in the seed coat, at the stage that immediately follows that in which CELLOX2 is expressed and when CELLOX2 already shows a decreased expression, suggesting a sort of relay regulation. The seed coat, also known as testa, surrounds the embryo throughout its development and dormancy, providing protection from

mechanical damage and pathogens, regulating germination, dispersal and seed viability in hostile environments (Ben-Tov et al., 2015a; Haughn & Chaudhury, 2005; Huang et al., 2008; Yang et al., 2011). Other BBE- like family members do not appear to be expressed in the seed coat; thus, CELLOX2 and CELLOX1 may play a unique role in this tissue as BBE-like oxidases.

At present, it is not known whether a homeostatic control of defense signaling and protection itself exists during seed development. However, some mechanisms of defense in seed have been showed, such as the presence of chemical defense metabolites, like hydroxyphenols, hydrogen cyanide released upon hydratation, proteins such as beta-1,3 glucanases, anti-fungal proteins against fungi and Gram-positive bacteria or hydrolases such as nucleases, proteases and chitinases(De Bolle et al., 1995; Hendry et al., 1994; Raviv et al., 2017; Rose et al., 2006; Terras et al., 1995). This evidence may provide a frame for further hypotheses about the role of these oxidases in seeds in terms of defense.

On the other hand, our results suggest a role of CELLOXs in seed development. Other enzymes involved in seed polysaccharides modifications such as those encoded by *RUBY*, *CESA5*, *IRX1-1* and *FEI2* (Griffiths et al., 2015; Harpaz-Saad et al., 2011; Mendu et al., 2011; Sullivan et al., 2011; Šola et al., 2019) have been shown to be involved in seed development.

Phenotypic analysis performed in the single knockout mutants obtained, CELLOX1 KO and CELLOX2 KO, and in the over-expressing CELLOX1 (CELLOX1 OE), has highlighted differences mainly in CELLOX1 OE transgenic plants compared to wild type. Indeed, CELLOX1 OE shows a larger seed area after hydration and a more detailed analysis of seed surface reveals a *columella* with a reduced size. Despite the larger size of the seed, a lower content of cellulose was observed by Direct Red 23 staining, which revealed a lower intensity in the CELLOX1 OE seeds. This observation is consistent with the results of monosaccharide composition analysis of the de-mucilaged AIS of these plants, upon sequential TFA/H_2SO_4- hydrolysis. Indeed, CELLOX1 OE shows a significant sharp reduction in the amount of cellulose-derived glucose compared to the wild type and the other genotypes. Conversely, hemicellulose–derived sugars like arabinose, galactose and xylose increase in this mutant, likely as a compensative effect for the cellulose decrease. Notably, the total amount of sugars does not change, but only the composition in monosaccharides. These data are consistent with CELLOXs being cellodextrin oxidases and suggest that their activity influences the structure of the seed coat.

Modification in cellulose and hemicelluloses composition could also influences mucilage density and adhesion to seed coat (Voiniciuc, Schmidt, et al., 2015). Mucilage has several roles like seed hydratation for the germination, seed dispersal, protection and interaction with soil microbiome and much is still to be discovered (Ben-Tov et al., 2015b; Engelbrecht & García-Fayos, 2012; Huang et al., 2008; Penfield et al., 2001; Raviv et al., 2017; Saez-Aguayo et al., 2014; Western, 2012; Yang et al., 2013). CELLOX1 OE plants do not show any defect in germination rate or in mucilage extrusion, so this mutation does not compromise seed viability. The only phenotypic difference observed in the mucilage is in CELLOX2 KO as a reduction, compared to the other genotypes analyzed. This result is in agreement with the CELLOX2 KO lower density of the adherent mucilage layer highlighted by the FITC–dextran staining compared to the wild type. The greater porosity of mucilage layer is found also in CELLOX1 KO mutant. However, the monosaccharide composition of both CELLOX1 KO and CELLOX2 KO do not show significant changes, except for an increase in the amount of galactose in the TFA-hydrolyzed de-mucilaged AIS fraction. Differences in the composition may be too subtle in the single KO mutants, which may act redumdantly, and may become more evident the homozygous double CELLOX1-CELLOX2 knockout mutant, the obtation of which is in progress. Phenotype variations will be better studied in these double knockout mutant. Overexpressing CELLOX2 are also being generated. It will be possible to assess whether, given that CELLOX1 and CELLOX2 have a similar enzymatic behavior, the overexpression of CELLOX2 leads to changes similar to those observed in CELLOX1 OE plants.

Taken together, my results show that CELLOX1 and CELLOX2 are important in defense signaling modulation, as DAMP/MAMP oxidases, with a possible involvement in seed development. Being the seed used as a model to study the cell wall (Arsovski et al., 2010; Dean et al., 2007; Haughn & Western, 2012), it is conceivable that CELLOXs can somehow influence cell walls polysaccharides composition. Since cell walls are important sources of food, fiber and biofuel, the chance to modulate the biotic stress resistance and sugars distribution without altering the viability of the seed or the plant growth would be a very interesting and useful tool for further studies and applications.

MATERIALS AND METHODS

Plants

A. thaliana plants, Col-0 and Col-2 ecotypes, were grown on MS/2 medium under long day conditions 16 h / 8 h at 22 °C in growth chamber or in soil under long day conditions (16 h light) in a greenhouse at 22 °C.

N. tabacum used for the transient expression of GFP- and RFP- tagged CELLOX2 *(At5g44360.1/BBE23)* for confocal analysis and total proteins extraction.

Yeast

Pichia pastoris X-33 was utilized for *CELLOX2* (*At5g44360.1)* heterologous expression. *Pichia* was grown in Yeast Extract Peptone Dextrose Medium [YPD; 1% yeast extract, 2% peptone, 2% dextrose (D-glucose)]. The transformed *Pichia* was grown in YPD containing 100 μg mL^{-1} Zeocin™ and in solid YPD (YPDS) containing 2 % agar and zeocin, according to instructions of the manufacturers of the *Pichia* Expression kit (Invitrogen). *Pichia* was grown at 28 °C in growth chamber for 48 h.

Fungi

Botrytis cinerea was utilized for the infection assay on *Arabidopsis* leaves. The fungus was grown on MEP medium containing 2 % malt extract, 1 % peptone, 1.5 % micro agar., at 25 °C.

Bacteria

E. coli electrocompetent strains One Shot Top10 (ThermoFisher) were transformed to amplify the constructs. *E. coli* was grown at 37 °C for 24 h in Low Salt medium (LSLB) containing 1 % tryptone, 0.5 %NaCl, 0.5 % Yeast Extract (2 % agar), and in Luria-Bertani (LB) medium with 1 % tryptone, 0.5 % yeast extract, 1 % NaCl (1.5 % agar).

A. tumefaciens strains GV3101 used for the agroinfiltration for the *CELLOX2* (*At5g44360.1)* transient plant transformation. The bacteria were grown at 28 °C for 48 h in LB medium.

Transgenic plants

T-DNA insertional lines were obtained from the European Arabidopsis Stock Center (NASC). For the *At4g20860* (*CELLOX1)* were genotyped the lines WiscDsLox504A05 (NASC ID N859101), SALK_131268 (NASC ID N631268), respectively *cellox1-1* and

*cellox1-2 (*CELLOX1 KO*)*. For the *At5g44360 (CELLOX2*) was genotyped the line WiscDsLox472A5 (NASC ID N857391), named *CELLOX2 KO*.
Overexpressing lines of *CELLOX1* (Locci et al., 2019) and *OGOX1* (Benedetti et al., 2018), previously obtained in the laboratory, were also used.

Constructs and transgenic plant

The expression vector utilized for the heterologous expression of *CELLOX2 (At5g44360.1/BBE23)* in X33 *Pichia* was pGAPZalfa A (Invitrogen). The vector possesses the α-factor mating signal sequence for secretion of the protein. This vector uses the GAP promoter to constitutively express recombinant proteins in *Pichia pastoris*. After *Pichia* transformation by electroporation, proteins can be secreted because of the presence I signal peptide of the α-factor, and they are expressed as fusions to a C-terminal peptide containing the myc epitope for detection and a polyhistidine tag for purification. Selection of these vectors is based on the dominant selectable marker, Zeocin™, which is bifunctional in both *Pichia* and *E. coli*.
In collaboration with Dr. Manuel Benedetti (University of L'Aquila, Italy) H-BBE23 and FHS-BBE23 constructs were obtained, provided by SUMOstar system (LifeSensors Inc. Malvern) for the heterologous expression of *At5g44360.1/BBE23.*

Gateway system vectors were used for *Agro* and plant transformation with the construct35S::*CELLOX2*GFP/RFP. In particular the pDONR™221 (Invitrogen) Kanamycin and Zeocin resistant, and the pK7FWG2 (V141) for the eGFP C-Term tag and the pB7RWG2 (V215) for the mRFPC-Term tag, kanamycin resistant (Karimi et al., 2002). The insert CELLOX2 was isolated and amplified by the genomic DNA (*CELLOX2* has not introns and the transcript is not available in seedlings) through PCR using the primers modified to contain attB sites for the insertion in the pDONR™for the BP and LR reactions by the clonase II enzyme according to the manufacturer's protocol (Gateway BP Clonase II Enzyme mix, Invitrogen).The primer also did not contain the STOP codon to permit the tag fusion. The insert was amplified using the Phusion high fidelity DNA polymerase (ThermoFisher). Primers used were:
"Cellox2DonrFw":
5'-GGGACAAGTTTGTACAAAAAAGCAGGCTTTATGAGAACACTTGAAGCTTTTG-3'
"Cellox2DonrNostopRv":
5'-GGGGACCACTTTGTACAAGAAAGCTGGGTCGACAATCAAAGGAGGAACACTTTG-3'.

The constructs obtained were all sequenced by the BioFab labs and checked. The plasmids and the insert were purified respectively using the QIA prepSpin Miniprep kit and the Promega wizard clean up kit.
For genotyping, in order to obtain the homozygous mutant line, and for the semi quantitative Q-PCR analysis, the following primers were used:
For *cellox1-1*:
LP 5′-CGTTTGATGGATGTAAATGGG-3′
RP 5′-TATTCTCGGTCCGCTTAAACC-3′.

For *CELLOX1 KO* (*cellox1-2):*
LP 5′-AGCATCAACCTCACAGACGA-3′
RP 5′-CCGAATCCTCCTCCGCTAAT-3′.

For CELLOX2 KO(*At5g44360/BBE23)* mutant:
LP 5′-CGCCTTTCATCATACTCGATC-3′
RP 5′-ATTGGTTGGATCAATCTTCCC-3′.

For the T-DNA insertion the specific left primer T-DNA p745 was used (5′-AACGTCCG-CAATGTGTTATTAAGTTGTC-3′).

Primers for ubiquitin (UBQ5) were:
LP 5′GTTAAGCTCGCTGTTCTTCAGT-3′
RP 5′-TCAAGCTTCAACTCCTCCTTTC-3′.

PCR to genotype was carried out using the KAPA Taq PCR kit (Sigma-Aldrich).

The modified pBI121 vector (Benedetti et al., 2015) was used to obtain the untagged and overexpressing35S::*CELLOX2* construct. Both the insert and the plasmid were cut with restriction enzymes BamHI and SacI.
Primer used were:
"BamHI23Fw":
5′ –CATAA**GGATCC**ATGAGAACACTTGAAGCTTTTGC-3′
"SacI23Rv":
5′ – CTAAG**GAGCTC**TTAGACAATCAAAGGAGGAACAC-3′

The following primers were designed to amplify the promoters of *CELLOX2* and *CELLOX1* promoters for insertion in the pBI121 modified vector lacking the 35S promoter and carrying the reporter gene GUS.
The restriction site of BamHI was added:

"pBBE23_LP":
5'- GCGCGC**GGATCC**TACTATGAATAAAGAATTGAAAATT -3'
"pBBE23_RP":
5' –GCGCGC**GGATCC**CTTTAGTGTTTTGCTTTTCTTG -3'
"pCELLOX_LP":
5'- CGC**GGATCC**GGTCTGTGATCTGTCAGACT -3'
"pCELLOX_RP":
5'- CGC**GGATCC**ATCTTTTTCTATTTTTGGTTTCTT -3'

Treatments

For the analysis of the expression of *CELLOX2* by semiquantitative RT-PCR (sqRT-PCR), 10-day-old Col-0 seedlings grown in liquid medium were treated 1 h with the elicitors flg22 (10 nM), elf18 (10 nM), OGs (50 μg mL^{-1}), and cellotriose (CD3; 25 μg mL^{-1}).

DNA and RNA extraction and quantification

The genomic DNA was extracted according to the Edward method modified. The Edward buffer was prepared with Edward buffer (200 mM Tris-HCl pH 7.5, 250 mM NaCl, 25 mM EDTA, 0.5 % SDS). The *Arabidopsis* leaf or seedling was put into a tube (2 mL) with a 0.5 cm diameter bead and frozen in liquid nitrogen, then 200 μl of Edward buffer was added, and the tissue was grinded by the "mixer mill" for 1 min at 24/s frequency. Once that the tissue was thawed, it was mixed by vigorously vortexing, followed by a centrifuge cycle of 16000xg for 5 min. RNAaseA (10 mg mL^{-1}) was added and vortexed. The sample was incubated at 56 °C for 20/30 min, after that spinned at 14000xg for 5 min at room temperature. 150 μl of supernatant were recovered and put into 1.5 ml tube. 150 μl of isopropanol were added to the supernatant and vortexed. The sample was left at room temperature for 10 min and for 5 min on ice, then it was centrifuged at 14000xg for 10 min at room temperature; supernatant was discarded. The pellet was washed twice with 1 mL of ethanol 70 %, incubated for 5 min at room temperature and centrifuged for 5 min at 16000xg. Ethanol was removed. The gDNA was dried for 4/5 min in the flow hood and finally redissolved in 40 μl of nuclease-free water. The DNA was quantified by gel electrophoresis run, using as standard the lambda DNA fragment.

The RNA was extracted according to the NucleoZOL protocol (Macherey-Nagel). The RNA was extracted from 10-day-old seedlings, grown in liquid MS/2, in 16 h light/8 h dark cycle in the growth chamber. The tissue samples, in a 2 mL Eppendorf with a bead in each, were frozen and homogenized by the "mixer mill" for 1 min at 24/s frequency. 500 μl of NucleoZol per 50 mg of tissues were added. Rnase-free

water (nuclease-free) was added to the lysate (200 µl per 500 µl NucleoZOL). The sample was shaken vigorously for 15 s, incubated at room temperature for 5 min and centrifuged the samples for 15 min at 12000xg at 4 °C. After this step, a semisolid pellet containing DNA, proteins and polysaccharides forms at the bottom of the tube and the RNA is still solubilized in the supernatant. Next, the supernatant (500 µl) was transferred to a tube containing 500 µl of isopropanol ant vortexed. The samples were incubated at room temperature for 10 min. The samples were centrifuged for 10 min at 12000xg at 4° C. The supernatant was removed and discarded. The washes followed for two times. In particular, 75 % ethanol (500 µl) was added and the sample was and centrifuged for 3 min at 8000xg, 4 °C; ethanol was removed from the pellet. Sample was centrifuged again at 8000xg at 4 °C for 2 min and the sample was left under the hood to permit the evaporation of the remnant ethanol. Finally, the pellet was dissolved in 40 µl of nuclease-free water.

RNA was quantified at the spectrophotometer by measuring the absorbance of a diluted RNA (1 : 250) at 260 and 280 nm with the Biorad smart spec plus spectrophotometer. The nucleic acid concentration is calculated using the Beer-Lambert law, A = ecl, which predicts a linear change in absorbance with concentration. The quality of RNA was evaluated by 1.5 % (w/v) agarose gel electrophoresis carried out at 120 V for 15 min. 5 µl of RNA Loading Buffer was added to 1 µg of RNA, and water DNAse-free was added up to a final volume of 10 µl, then the sample was heated at 70 °C for 5 minutes. The gel image was detected with Gel Doc™ XR+ System.

Expression analysis by RT-PCR and quantitative RT-PCR

The RNA extracted was treated with DNAse digestion, performed in a 10 µl reaction mix containing 2 µg of RNA, 1 µl of rQ1 DNase 10X Reaction Buffer (PROMEGA), 1 µl of rQ1 RNase-free DNase (PROMEGA) and nuclease free water up to 10 µl. Samples were incubated at 37 °C for 30 min to allow the digestion reaction then 1 µl of rQ1 DNase Stop Solution was added and the samples were incubated at 70 °C for 10 min to inactivate the DNase. For qRT-PCR, cDNA was synthesized with anchored-oligo (dT)15 primers and random primers (PROMEGA). In detail, 10 µl of reaction mix contained 2µl of ImProm.II™ 5X Reaction Buffer (PROMEGA), 1µl of MgCl2 (25 mM), 0.625 µl of dNTPs (10 mM), 0.25 µl of random primers, 0.25 µl of oligo(dT)s, 0.5 µl of ImProm.II™ Reverse Transcriptase (PROMEGA), the 2 µg of RNA previously treated with the DNAse, and H_2O up to final volume. Samples were incubated 10 min at 25 °C to allow primers annealing, then at 42 °C for 1 h in order to allow the extension reaction and 15 min at 70 °C to inactivate the Reverse

Transcriptase. Real-time quantitative PCR analysis was performed using a CFX96 Real-Time System (BIO-RAD). cDNA, corresponding to 50 ng of total RNA, was amplified in a 10 μL reaction mix containing 1 × Go Taq qPCR Master Mix (PROMEGA) and 0.5 μM of each primer. Expression levels of each gene were evaluated relatively to UBQ5.

Seed sterilization and plant growth

Seeds were treated with 1 mL of sterilization solution (0.01 % SDS, 1.6 % NaClO, H_20 up to final volume) for 7 min, with shacking. Seeds were washed 4 times in 1 mL of sterile water by centrifuge cycles at 6000g for 1 min. For stratification, seeds were left in 400 μl of sterile water for 4 days at 4 °C in dark conditions. All steps were carried out under the hood. Seeds were sown on plates containing solid MS/2 medium (Murashige Skoog Medium basal salt; 2.15 g L^{-1}, 1 % sucrose, 0.8 % plant agar, pH 5.5 adjusted with KOH), and grown at 22 °C and 70 % relative humidity under a 16 h light/ 8 h dark cycle. Adult plants were transferred on soil at 22 °C and 70 % relative humidity under a 16 h light/8 h dark cycle (approximately 120 μmol m^{-2} s^{-1}) in a growth chamber or in the greenhouse.

Total protein extraction and quantification

The extraction buffer was prepared according to the tissue characteristics, in this case *N. tabacum* leaves: 50 mM TRIS HCl pH 6.8, 0.7 M NaCl, protease inhibitor cocktail (1 : 1000) and H_20 up to final volume. Samples were ground by mortar and pestle (always using liquid N_2) and 1 mL of extraction buffer was added for 1 g of sample. Also the protease inhibitors (1 μl each) were added, then the samples were kept under shaking at 4 °C for 30 min, and centrifuged at 1000xg for 10 min. The supernatant was recovered for each sample, and centrifuged at 1000xg for 10 min. The supernatant was recovered again. The total proteins extracted were quantified by Bradford Assay using the BioRad solution (Bradford, 1976). BSA 1 mg mL^{-1} was prepared for the standard curve.

SDS-PAGE, Western Blot

For the SDS-PAGE, the running gel 8 % in 10 mL of final volume was prepared: H_2O up to volume, 30 % acrylamide mix 2.7 mL, 1.5 M Tris (pH 8.8, BIORAD) 2.5 mL, 10 % SDS 0.1 mL , 10 % ammonium persulfate (APS) 0.1 mL, and TEMED 0.006 mL. Stacking gel 5 % in a final volume of 2 mL: H_20 up to volume, 30 % acrylamide mix

0.33 mL, 1 M Tris (pH 6.8, BIORAD) 0.25 mL, 10 % SDS 0.02 mL, 10 % APS 0.02 mL, TEMED 0.002 mL. Spacers of 0.75 mm were used (volume around 20 µl). The loading buffer containing β-mercaptoethanol, bromophenol blue, and SDS 10 %, was added to the proteins to a final volume of 20 µl, and then boiled at 100 °C for 5 min to denature the proteins. The samples ran at 20 mA, constant Amperage.
The western blot was performed according to the BIORAD T.B TURBO KIT. The transfer of the proteins on the nitrocellulose membrane was performed using the Trans-Blot® Turbo™ Transfer System. The nitrocellulose membrane was left with the blocking solution (BSA 5 %, tween 0.2 %, TBS 1 X, H2O up to volume) for 1 h shacking. Then 3 washing cycles (20 min for each) were done with the solution TBS 1 X and tween 0.2 %. Discarded the washing solution, the first antibody [anti-myc (SANTA CRUZ) for the *Pichia CELLOX2 (*At5g44360) secretion system and anti-GFP (SANTA CRUZ) for the CELLOX2 (At5g44360) derived from the agroinfiltrated *N. tabacum*] was added and left overnight shacking. Washed 3 times for 20 min each with the washing solution. Put the second antibody (1 : 6000, IgG Alkaline phosphatase antibody SIGMA) with 2.5 % BSA, TBS 1 X and tween 0.2 %, left shacking for 1 h. Washed again 3 times for 20 min each with the washing solution. Finally the membrane was treated with the Clarity Western ECL Substrate (BIORAD) and the proteins detected with the Gel Doc™ XR+ System. The standard used was the Precision Plus Protein TM Dual Color Standards (BIORAD).

Acetone protein precipitation according to the Thermo scientific procedure.
Pichia medium (700 µl), where *CELLOX2 (*At5g44360/BBE23) was supposed to be secreted, was taken to precipitate the proteins. The medium was centrifuged at max speed for 5 min and the the supernatant transferred in a 2 mL Eppendorf tube. Cold acetone (pre-cooled at -20 °C) was added four times the sample volume. Vortexed and incubated for 60 min at -20 °C. Centrifuged for 10min at 15000xg x 10 min and decanted the supernatant. The pellet with the precipitated proteins was kept. Finally, the acetone was left to evaporate from the uncapped tubes at room temperature for 30 min under the hood.

Xylenol orange assay
H_2O_2 produced was measured using the xylenol orange colorimetric assay. The xylenol orange solution was prepared: 250 mM H_2SO_4, 1mM xylenolorange, 1 M sorbitol, 22.5 mM $NH_4Fe(SO_4)$ and H_20 up to volume. The assay was performed as previously described (Gay et al., 1999). Mix of reaction consisted of 50 mM Tris-HCl

pH 7.5, 50 mM NaCl, 0.3 % NaN_3, 0.4 mM each substrate, and enzymes FHS-CELLOX1 and FHS-BBE23 incubated for 1 h at 37 °C. Enzymes were derived from BMM (Buffered Minimal Methanol) growth medium of transformed *Pichia*, filtered through a 0.2-μm filter, dialyzed and concentrated by vivaspin 10 kDa MWCO cut off, to a final concentration of 10 – 20 X. A standard curve was built with the xylenol orange solution and different and known H_2O_2 concentrations. After the incubation, xylenol orange solution was added to each sample and left to react for 15min in dark conditions. Finally the OD560 of all the samples was measured at the spectrophotometer.

Different cell-wall carbohydrates were used as substrates, such as cellodextrins with a polymerization degree between 2 and 6 (ELYCITIL S.A.; France), OGs, lactose (Sigma–Aldrich; A1206000), maltose (Sigma–Aldrich; M5885), galactose (Sigma–Aldrich; G0750), glucose (Sigma–Aldrich; G8270), xylose (Sigma–Aldrich; X3877), chitotriose (O-CHI3; Megazyme), chitohexaose (O-CHI6; Megazyme), O-BGTETB (MLG443; Megazyme): 3^1-β-D-cellotriosyl-glucose, O-BGTETC (MLG434 + 344; Megazyme): mixture of 3^2-β-D-cellobiosyl-cellobiose and 3^3-β-D-glucosyl-cellotriose, O-BGTRIA (MLG34; Megazyme): 3^2-β-D-glucosyl-cellobiose, O-BGTRIB (MLG43; Megazyme): 3^1-β-D-cellobiosyl-glucose, N-acetyl-muramic acid (NAM; Carbosynth, MA05012).

Xylenol orange assay was also used for determine the pH optimum of enzymatic relative activity (%) of FHS-CELLOX1 and FHS-CELLOX2. Different pH values were tested in a range of pH 5 to pH 12, using [0.4 mM] cellobiose as substrate.

Agroinfiltration

The infiltration buffer [MES 50 mM, pH 5.6 (pH adjusted with KOH), 2 mM v, 200 mM acetosyringone, 0.5 % glucose] was used to resuspend the transformed *A. tumefaciens* for inoculation. OD at 600 nm was measured to have a final value of 0.1 and 0.2 for each sample for infiltration of *N. tabacum* leaves using needless a syringe. The infiltrated leaves were left for 48 h in the greenhouse before confocal microscope visualization, using a Zeiss LSM 780 microscope.

Floral dip

A. tumefaciens colonies transformed with the construct of interest were grown in LB broth media with antibiotics for selection of the transformed strains, overnight at 28 °C, shaking at 210 rpm. The next day the starter culture was diluted in a larger

volume of LB with antibiotics for selection, and it was grown overnight at 28 °C at 160 rpm. The OD at 600 nm of each culture was checked, for dilution to OD at 600 nm in the range of 0.8 and 1.00. The Floral Dip solution contained 5 % sucrose, 10 mM $MgCl_2$, 100 μM acetosyringone. The *Agrobacterium* culture (200 mL) was centrifuges at 8000 rpm for 10 min at room temperature. The pellet was resuspended in the floral dip solution. The suspension was incubated for 2 hours and 0.01 %. Silwet was added. Arabidopsis plants 4 weeks after germination were used. All the opened flowers and siliques were cut. The plants were checked for the presence of unopened flower buds and dipped in the suspension for 1 min. The dipped plants were wrapped with a plastic to maintain an high relative humidity and left in the grow chamber for 2-3 days before removing the plastic.

Ruthenium Red Staining and seed and mucilage areas measurement

Mucilage area was measured according to Wang et al (2019), with some modifications. About 50 seeds from batches grown simultaneously and under same conditions were used to quantify the seeds and adherent mucilage areas. Seeds were placed in a clean (but not necessarily sterile) microfuge tube. Distilled H_2O (500 μl) was added for seeds imbibition for the seeds to hydrate and release the mucilage from the epidermal seed coat, and the tube was shaken (~ 300 rpm) on an orbital shaker for 40′ at room temperature to remove the non-adherent layer. Supernatant was carefully removed with a pipet and replaced with 500 μl of 0.01 % ruthenium red solution for 5′. The ruthenium red solution was removed and replaced with dH_2O for washing before the observation and the acquisition of images at optical microscope (4 X) with a bright-field.

The area (mm^2) of the whole seed and adherent mucilage was measured using the software ImageJ (Schneider et al., 2012) and data were normalized on the average Col-0 seed area. The experiment was repeated three times.

Infection assay of *Botrytis cinerea* on *Arabidopsis* leaves

B. cinerea was grown at 25 °C for 10-15 days in MEP media. Conidia were harvested with 10-20 mL of sterile water using a glass rod to detach spores on the Petri plate and the water with the spores have been slid through a filter miracloth to remove the mycelium debris. After centrifugation for 8 min at 5000 rpm, spores were recovered and resuspended in 3-5 mL of sterile PDB. The spores were counted with a hemocytometer, and diluted to 5 X 10^5 spores ml^{-1} and incubated at RT for 2 - 4 hours

to allow germination. 4 – week - old Arabidopsis plants were used for infection. Spores were inoculated by placing a drop of spore suspension in PDB on each half of the upper side of each leaf. Plants were wrapped to avoid contamination and desiccation and left in the grow chamber. Infected leaves were detached two days after and pictures were taken.

Quantification and statistical analysis

Variation in gene expression was analyzed through quantitative real-time PCR analysis using the Pfaffl method (Pfaffl, 2001). The statistical significance of the difference in gene expression between specific samples is analyzed through Student's t test. Densitometry analysis for the quantification of g DNA, amplified insert and vectors was performed by the software ImageJ (https://imagej.nih.gov/ij/). The germination rate was obtained considering the germinated seeds (seeds which showed the radicle) out of the sum of germinated and not germinated ones belonging to the same plate.

Statistical analyses for ANOVA followed by post-hocTukey's HSD test (95% family-wise confidence level, alpha level 0.05) and for the compact letter display (cld) were performed usingthe software R 3.6.3 (https://www.r-project.org/) and Rstudio, PBC, Boston, MA (http://www.rstudio.com/). Unpaired Student's t test was calculated on GraphPad (https://www.graphpad.com/quickcalcs/ttest1.cfm).

Extraction of total mucilage

Total mucilage extraction was performed as previously described (Voiniciuc, Schmidt, et al., 2015) with some modifications. Seeds (25 mg for each genotype) were weighted and 1.4 mL of H_2O was added. Seeds were shaken using a mixer miller at 30 Hz for 15 ' and for other 15 ' after turning the samples 180 ° to remove the total mucilage. Seeds were left to settle for 1-2 '. 1 mL of mucilage-containing supernatant was removed from each sample and transferred to a clean tube. Samples were dried under a stream of N_2 gas at 60 °C.

Alcohol Insoluble solids (AIS) extraction from mature whole seeds

Extraction was performed according to (Dean et al., 2019). The same seeds from which total mucilage was extracted were used (originally 25 mg), and 1-mm zirconia

beads were added to each tube. Seeds were homogenized by mixer mill 30 Hz for 20'', repeated for two times. One mL of 70 % (v/v) EtOH was added, samples were vortexed and incubated at 65 °C in a heat block for 10'. Samples were vortexed for 10', centrifuged at 16000xg for 15' and the supernatant was removed. The pellet was washed with 1 mL of 70 % (v/v) EtOH, 80 % (v/v) MeOH, 100 % (v/v) MeOH for two times, and then with 100 % (v/v) acetone for two times. Each washing step consisted of 10' vortex and centrifuge 16000xg for 15'. Pellet of each sample was resuspended in a small amount of 100 % acetone and transferred to a new tube leaving the beads behind. Pellet was dried under fume hood.

The AIS was destarched in a buffer containing 100 mM KH_2PO_4, 5 mM NaCl, 0.02 % (w/v) NaN_3, pH 7. Samples were heated at 70 °C for 10'. Alpha- amylase Type I-A (Sigma A-4268; 5 U/ mg AIS) was addes in the pre- warmed AIS, and the samples were left to incubate at 37 °C for 24 h in a rotary shaker (Zablackis et al., 1995). After centrifugation at 25000xg for 20', the supernatant was removed, and the pellet was washed with ultrapure H_2O and 80 % acetone. Each wash consisted of vortexing and centrifuging at 25000xg for 5'. Supernatant of each genotype was discarded and the pellet was dried under a stream of N_2 gas at 60 °C. The resulting AIS was weighted.

Hydrolysis and Determination of Monosaccharide Composition by HPAEC

After total mucilage and AIS extraction, 5 mg mL^{-1} D-erythritol was added as an internal standard in all the samples (Dean et al., 2019). Neutral sugar standards such as fucose (Sigma–Aldrich, F8150), arabinose (Sigma–Aldrich, A3131), rhamnose (Sigma–Aldrich, W373011), galactose Sigma–Aldrich, G0750), glucose (Sigma–Aldrich, G8270), mannose (Sigma–Aldrich, M6020), and xylose (Sigma–Aldrich, X3877) and acid sugar standards, galacturonic acid (Sigma–Aldrich, 48280), glucuronic acid (Sigma–Aldrich, G5269) and gluconic acid (Sigma–Aldrich, G9005) were prepared and processed in the same way of the total mucilage and AIS. Standard calibration curves were then used to quantify monosaccharides amounts.

A saponification step was performed for the demethylation of pectin before hydrolysis. NaOH (1 M) was added and samples incubated for 1 h, RT. Then, 1 M HCl was added, and samples were centrifuged for 5'. Supernatant was removed. The pellet was dried and subjected to hydrolysis with trifluoroacetic acid (TFA). Samples were treated with 2 M TFA, incubated for 90' at 121 °C, washed with isopropanol and dried with a stream of N_2 gas at 40 °C. The hydrolysate was dissolved in 200 µl

of bidistilled H_2O, vortexed and centrifuged 5' at 14000xg. The supernatants were transferred to new tubes for HPAEC-PAD analysis.

The residual pellet was hydrolyzed with 72 % (v/v) sulfuric acid to hydrolyze cellulosic material (Dean et al., 2019; Macquet et al., 2007; Saeman et al., 1954). Samples were incubated for 2 h in ice, vortexing every 30 ' for 5–10 sec. Then, samples were diluted with water to a sulfuric acid concentration of 4 % (v/v), and left for 1 h at 121 °C. Samples were washed with isopropanol and dried. Finally, 200 µl of bidistilled H_2O was added and samples were centrifuged at 16000xg for 1' and the supernatant was collected and transferred to new tubes.

All samples were filtered through cellulose acetate membrane (pore size 0.22 µm) Corning® Costar® Spin-X® centrifuge tube filters before HPAEC-PAD analysis. AIS samples were diluted 5 X.

Samples were analyzed by high-performance anion-exchange chromatography with pulsed amperometric detection (HPAEC-PAD) using a 3 × 150 mm anionic exchange column Carbopac PA20 with guard column (Dionex Thermo Fischer) mounted on a ICS3000 (Dionex Thermo Fischer) HPLC. Before injection of each sample, the column was washed with 200 mM NaOH for 5 min, then equilibrated with 6 mM NaOH for 10 min. Separation was obtained at a flow-rate of 0.4 mL/min applying an isocratic elution with 6 mM NaOH for 20 min then a linear gradient from 6 mM NaOH to 800 mM NaOH for 10 min. Monosaccharides were detected by using a pulsed gold amperometric detector set on waveform A, according to the manufacturer's instructions. Peaks were identified and quantified by comparison with the standard mixture.

Sugars from mucilage were normalized to the mass of seed extracted, and sugars from whole-seed AIS were normalized to the mass of AIS and to the internal standard.

Direct Red 23 and FITC dextran staining

Seed cellulose was stained with Direct Red 23 dye (also known as Pontamine Fast Scarlet 4BS; Sigma-Aldrich, 212490-50G) (Anderson et al., 2010; Mendu et al., 2011; Voiniciuc, Schmidt, et al., 2015). Approximately 50 seeds for each genotype were imbibited in ultrapure H_2O and shaked at ~100 rpm for 15'. H_2O was removed and

0.025 % (w/v) Direct Red 23 in 50 mM NaCl solution was added to seeds, and left for 60' shaking at ~ 100 rpm, under dark condition. Staining solution was removed and seeds were washed with ultrapure H_2O. Seeds were imagined using a confocal microscope Zeiss LSM 780 (552-nm excitation and 600- to 650-nm emission). For FITC – dextran staining (Voiniciuc, Schmidt, et al., 2015), seeds were firstly imbibited in 100 mM sodium acetate pH 4.5 for 10'. Then, 1 mg mL^{-1} of FITC – dextran 70 kDa molecules (Sigma-Aldrich; 46945) was added to seeds and incubated for 30', shaking at ~ 125 rpm under dark condition. Subsequently, seeds were directly observed at confocal microscope Zeiss LSM 780 (488-nm excitation and 502 – 542 -nm emission).

Scanning Electron Microscope (SEM)

SEM was used to examine epidermal morphology of dry seeds. Wild-type and CELLOXs mutants seeds were mounted without any preparation on aluminium stubs and observed by Scanning Electron Microscopy (FESEM Gemini 500, Zeiss) equipped whit Peltier MK3Coolstage (Zeiss) at 10 kV, 20 Pa (VP), 4 °C. The SEM observations were carried out at different magnifications (400 X, 1000 X and 3000 X). SEM imaging was carried out in collaboration with Dr. Moira Giovannoni, University of L'Aquila, Italy.

Bioinformatic analyses

Bioinformatic analyses were performed through these following software and database. For genetic and molecular data the databases The Arabidopsis Information Resource (TAIR) and Uniprot (https://www.uniprot.org/) were used.

For sequence alignment DNAMAN (https://www.lynnon.com/). For molecules modeling PDB server and the software PyMOL were used (https://www.wwpdb.org/; https://pymol.org/2/). Web server APBS-PDB2PQR (Dolinsky et al., 2004); https://server.poissonboltzmann.org/pdb2pqr) was used for prediction of electrostatic potential surfaces at different pH. Predicted signal peptide and membrane-spanning regions was studied by the tool SignaIP 4.1 (http://www.cbs.dtu.dk/services/SignalP/). For localization of transcripts was used eFP Browser (Schmid et al., 2005; Winter et al., 2007); https://bar.utoronto.ca/efp/cgi-bin/efpWeb.cgi). Differential expression analyses were performed by Genevestigator

(Hruz et al., 2008), though the *Arabidopsis* RNAseq data and Affymetrix *Arabidopsis* ATH1 Genome Array provided by the software.

Section III

Damage-Associated Molecular Patterns during plant graft formation

Summary

Plant grafting is characterized by tissue fusion and vascular reconnection and involves responses to wounding, which in part overlap with responses to pathogens. The molecular mechanisms of graft formation remain unknown. Oligogalacturonides (OGs), previously implicated in the wound response, and cellodextrins (CDs) are DAMPs (Damage-Associated Molecular Patterns) derived from the degradation of the plant cell wall. A mechanism for maintaining the homeostasis of OGs and CDs activity is represented by their oxidases, respectively OGOXs and CELLOX, belonging to the family of the Berberine-Bridge Enzyme-like (BBE-like) family. OGOX1 and CELLOX1 show a differential expression during the grafting process. I have undertaken the study of the role of OGs and CDs and their oxidases in the process of grafting, characterized by a complex cross-talk among different signals including hormones, especially auxin and cytokinin. It is known that OGs antagonize the action of auxin. In this work I found that CDs, like OGs, inhibit auxin responses. However, the expression of the auxin-regulated DR5::GUS gene shows a positive effect on the response to CDs in meristematic cells. I also show that OGs and CDs influence the grafting process, at the level of vascular tissue formation and differentiation. This research could contribute to shed a light on the unclear role of DAMPs in plant development and deepen the still unknown molecular mechanism of the graft formation, leading to a possible biotechnological optimization of the grafting process and vascular development.

INTRODUCTION

Grafting consists of cutting and joining the shoot of one plant, the scion, and the root of a different plant, the rootstock, so that they become one. Grafting induces responses to the wound itself and, when successful, tissue healing as well as fusion and vascular reconnection (Melnyk, 2017d; Melnyk & Meyerowitz, 2015).

Much is unknown about the molecular mechanisms of graft formation. At the graft junction, a pluripotent callus is formed that fills the gap, seals the two parts together and later differentiates by forming epidermal, mesophyll and vascular tissues. In grafted *Arabidopsis* hypocotyls, tissues adhere 1-2 days after grafting and the phloem connects after three days. The xylem connects after seven days (Melnyk et al., 2018).

Hormones play an important role in the process. The synthesis of auxin, which promotes vascular differentiation and reconnection, is induced, and the junction of hypocotyls is inhibited when cotyledons, which produce auxin, are cut or treated with auxin inhibitors. Cytokinins are also involved in the process. A correct balance between auxin and cytokinins induces cambium proliferation and development, and this is considered a key factor for a successful grafting. Indeed, genes associated with cell division and vascular formation as well as with auxin responsiveness are activated symmetrically in the two grafted ends (Melnyk et al., 2018). Moreover, specific genes are regulated in grafted cut sites compared to separated (non-grafted) sites; many of these graft-specific genes respond asymmetrically at the graft junction, suggesting that different events occur in the two parts that lead to a successful grafting.

At the very early stages, events occurring at the graft junction are manly related to the effects of the tissue injury that follows the cut (wounding). The vulnerability, especially to pathogens, caused by rupture of cell wall integrity due to wounding is compensated by the plant by the activation of the immune system for defense (Couto & Zipfel, 2016). Activation may in part depend on the recognition of self-molecules released upon cell and tissue damage that act as danger signals; these molecules can also be released during pathogen infection. These endogenous elicitors are indicated as damage-associated molecular patterns (DAMPs) (De Lorenzo et al., 2018; Gust et al., 2017). Like DAMPs, non-self molecules [pathogen/microbe-associated molecular patterns (PAMPs/MAMPs)] act as danger signals. Both DAMPs and MAMPs induce a similar type of immunity, indicated as Pattern-Triggered Immunity (PTI). Mechanical wounding alters almost 8% of the *Arabidopsis* transcriptome and changes show high degree of overlap with those typical of PTI (Cheong et al., 2002; Gramegna et al., 2016).

The cell wall appears to play an important role during the whole grafting process. DAMPs released from the cell wall are likely to be relevant in the early grafting process. Among DAMPs, oligogalacturonides (OGs) are released from the degradation of unmethylesterified homogalacturonan (HGA), a major component of pectin in the plant cell wall, by the action of endogenous pectic enzymes and especially polygalacturonases (PGs) induced by mechanical damage or produced by pathogens during microbial infection. The activity of OGs as DAMPs is well documented (Ferrari et al., 2013). OGs have been implicated in wound signaling (Duran-Flores & Heil, 2016; Savatin, Gramegna, et al., 2014). For example, a tomato PG has been described to be responsible for the production of OGs after wounding (Bergey et al., 1999). Another class of DAMPs that can be released upon mechanical injury is represented by cellodextrins (CDs), derived from the degradation of cellulose (Aziz et al., 2007). CDs also induce the typical immunity responses (Johnson et al., 2018b).

Because immunity is costly, developmental processes and immunity must be finely coordinated and integrated to optimize a plants interaction with its environment (Kliebenstein, 2016). Plant hormone crosstalk is essential in this coordination (Huot et al., 2014). Auxins can negatively impact plant defense by interfering with other hormone signaling pathways or with PTI (Bellincampi et al., 1993; Branca et al., 1988; Denance et al., 2013; Savatin et al., 2011). Interestingly OGs are capable of antagonizing the action of auxin (Ferrari et al., 2008). For example, OGs inhibit the IAA-induced expression of GUS driven by the synthetic promoter DR5, and the accumulation of transcripts of early genes up-regulated by IAA (Savatin et al., 2011). Elevated OGs levels reduce plant growth, suggesting that the release of OGs plays a role in the growth-defense trade-off (Benedetti et al., 2015). On the other hand, it has been shown that CDs can regulate the expression of genes involved in growth and root development, but it is not known whether they can antagonize the action of auxin (Johnson et al., 2018b).

It can be hypothesized that both OGs and CDs play a role also later during the grafting process, when extensive biosynthesis and remodelling of polysaccharides take place to reconstruct the cell wall (Notaguchi et al., 2020). Adhesion between the scion and the rootstock, which occurs before callus formation, is mediated by high levels of HGA at graft junction (Sala et al., 2019), likely due to intermolecular $Ca2^{++}$-mediated ionic bridges referred to as "egg-boxes" that allow the formation of an adhesion gel structure (Decreux & Messiaen, 2005). Recently a new model for cell wall morphogenesis has been proposed that foresees that the cell wall expansion and

shaping is driven by nanofilament of HG (Haas et al., 2020). The methylation/demethylation of HGA also strongly influences the cell wall remodeling. At a later stage upon grafting, fibrillar and membranous material, mainly composed by pectin and proteins (extensins), is deposited extracellularly and appears on the surface of the callus cells, together with numerous bead-like structures, also rich in cell wall polysaccharides, that are present along the connection between scion and stock. The extracellular material subsequently seals the graft union. Several cell wall modification enzymes and proteins, such as β-1,4 glucanase, β-1,3 glucanase, xyloglucan hydrolase and expansins are up-regulated after grafting, in particular in proliferated cambial cells or pith region at the graft site (Notaguchi et al., 2020). The regulation of the expression of cell wall remodeling proteins and enzymes requires a fine and complex cross-talk between hormones.

Cytokinins regulate the expression of cell wall remodeling enzymes like pectin-modifying enzymes, expansins and laccases and play a role in monitoring the cell wall integrity (Bacete & Hamann, 2020). Moreover, they also modulate the defense responses (Kondo et al., 2011). In particular, among the Arabidopsis Response Regulators (ARRs) that mediate the cytokinin signaling, ARR5 and ARR6 are involved in the formation of protoxylem vessels. Mutants defective in ARR6 are more resistant to *Plectosphaerella cucumerina*, a necrotrophic fungus, and more susceptible to *Ralstonia solanacearum*, a vascular bacterium. Notably, *arr6* plants have a cell wall composition altered in the pectin fraction and enriched in potential DAMPs in comparison with the wild type.

A fine balance and homeostasis of hormones and possible regulatory signals such as OGs and CDs may therefore be crucial for a successful grafting. Indeed, at a very high level, the release of OGs has been shown to cause a deleterious hyper-immunity and eventually death. A possible mechanism by which the homeostasis of OGs and CDs can be maintained is represented by inactivating oxidases. Four OG oxidase (OGOX1-4) and one cellodestrin oxidase (CELLOX1), belonging to the berberine-bridge enzyme-like (BBEl) family (Daniel et al., 2015), have been so far identified (Benedetti et al., 2018; Locci et al., 2019). Oxidation of OGs and CDs is accompanied by the formation of H_2O_2.

The role of cell wall-derived DAMPs in grafting has never been studied. To elucidate their role as possible signals, I investigated, in this part of the work, the effects of OGs and CDs on processes that are relevant in grafting. I also studied the involvement of OGOX1 and CELLOX1 in the formation of the graft junction using a reverse genetics approach.

RESULTS AND DISCUSSION

Cellotriose has a dual action on early auxin-regulated gene expression

In order to better understand the biology of cellodextrins, I first investigated whether they antagonize auxin (IAA) responses, as previously described for OGs (Savatin et al., 2011). The expression of some of early auxin-responsive genes such as members of the Auxin/Indole-3-Acetic Acid (*AUX/IAA*) family and of the small auxin upregulated RNA (*SAUR*) family genes was analyzed after a 1-h treatment with cellotriose (CD3) in the presence and in the absence of IAA in Col-0 *Arabidopsis* seedlings. In parallel, OGs with and without IAA were used as controls (Figure III.1.).

In seedlings treated with CD3 combined with IAA, there was a reduced level of

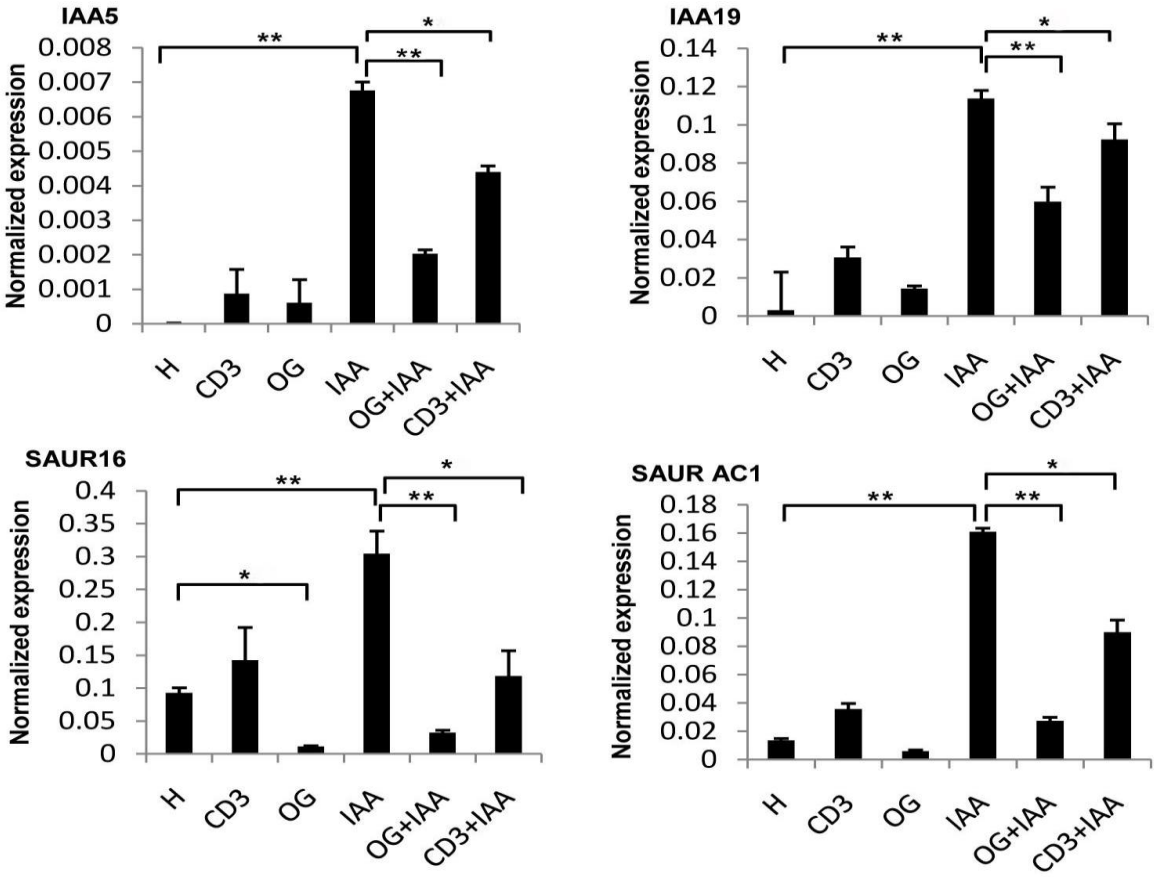

Figure III.1. Expression of early auxin response genes in *Arabidopsis* seedlings after treatment with IAA, OGs and cellotriose (CD3). Expression in the whole seedling of the early auxin (IAA)-responsive genes *IAA5* and *IAA19 (*members of the AUX/IAA family), and *SAUR16* and *SAUR AC1* (members of the Small Auxin Up-Regulated RNA family). Seedlings were treated for 1 h with oligogalacturonides (OG, 100 µg mL $^{-1}$) or cellotriose (CD3, 100 µg mL $^{-1}$) alone or in combination with 1.5 µM IAA. Treatment with water (H) was used as a control. Transcript levels were analyzed by qRT-PCR and normalized to *UBQ5* expression. Average ± SD ; *= p< 0.05; **= p< 0.0001.

IAA5, IAA19, SAUR AC1, SAUR16 gene induction compared to the high expression of these genes in seedlings treated with IAA alone. These data reveal that the CD3 antagonizes IAA in the whole *Arabidopsis* seedling similarly to OGs action. It has to be noted a slight increase, albeit not significant, of *IAA19* and *SAUR16* transcripts in the treatment with CD3 alone compared to the basal expression that needs to be further examined.

To corroborate the results on the inhibitory effect of CD3 on auxin responses, a qualitative analysis of the expression of pDR5::GUS was performed on the entire *Arabidopsis* seedling after CD3 and IAA treatment to study whether the spatial distribution of IAA is perturbed after treatment with CDs. In parallel pDR5::GUS expression was analyzed upon OG treatment. Surprisingly, while an overall reduction of DR5 induction on the entire tissues was detected in the combined IAA + CD3 treatment, a marked intensification of GUS signal only at the level of both foliar and radical apical meristem was observed. Instead, the OG treatment completely suppressed the auxin-induced GUS expression at the apical level of the leaf and the root (Figure III.2.).

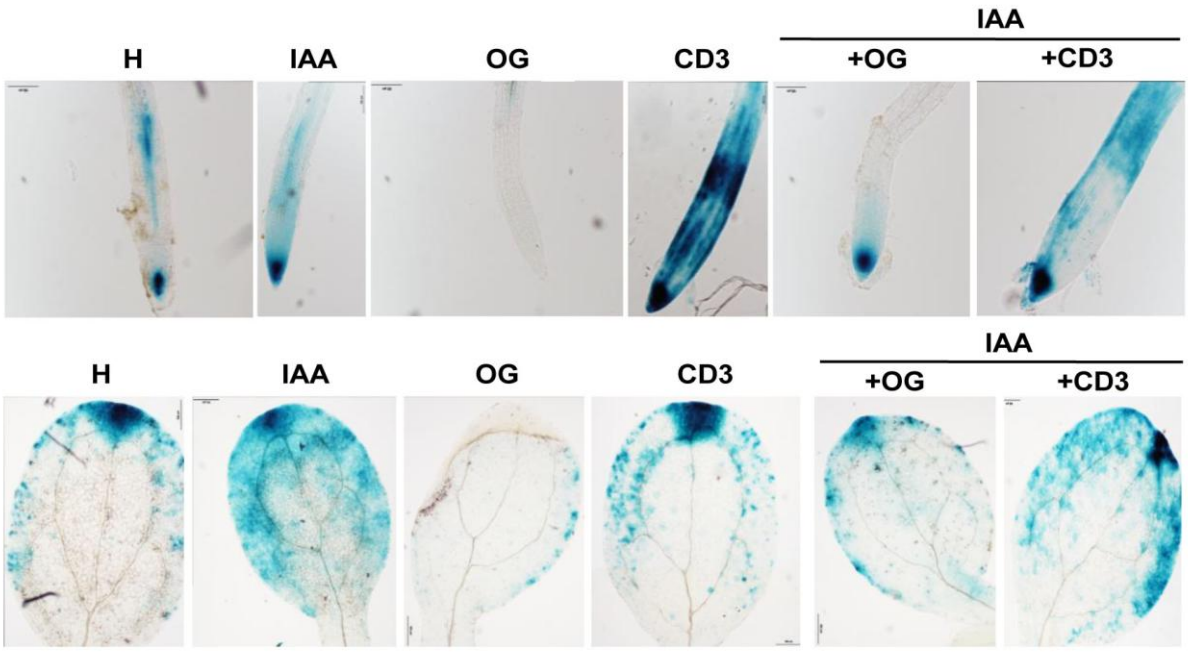

Figure III.2. Expression of pDR5::GUS in the *Arabidopsis* root apex and leaf upon treatment with auxin, OG and cellotriose (CD3). Upper and bottom panels show root apex and leaves, respectively, from pDR5::GUS whole seedlings treated with oligogalacturonides (OG, 100 μg mL $^{-1}$), cellotriose (CD3, 100 μg mL $^{-1}$) alone and in combination with 1.5 μM IAA**. Treatment** with water (H) was used as a control. Images were taken by optic microscope (roots 10 X , leaves 4 X). Scale bar 100 μm.

These results suggest that OGs and CDs are both modulators of the IAA signaling with a different mode of action. The total absence of GUS activity at the apical meristems in the treatment with OGs alone is consistent with the well-known capability of OGs of inhibiting auxin-regulated expression. CD3 also show inhibitory activity on the auxin responses and this may occur through pathways similar to those induced by OGs, which have been hypothesized to target auxin expression likely at the level of processes occurring at the promoter level. However, the increase of GUS activity at the apical meristems observed in the treatment with CD3 alone reflects instead a positive effect of CD3 on the auxin responses. An increase of IAA levels, for example due to an inhibition of IAA transport, may explain this effect. Further experiments are necessary to elucidate the action of CD3 on the expression and spatial distribution of proteins involved in the transport of IAA as for example the PIN proteins.

OGs, CDs and their oxidation influence the phloem reconnection and vascular formation.

Because both OGs and CD3 affect auxin-regulated responses, I investigated whether they play a role in grafting and tissue regeneration, where the balance between auxin and cytokinin plays an important role. First, I examined the phloem connectivity in

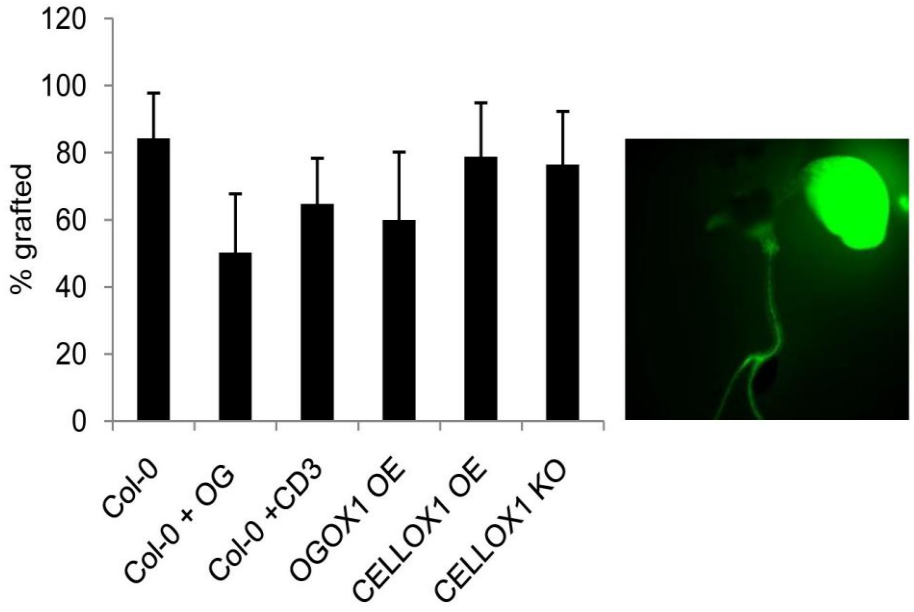

Figure III.3 . Vascular reconnection in wild-type plant treated with OGs or CD3 and in self-grafted mutant plants. Number of seedlings (%) that show the CFDA signal and considered as grafted, out of the total seedlings analyzed. Each genotype was self-grafted 7 days after germination (short-light cycle), and the CFDA assay was performed at 5 days after grafting (DAG). Col-0 + OG and Col-0 + CD3 are intended as Col-0 self-grafted with respectively OGs [100 μg mL $^{-1}$] and CD3 [25 μg mL $^{-1}$]. The plot is the average ± SD of three experiments performed at different times. On the right, the picture of a grafted Col-0/Col-0 seedling showing the CFDA signal in the phloem vasculature. It is possible to observe the CFDA-agar drop on the cotyledon

grafted wild-type plants treated with OGs and CDs. Phloem connectivity is used as evidence of a successful grafting, and is studied by using mobile dyes, such as the fluorescein derivative CarboxyFluorescein Diacetate (CFDA), applied to a leaf and monitoring the source to sink transport from the scion to the rootstock (Figure III.3.). Arabidopsis seedlings were treated with OGs and cellotriose (CD3). The attachment rate showed a slight, albeit not significant, decrease, in particular upon treatment with OGs (Figure III.3.). This result needs to be corroborated with a higher number of replicates. The experiment with CD3 will be repeated using higher concentrations. The decreased rate attachment after OG treatment may be explained by the antagonism between OGs and auxin. Auxin has a key role in the vascular formation, and when applied exogenously to undifferentiated tissues, promotes the formation of vascular strands. Moreover, auxin is involved in wounding healing and the grafting induces the expression of auxin biosynthesis genes (Nanda & Melnyk, 2018).
In parallel, mutants or transgenic plants altered in the expression of oxidases that inactivate these molecules were analyzed. Indeed, analysis of the transcriptional dynamics occurring in Arabidopsis during healing of grafted tissues shows a differential expression for *OGOX1*, *CELLOX1* and other BBE-like members (Melnyk et al., 2018). This is not surprising, because grafting involves the rupture of the cell wall and likely the release of OGs and CDs (Melnyk & Meyerowitz, 2015; Nanda & Melnyk, 2018). In particular, *OGOX1* is up-regulated and *CELLOX1* is down-regulated in the grafted bottom compared with the not-grafted separated bottom. No differences are detected at the level of grafted and separated top, revealing an asymmetric expression for these genes at the graft site (Figure III.4.).

In my experiments, OGOX1 and CELLOX1 self-grafted mutants did not show significant differences with the wild type in terms of percentage of successfully

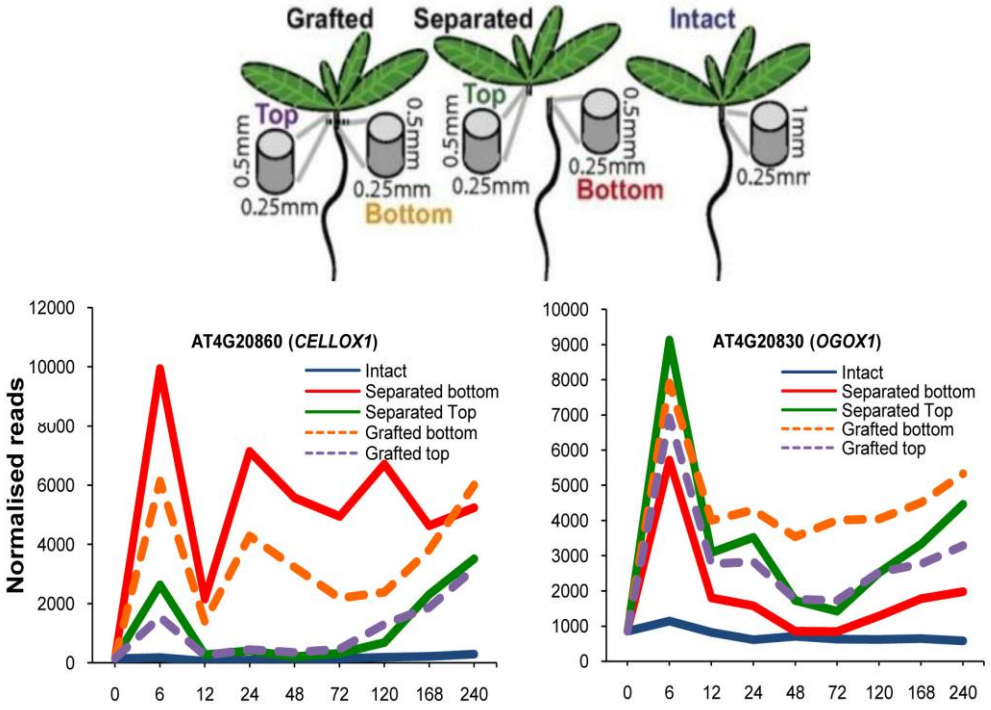

Figure III.4. Differential gene expression profile of *CELLOX1* and *OGOX1* after grafting. *CELLOX1* expression is down-regulated at the grafted bottom, compared to the separated bottom (not grafted). On the contrary, *OGOX1* is up-regulated in the grafted bottom compared to the separated bottom. Graph were on the basis of the data of Melnyk et al. (2018)

grafted seedlings; however, a trend to a decrease was observed in OGOX1 OE plants. A useful system to study *de novo* vascular regeneration is the so called VISUAL (Vascular Cell Induction Culture System Using Arabidopsis Leaves) assay, in which xylem and phloem cell differentiation can be ectopically induced in *Arabidopsis* leaves. The enzyme glycogen synthase kinase 3 (GSK3) plays a central role in the vascular meristem maintenance by suppressing xylem cell differentiation, and inhibiting the GSK3 activity by using the kinase inhibitor bikinin induces ectopic xylem and phloem cell differentiation that can be observed using a fluorescence stereoscope under UV light (exploiting the auto-fluorescence of the vascular cells) in cotyledons. A large number of vascular cells is generated in only four days after the addition of bikinin (Kondo et al., 2016). Normally the differentiation rates of ectopic xylem cells in the VISUAL assay are between 50-70 % in terms of xylem area per whole leaf area.

Vascular differentiation was therefore examined using the VISUAL assay in Col-0 seedlings treated with OGs [100 μg mL $^{-1}$], CD3 [25 μg mL $^{-1}$] and then treated with bikinin 4 days before the observation. In cotyledons treated with OGs and CD3 there was a strong decrease of vascular cells, with differentiation rates of 20 % and 23 % respectively compared to 57 % of untreated Col-0. These results indicate that OGs and CDs inhibit the ectopic vascular differentiation, likely because they interfere with the hormones, particularly the IAA that is antagonized by OGs.

In parallel, vascular differentiation was examined in the mutants CELLOX1 OE, CELLOX1 KO, OGOX1 OE and Col-0 seedlings treated with OGs or CD3 and then treated with bikinin 4 days before the observation. The same genotypes not treated with bikinin were used as negative controls. The percentage of the area of the vascular cells formed out of the area of the entire leaf was measured. Both cotyledons CELLOX1 OE and OGOX1 OE plants showed a higher increase of vascular cells as compared to the wild type plants with an ectopic formation of xylem/phloem of 67 % (vessels/leaf area) for CELLOX1 OE plants and 65 % for OGOX1 OE plants, respectively, compared to a value of 57 % obtained with Col-0 plants. This suggests that the accumulation of endogenous OGs and CDs may interfere with a successful vascular differentiation during grafting, which may be therefore favored by their inactivation by CELLOX1 and OGOX1. In the CELLOX1 and OGOX1 overexpressing plants, the hydrogen peroxide produced by the oxidation of CDs and OGs may *per se* trigger the differentiation. Conversely and in agreement with this hypothesis, CELLOX1 KO showed a slight decrease of the ectopic cells area, with a value of 44 %. (Figure III.5.).

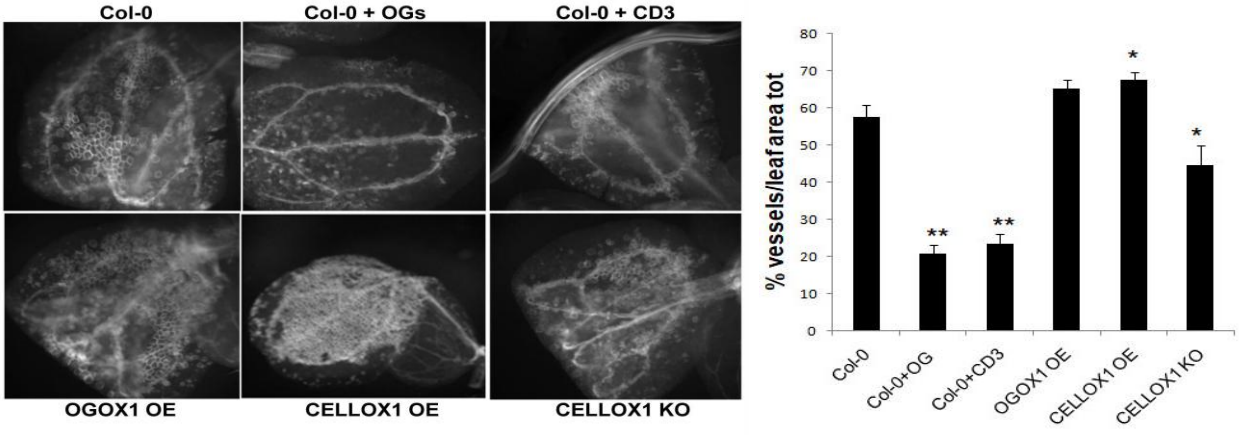

Figure III.5. VISUAL assay on OGOX1 OE, CELLOX1 OE, CELLOX1 KO and Col-0 cotyledons treated with OGs and cellotriose (CD3). In the left panel leaves of each mutant treated with bikinin, observed at the fluorescence stereoscope. In the right panel, the area (%) of ectopic vessels out of the area of the whole leaf (average ± SE) is shown. The experiment was repeated 3 times for CELLOX1 OE, OGOX1 OE, and CELLOX1 KO; 2 times for the treatment of Col-0 with OGs [100 μg mL $^{-1}$] and CD3 [25 μg mL $^{-1}$] . Ectopic formation of vascular cells was induced by bikinin in all the samples. T-student. *= $p < 0.05$; **= $p < 0.0001$.

Many genes are transcriptionally activated at the graft site and can be exploited as markers to monitor the process of grafting; in particular the promoter reporter fusions of two cytokinin-responsive genes, *ARR5* and the *HIGH CAMBIAL ACTIVITY 2* (*HCA2*), have been useful for this purpose (Melnyk et al., 2018). Activation of these promoters occurs at graft junction, and the intensity of the reporter signal is monitored by confocal microscopy as a quantitative measure of the gene expression.
I performed preliminary experiments on transgenic plants carrying the construct pARR5::RFP, available in the laboratory of Dr. Melnyk (SLU, Uppsala). CELLOX1 OE, OGOX1 OE and CELLOX1 KO seedlings were grafted with the seedlings of pARR5::RFP as a scion. The fluorescence signals in pARR5::RFP seedlings grafted with each mutant did not show macroscopic differences compared with the wild type, although in many cases a slightly lower fluorescent was observed (Figure III.6.). These experiments need to be repeated with a quantitative evaluation of the effects. Moreover, further analyses with pARR5::RFP used as both scion and rootstock, and pHCA2::GFP seedlings as rootstock must be performed, also in the presence of OGs and CD3.

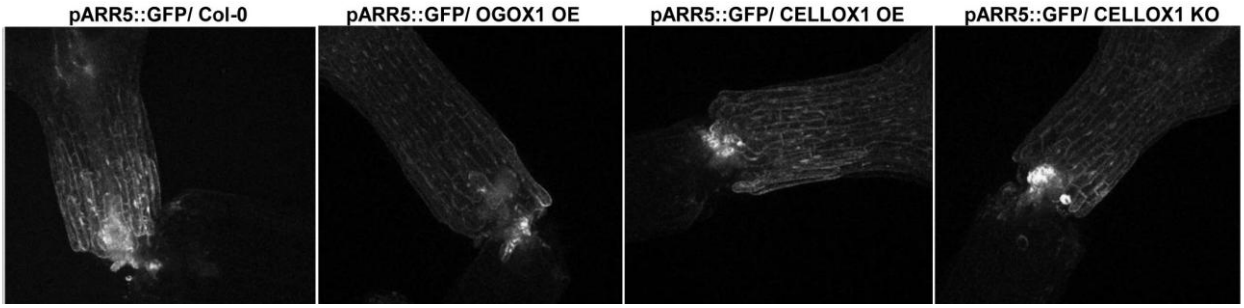

Figure III.6. *ARR5* expression in transgenic pARR5::GFP seedlings grafted with OGOX1 and CELLOX1 mutants. *ARR5* is a gene activated specifically at the graft junction and used as a marker. Its expression is monitored following the intensity of the GFP fluorescence in plants expressing the transcriptional fusion pARR5::GFP. Seedlings were observed 4 days after grafting (DAG). pARR5::GFP is the scion and Col-0 and mutants are the rootstocks. Confocal images.

Taken together, albeit preliminary, these results are very promising, as they suggest a role of OGs and CDs in the grafting process, particularly in the process of vascular tissue formation and differentiation. Moreover, expression analyses of auxin-related genes indicate that CDs antagonize auxin, and, interestingly, seem to have a dual role, with a positive effect on the response to auxin of meristematic cells. Further studies are needed to better understand the dynamics of the interaction between DAMPs and the hormonal activity and to deepen our understanding of the role of OGs and CDs in grafting and vascular formation.

MATERIALS AND METHODS

Plants

Arabidopsis thaliana plants, Col-0 ecotype, were grown on MS/2 medium under short- and long-day conditions, respectively 8 h/ 16 h at 22 °C and 16 h/ 8 h in growth chamber in a greenhouse at 22 °C.

Transgenic seeds of pSUC2::GFP were kindly provided by Dr. Ruth Stadler. The seeds of pARR5::RFP and pHCA2::RFP were kindly provided by Dr. Charles Melnyk.

Seed sterilization and plant growth

Seed sterilization was performed as described in Section II, page 55. Seedlings were grown in MS/2 medium at 22 °C and 70 % relative humidity under a 16 h light/ 8 h dark for the xylem morphology assay and 8 h light/ 16 h dark cycle for the grafting assay.

Grafting assay

The grafting assay was performed as previously described (Melnyk, 2017b, 2017c). The seedlings were grown vertically to ensure the correct hypocotyl growth. Short-day grown plants were grafted 7 days after germination. For adding or removing sterile water during grafting, the Petri dishes were prepared with two Whatman circles (Whatman 3 MM Chr cellulose 46 x 57 cm) and one Hybond membrane (Hybond N membrane, 20 cm x 3 m) previously sterilized. The grafting was performed under a laminar flow hood, using a stereoscope, previously cleaned with 70 % EtOH. *Arabidopsis* seedlings (6-12) were placed in a row on the Hybond membrane in the Petri dish. The Ultra Fine Micro Knives (by Fine Science Tools, 10315-12) was used to cut the samples and fine forceps to move gently the seedlings. For each seedling one cotyledon was cut off and discarded to allow the shoot to lie flat on the membrane. Then a transverse cut was done through the hypocotyl, close to the shoot. The cut shoot from one plant was taken and placed closer to the cut root from another plant. Using the forceps, the shoot at the level of the cotyledon was gently pushed until the cut root to align and to join the pieces together. After grafting, the lid was placed on the petri dish, and the plates were sealed with a layer of Parafilm. The dishes were moved into the grow chamber at 20-22 °C for at least 4-5 days. The plates were mounted vertically in short-day conditions.

Phloem connectivity assay: CFDA assay

The CFDA assay was performed as previously described (Melnyk, 2017c) on seedlings at 4 days after grafting. 5(6)-Carboxyfluorescein diacetate (CFDA) in powdered form (1 mg) was dissolved in 10 μl of DMSO. CFDA-DMSO (5 μl) was added to 1 mL of 0.8 % bacto-agar previously molten (1 mM of CFDA final concentration). A small drop of molten CFDA-agar (1-2 μl) was pipetted on the cotyledon of the grafted seedlings. Previously, each cotyledon had to be wounded by gently pressing on it with fine forceps. Then, the seedlings were left for 1 hour, and the number of plants that showed the CFDA signal were scored under a fluorescence stereoscope with a GFP or YFP filter, focusing on the rootstock vasculature, below the graft junction.

VISUAL ASSAY with *Arabidopsis* cotyledons

The VISUAL ASSAY was performed according to Kondo et al. (2016). All the steps were carried out under the hood, in sterile conditions. The liquid growth medium was prepared: 2.2 g L^{-1} MS basal medium, 10 g L^{-1} sucrose, and 0.5 g L^{-1} MES (2-morpholinoethanesulfonic acid monohydrate) in Milli-Q and the pH was adjusted to 5.7 using KOH. Liquid growth medium (10 mL) was added to each well of a 6 well-plate and 10-15 seeds were sown per well. Then the plate was sealed using a surgical tape and incubated at 22 °C under continuous light (neutral fluorescent lamp; 44-45 umol m^{-2} s^{-1}) for 6 days, on a rotary shaker (110 rpm). The induction medium was prepared: 2.2 g L^{-1} MS Basal Medium containing 50 g L^{-1} D (+)- glucose in MilliQ and the pH was adjusted to 5.7 with KOH. 2.4-D (1.25 mg L^{-1}), kinetin (0.25 mg L^{-1}) and bikinin (10 μM) were added to the solution previously prepared. 2.5 mL of the induction medium were added into each well of a 12-well plate. The seedlings were cut across the middle section of the hypocotyls using surgical forceps. 4-6 cotyledons for each well were rescued and transferred in the well containing the induction medium. The plate was sealed and incubated at 22 °C under continuous light for 4 days (neutral white fluorescent lamp; 60-70 μmol^{-2} s^{-1} – the light intensity is stronger than for plant growth). Finally, the samples were fixed in fixative solution (acetic acid and ethanol at a ratio of 1 : 3) overnight. Then, the clearing solution (chloral hydrate, glycerol and distilled water at a ratio of 8 : 1 : 2) was added and left for over 3 hours. The cotyledons were mounted on a glass slide and observed under a bright field microscope, under UV exposure to observe the auto-fluorescence from xylem secondary cell walls for more visible images.

Quantitative RT-PCR analyses of early auxin responsive genes expression after DAMP treatment

For gene expression analysis, 10-day-old Col-0 seedlings (grown in liquid MS/2 sucrose 0.5 %) were treated for 1 h with CDs with a degree of polymerization of 3 (100 μg mL^{-1}), OGs (100 μg mL^{-1}) and IAA 1.5 μM (SIGMA, 87-51-4) as controls (Savatin et al., 2011). Gene expression analyses were performed on RNA extracted from plant tissues with Trifast Reagent (Euroclone, https://www.euroclonegroup.it/) according to the manufacturer's protocol. Complementary DNA was synthesized in a 20-μl reaction mix using ImProm.II™ Reverse Transcriptase (Promega). Real-time quantitative PCR analysis was performed using a CFX96 Real-Time System (Bio-Rad, http://www.bio-rad.com/) and the reaction was carried out in a mix containing 1× Go Taq qPCR Master Mix (Promega) and 0.5 μl of each primer. The expression levels of each gene, relative to UBQ5, were determined using a modification of the Pfaffl method (Pfaffl, 2001) as previously described (Ferrari et al., 2006).

The following primers were used.

UBQ5 (*AT3G62250*):
LP 5'–GTTAAGCTCGCTGTTCTTCAGT-3'
RP 5'- TCAAGCTTCAACTCCTTCTTTC-3'.

IAA5 (*AT1G15580*):
LP 5'-ACCGAACTACGGCTAGGTCT-3'
RP 5'- CTGTTCTTTCTCCGGTACGA-3'.

IAA19 (*AT3G15540*):
LP 5'-CGAAAGTGGGGTTAGGGTAT-3'
RP 5'- CTAGAAACATCCCCCAAGGT-3'.

SAUR16 (*AT4G38860*):
LP 5'-ACAATGCTACGACGAGGAAG-3'
RP 5'- CTTCTTCACAAGGGATGGTG-3'.

SAUR-AC1 (*AT4G38850*):
LP 5'-AAGGGAATCATCGTCGACAC-3'
RP 5'- TATTGTTAAGCCGCCCATTG-3'.

Histochemical Localization of GUS Activity

The pDR5::GUS construct and transgenic plants have been previously described (Ulmasov et al., 1997). 10-day-old PDR5::GUS seedlings (grown in liquid MS/2 sucrose 0.5 %) were treated for 1 h with cellotriose (100 μg mL^{-1}), OGs (100 μg mL^{-1}) and IAA 1.5 μM (SIGMA, 87-51-4) as controls (Savatin et al., 2011). Histochemical GUS staining was performed by incubating whole pDR5::GUS seedlings in GUS staining buffer containing 50 mM sodium phosphate (pH 7.0), 0.5 mM potassium ferrocyanide, 10 mM EDTA, 0.1 % (v/v) Triton X-100, 2 % (v/v) dimethyl sulfoxide, and 1 mM 5-bromo-4-chloro-3-indolyl-D-glucuronide at 37 °C for 24 h (Jefferson, 1987).

Section IV

References

Aloni, R. (1980). Role of auxin and sucrose in the differentiation of sieve and tracheary elements in plant tissue cultures. *Planta*, *150*(3), 255-263. https://doi.org/10.1007/BF00390835

Aloni, R. (1987). Differentiation of vascular tissues. *Annual Review of Plant Physiol.*, *38*, 179-204. (NOT IN FILE)

Anderson, C. T., Carroll, A., Akhmetova, L., & Somerville, C. (2010). Real-time imaging of cellulose reorientation during cell wall expansion in Arabidopsis roots. *Plant Physiology*, *152*(2), 787-796. https://doi.org/10.1104/pp.109.150128

Arsovski, A. A., Haughn, G. W., & Western, T. L. (2010). Seed coat mucilage cells of *Arabidopsis thaliana* as a model for plant cell wall research. *Plant Signaling & Behavior*, *5*(7), 796-801. https://doi.org/10.4161/psb.5.7.11773

Arsovski, A. A., Popma, T. M., Haughn, G. W., Carpita, N. C., McCann, M. C., & Western, T. L. (2009). AtBXL1 encodes a bifunctional beta-D-xylosidase/alpha-L-arabinofuranosidase required for pectic arabinan modification in Arabidopsis mucilage secretory cells. *Plant Physiology*, *150*(3), 1219-1234. https://doi.org/10.1104/pp.109.138388

Aziz, A., Gauthier, A., Bézier, A., Poinssot, B., Joubert, J. M., Pugin, A., Heyraud, A., & Baillieul, F. (2007). Elicitor and resistance-inducing activities of beta-1,4 cellodextrins in grapevine, comparison with beta-1,3 glucans and alpha-1,4 oligogalacturonides. *Journal of Experimental Botany*, *58*(6), 1463-1472. https://doi.org/10.1093/jxb/erm008 (NOT IN FILE)

Aziz, A., Heyraud, A., & Lambert, B. (2004). Oligogalacturonide signal transduction, induction of defense-related responses and protection of grapevine against *Botrytis cinerea*. *Planta*, *218*(5), 767-774. https://doi.org/10.1007/s00425-003-1153-x. (NOT IN FILE)

Bacete, L., & Hamann, T. (2020). The role of mechanoperception in plant cell wall integrity maintenance. *Plants (Basel)*, *9*(5). https://doi.org/10.3390/plants9050574

Bellincampi, D., Dipierro, N., Salvi, G., Cervone, F., & De Lorenzo, G. (2000). Extracellular H_2O_2 induced by oligogalacturonides is not involved in the inhibition of the auxin-regulated *rolB* gene expression in tobacco leaf explants. *Plant Physiology*, *122*(4), 1379-1385. https://doi.org/10.1104/pp.122.4.1379

Bellincampi, D., Salvi, G., De Lorenzo, G., Cervone, F., Marfa, V., Eberhard, S., Darvill, A., & Albersheim, P. (1993). Oligogalacturonides inhibit the formation of roots on tobacco explants. *The Plant Journal*, *4*(1), 207-213. https://doi.org/10.1046/j.1365-313X.1993.04010207.x

Ben-Tov, D., Abraham, Y., Stav, S., Thompson, K., Loraine, A., Elbaum, R., de Souza, A., Pauly, M., Kieber, J. J., & Harpaz-Saad, S. (2015a). COBRA-LIKE2, a member of the glycosylphosphatidylinositol-anchored COBRA-LIKE family, plays a role in cellulose deposition in Arabidopsis seed coat mucilage secretory cells. *Plant Physiology*, *167*(3), 711-724. https://doi.org/10.1104/pp.114.240671

Ben-Tov, D., Abraham, Y., Stav, S., Thompson, K., Loraine, A., Elbaum, R., de Souza, A., Pauly, M., Kieber, J. J., & Harpaz-Saad, S. (2015b). COBRA-LIKE2, a member of the glycosylphosphatidylinositol-anchored COBRA-LIKE family, plays a role in cellulose deposition in arabidopsis seed coat mucilage secretory cells. *Plant Physiol*, *167*(3), 711-724. https://doi.org/10.1104/pp.114.240671

Benedetti, M., Pontiggia, D., Raggi, S., Cheng, Z., Scaloni, F., Ferrari, S., Ausubel, F. M., Cervone, F., & De Lorenzo, G. (2015). Plant immunity triggered by engineered in vivo release of oligogalacturonides, damage-associated molecular patterns. *Proc. Natl. Acad. Sci. U. S. A.*, *112*(17), 5533-5538. https://doi.org/10.1073/pnas.1504154112 (NOT IN FILE)

Benedetti, M., Verrascina, I., Pontiggia, D., Locci, F., Mattei, B., De Lorenzo, G., & Cervone, F. (2018). Four Arabidopsis berberine bridge enzyme-like proteins are specific oxidases that inactivate the elicitor-active oligogalacturonides. *Plant Journal*, *94*(2), 260-273. https://doi.org/10.1111/tpj.13852

Bergey, D. R., Orozco-C rdenas, M. L., De Moura, D. S., & Ryan, C. A. (1999). A wound- and systemin-inducible polygalacturonase in tomato leaves. *Proceedings of the National Academy of Sciences, USA*, *96*(4), 1756-1760. (IN FILE)

Boller, T., & Felix, G. (2009). A renaissance of elicitors: perception of microbe-associated molecular patterns and danger signals by pattern-recognition receptors. *Annual Review of Plant Biology*, *60*, 379-406. (NOT IN FILE)

Bradford, M. M. (1976). A rapid and sensitive method for the quantitation of microgram quantities of protein utilizing the principle of protein-dye binding. *Analytical Biochemistry*, *72*, 248-254. (NOT IN FILE)

Branca, C., De Lorenzo, G., & Cervone, F. (1988). Competitive inhibition of the auxin-induced elongation by α-D-oligogalacturonides in pea stem segments. *Physiologia Plantarum*, *72*(3), 499-504. https://doi.org/10.1111/j.1399-3054.1988.tb09157.x

Broekaert, W. F., & Pneumas, W. J. (1988). Pectic polysaccharides elicit chitinase accumulation in tobacco. *Physiologia Plantarum*, *74*, 740-744. https://doi.org/10.1111/j.1399-3054.1988.tb02046.x (NOT IN FILE)

Brutus, A., Sicilia, F., Macone, A., Cervone, F., & De Lorenzo, G. (2010). A domain swap approach reveals a role of the plant wall-associated kinase 1 (WAK1) as a receptor of oligogalacturonides. *Proceedings of the National Academy of Sciences, USA*, *107*(20), 9452-9457. https://doi.org/10.1073/pnas.1000675107

Burton, R., & Fincher, G. (2009). (1→3),(1→4)-β-D-glucans in cell walls of the Poaceae, lower plants, and fungi: a tale of two linkages. *Molecular Plant*, *2*(5). https://doi.org/10.1093/mp/ssp063

Cervone, F., Hahn, M. G., De Lorenzo, G., Darvill, A., & Albersheim, P. (1989). Host-pathogen interactions. XXXIII. A plant protein converts a fungal pathogenesis factor into an elicitor of plant defense responses. *Plant Physiology*, *90*, 542-548. (IN FILE)

Cheong, Y. H., Chang, H. S., Gupta, R., Wang, X., Zhu, T., & Luan, S. (2002). Transcriptional profiling reveals novel interactions between wounding, pathogen, abiotic stress, and hormonal responses in Arabidopsis. *Plant Physiology*, *129*(2), 661-677. https://doi.org/10.1104/pp.002857

Chitwood, D. H., & Timmermans, M. C. (2010). Small RNAs are on the move. *Nature*, *467*(7314), 415-419. https://doi.org/10.1038/nature09351

Claverie, J., Balacey, S., Lemaitre-Guillier, C., Brule, D., Chiltz, A., Granet, L., Noirot, E., Daire, X., Darblade, B., Heloir, M. C., & Poinssot, B. (2018). The cell wall-derived xyloglucan is a new DAMP triggering plant immunity in *Vitis vinifera* and *Arabidopsis thaliana*. *Frontiers in Plant Science*, *9*, 1725. https://doi.org/10.3389/fpls.2018.01725

Couto, D., & Zipfel, C. (2016). Regulation of pattern recognition receptor signalling in plants. *Nature Reviews Immunology*, *16*(9), 537-552. https://doi.org/10.1038/nri.2016.77

Custers, J. H., Harrison, S. J., Sela-Buurlage, M. B., van Deventer, E., Lageweg, W., Howe, P. W., van der Meijs, P. J., Ponstein, A. S., Simons, B. H., Melchers, L. S., & Stuiver, M. H. (2004). Isolation and characterisation of a class of carbohydrate oxidases from higher plants, with a role in active defence. *The Plant Journal*, *39*(2), 147-160. https://doi.org/10.1111/j.1365-313X.2004.02117.x

Dalling, J. W., Davis, A. S., Arnold, A. E., Sarmiento, C., & Zalamea, P.-C. (2020). Extending plant defense theory to seeds [review-article]. *Annual Review of Ecology, Evolution, and Systematics*, *51*(1), 123-141. https://doi.org/10.1146/annurev-ecolsys-012120-115156

Daniel, B., Konrad, B., Toplak, M., Lahham, M., Messenlehner, J., Winkler, A., & Macheroux, P. (2017). The family of berberine bridge enzyme-like enzymes: A treasure-trove of oxidative reactions. *Arch. Biochem. Biophys.*, *632*, 88-103. https://doi.org/10.1016/j.abb.2017.06.023 (NOT IN FILE)

Daniel, B., Pavkov-Keller, T., Steiner, B., Dordic, A., Gutmann, A., Nidetzky, B., Sensen, C. W., van der Graaff, E., Wallner, S., Gruber, K., & Macheroux, P. (2015). Oxidation of monolignols by members of the berberine-bridge enzyme family suggests a role in plant cell wall metabolism. *Journal of Biological Chemistry*, *290*(30), 18770-18781. https://doi.org/10.1074/jbc.M115.659631 (NOT IN FILE)

Daniel, B., Wallner, S., Steiner, B., Oberdorfer, G., Kumar, P., van der Graaff, E., Roitsch, T., Sensen, C. W., Gruber, K., & Macheroux, P. (2016). Structure of a berberine bridge enzyme-like enzyme with an active site specific to the plant family brassicaceae. *PLoS One*, *11*(6), e0156892. https://doi.org/10.1371/journal.pone.0156892 (NOT IN FILE)

Davis, K. R., Darvill, A. G., Albersheim, P., & Dell, A. (1986). Host-pathogen interactions. XXIX. Oligogalacturonides released from sodium polypectate by endopolygalacturonic acid lyase are elicitors of phytoalexins in soybean. *Plant Physiology*, *80*, 568-577. https://doi.org/10.1104/pp.80.2.568. (IN FILE)

Davis, K. R., & Hahlbrock, K. (1987). Induction of defense responses in cultured parsley cells by plant cell wall fragments. *Plant Physiology*, *85*, 1286-1290. https://doi.org/10.1104/pp.84.4.1286 (IN FILE)

De Bolle, M. F. C., Eggermont, K., Duncan, R. E., Osborn, R. W., Terras, F. R. G., & Broekaert, W. F. (1995). Cloning and characterization of two cDNA clones encoding seed- specific antimicrobial peptides from Mirabilis jalapa L. *Plant Molecular Biology*, *28*, 713-721. (ON REQUEST (11/03/95))

De Lorenzo, G., & Ferrari, S. (2002). Polygalacturonase-inhibiting proteins in defense against phytopathogenic fungi. *Current Opinion in Plant Biology*, *5*(4), 295-299. https://doi.org/10.1016/s1369-5266(02)00271-6

De Lorenzo, G., Ferrari, S., Cervone, F., & Okun, E. (2018). Extracellular DAMPs in plants and mammals: immunity, tissue damage and repair. *Trends in Immunology*, *39*(11), 937-950. https://doi.org/10.1016/j.it.2018.09.006

Dean, G. H., Sola, K., Unda, F., Mansfield, S. D., & Haughn, G. W. (2019). Analysis of monosaccharides from Arabidopsis seed mucilage and whole seeds using HPAEC-PAD. *Bio Protoc*, *9*(24), e3464. https://doi.org/10.21769/BioProtoc.3464

Dean, G. H., Zheng, H., Tewari, J., Huang, J., Young, D. S., Hwang, Y. T., Western, T. L., Carpita, N. C., McCann, M. C., Mansfield, S. D., & Haughn, G. W. (2007). The Arabidopsis MUM2 gene encodes a beta-galactosidase required for the production of seed coat mucilage with correct hydration properties. *The Plant Cell*, *19*(12), 4007-4021. https://doi.org/10.1105/tpc.107.050609

Decreux, A., & Messiaen, J. (2005). Wall-associated kinase WAK1 interacts with cell wall pectins in a calcium-induced conformation. *Plant and Cell Physiology*, *46*(2), 268-278. (NOT IN FILE)

Denance, N., Sanchez-Vallet, A., Goffner, D., & Molina, A. (2013). Disease resistance or growth: the role of plant hormones in balancing immune responses and fitness costs. *Frontiers in Plant Science*, *4*, 155. https://doi.org/10.3389/fpls.2013.00155

Denoux, C., Galletti, R., Mammarella, N., Gopalan, S., Werck, D., De Lorenzo, G., Ferrari, S., Ausubel, F. M., & Dewdney, J. (2008). Activation of defense response pathways by OGs and Flg22 elicitors in Arabidopsis seedlings. *Molecular Plant*, *1*(3), 423-445. https://doi.org/10.1093/mp/ssn019

Dolinsky, T., Nielsen, J., McCammon, J., & Baker, N. (2004). PDB2PQR: an automated pipeline for the setup of Poisson-Boltzmann electrostatics calculations. *Nucleic Acids Research*, *32*(Web Server issue). https://doi.org/10.1093/nar/gkh381

Du, J., Kirui, A., Huang, S., Wang, L., Barnes, W. J., Kiemle, S., Zheng, Y., Rui, Y., Ruan, M., Qi, S., Kim, S. H., Wang, T., Cosgrove, D. J., Anderson, C. T., & Xiao, C. (2020). Mutations in the pectin

methyltransferase QUASIMODO2 Influence cellulose biosynthesis and wall integrity in *Arabidopsis thaliana*. *The Plant Cell*, tpc.00252.02020. https://doi.org/10.1105/tpc.20.00252

Duran-Flores, D., & Heil, M. (2016). Sources of specificity in plant damaged-self recognition. *Current Opinion in Plant Biology*, *32*, 77-87. (NOT IN FILE)

Elo, A., Immanen, J., Nieminen, K., & Helariutta, Y. (2009). Stem cell function during plant vascular development. *Seminars in Cell & Developmental Biology*, *20*(9), 1097-1106. https://doi.org/10.1016/j.semcdb.2009.09.009

Engelbrecht, M., & García-Fayos, P. (2012). Mucilage secretion by seeds doubles the chance to escape removal by ants. *Plant Ecology*, *213*(7), 1167-1175. https://doi.org/http://dx.doi.org/10.1007/s11258-012-0074-9

Farvardin, A., Gonzalez-Hernandez, A. I., Llorens, E., Garcia-Agustin, P., Scalschi, L., & Vicedo, B. (2020). The apoplast: a key player in plant survival. *Antioxidants (Basel)*, *9*(7). https://doi.org/10.3390/antiox9070604

Felle, H. H., Herrmann, A., Hückelhoven, R., & Kogel, K. H. (2005). Root-to-shoot signalling: apoplastic alkalinization, a general stress response and defence factor in barley (Hordeum vulgare). *Protoplasma*, *227*(1), 17-24. https://doi.org/10.1007/s00709-005-0131-5

Ferrari, S., Galletti, R., Denoux, C., De Lorenzo, G., Ausubel, F. M., & Dewdney, J. (2007). Resistance to *Botrytis cinerea* induced in Arabidopsis by elicitors is independent of salicylic acid, ethylene, or jasmonate signaling but requires PHYTOALEXIN DEFICIENT3. *Plant Physiology*, *144*(1), 367-379. https://doi.org/10.1104/pp.107.095596 (NOT IN FILE)

Ferrari, S., Galletti, R., Pontiggia, D., Manfredini, C., Lionetti, V., Bellincampi, D., Cervone, F., & De Lorenzo, G. (2008). Transgenic expression of a fungal endo-polygalacturonase increases plant resistance to pathogens and reduces auxin sensitivity. *Plant Physiology*, *146*(2), 669-681. https://doi.org/10.1104/pp.107.109686

Ferrari, S., Galletti, R., Vairo, D., Cervone, F., & De Lorenzo, G. (2006). Antisense expression of the Arabidopsis thaliana AtPGIP1 gene reduces polygalacturonase-inhibiting protein accumulation and enhances susceptibility to Botrytis cinerea. *Molecular Plant-Microbe Interactions*, *19*(8), 931-936. (NOT IN FILE)

Ferrari, S., Savatin, D. V., Sicilia, F., Gramegna, G., Cervone, F., & Lorenzo, G. D. (2013). Oligogalacturonides: plant damage-associated molecular patterns and regulators of growth and development. *Frontiers in Plant Science*, *4*, 49. https://doi.org/10.3389/fpls.2013.00049 (NOT IN FILE)

Fontaine, T., Simenel, C., Dubreucq, G., Adam, O., Delepierre, M., Lemoine, J., Vorgias, C., Diaquin, M., & Latgé, J. (2000). Molecular organization of the alkali-insoluble fraction of *Aspergillus fumigatus* cell wall. *The Journal of Biological Chemistry*, *275*(36). https://doi.org/10.1074/jbc.M909975199

Franková, L., & Fry, S. C. (2020). Activity and action of cell-wall transglycanases. In Z. A. Popper (Ed.), *The Plant Cell Wall: Methods and Protocols* (pp. 165-192). Springer New York. https://doi.org/10.1007/978-1-0716-0621-6_10

Fry, S. C., Nesselrode, B. H., Miller, J. G., & Mewburn, B. R. (2008). Mixed-linkage (1→3,(1→4)-β-D-glucan is a major hemicellulose of Equisetum (horsetail) cell walls. *New Phytologist*, *179*(1), 104-115. https://doi.org/10.1111/j.1469-8137.2008.02435.x

Galletti, R., Denoux, C., Gambetta, S., Dewdney, J., Ausubel, F. M., De Lorenzo, G., & Ferrari, S. (2008). The AtrbohD-mediated oxidative burst elicited by oligogalacturonides in Arabidopsis is dispensable for the activation of defense responses effective against *Botrytis cinerea*. *Plant Physiology*, *148*(3), 1695-1706. https://doi.org/10.1104/pp.108.127845 (NOT IN FILE)

Galletti, R., Ferrari, S., & De Lorenzo, G. (2011). Arabidopsis MPK3 and MPK6 Play Different Roles in Basal and Oligogalacturonide- or Flagellin-Induced Resistance against Botrytis cinerea. *Plant Physiology*, *157*(2), 804-814. https://doi.org/10.1104/pp.111.174003

Gaut, B. S., Miller, A. J., & Seymour, D. K. (2019). Living with two genomes: grafting and its implications for plant genome-to-genome interactions, phenotypic variation, and evolution.

Annual Review of Genetics, *53*, 195-215. https://doi.org/10.1146/annurev-genet-112618-043545

Gay, C., Collins, J., & Gebicki, J. M. (1999). Hydroperoxide assay with the ferric-xylenol orange complex. *Analytical Biochemistry*, *273*(2), 149-155. (NOT IN FILE)

Gonzalez, A., Mendenhall, J., Huo, Y., & Lloyd, A. (2009). TTG1 complex MYBs, MYB5 and TT2, control outer seed coat differentiation. *Developmental Biology*, *325*(2), 412-421. https://doi.org/10.1016/j.ydbio.2008.10.005

Gramegna, G., Modesti, V., Savatin, D. V., Sicilia, F., Cervone, F., & De Lorenzo, G. (2016). GRP-3 and KAPP, encoding interactors of WAK1, negatively affect defense responses induced by oligogalacturonides and local response to wounding. *Journal of Experimental Botany*, *67*(6), 1715-1729. https://doi.org/10.1093/jxb/erv563

Gravino, M., Locci, F., Tundo, S., Cervone, F., Savatin, D. V., & De Lorenzo, G. (2017). Immune responses induced by oligogalacturonides are differentially affected by AvrPto and loss of BAK1/BKK1 and PEPR1/PEPR2. *Molecular Plant Pathology*, *18*(4), 582-595. https://doi.org/10.1111/mpp.12419

Gravino, M., Savatin, D. V., Macone, A., & De Lorenzo, G. (2015). Ethylene production in *Botrytis cinerea*- and oligogalacturonide-induced immunity requires calcium-dependent protein kinases. *The Plant Journal*, *84*(6), 1073-1086. https://doi.org/10.1111/tpj.13057

Griffiths, J. S., Sola, K., Kushwaha, R., Lam, P., Tateno, M., Young, R., Voiniciuc, C., Dean, G., Mansfield, S. D., DeBolt, S., & Haughn, G. W. (2015). Unidirectional movement of cellulose synthase complexes in Arabidopsis seed coat epidermal cells deposit cellulose involved in mucilage extrusion, adherence, and ray formation. *Plant Physiology*, *168*(2), 502-520. https://doi.org/10.1104/pp.15.00478

Griffiths, J. S., Tsai, A. Y., Xue, H., Voiniciuc, C., Sola, K., Seifert, G. J., Mansfield, S. D., & Haughn, G. W. (2014). SALT-OVERLY SENSITIVE5 mediates Arabidopsis seed coat mucilage adherence and organization through pectins. *Plant Physiology*, *165*(3), 991-1004. https://doi.org/10.1104/pp.114.239400

Gust, A. A., Biswas, R., Lenz, H. D., Rauhut, T., Ranf, S., Kemmerling, B., Gotz, F., Glawischnig, E., Lee, J., Felix, G., & Nurnberger, T. (2007). Bacteria-derived peptidoglycans constitute pathogen-associated molecular patterns triggering innate immunity in Arabidopsis. *Journal of Biological Chemistry*, *282*(44), 32338-32348. (NOT IN FILE)

Gust, A. A., Pruitt, R., & Nürnberger, T. (2017). Sensing danger: key to activating plant immunity. *Trends in Plant Science*, *22*(9), 779-791. https://doi.org/10.1016/j.tplants.2017.07.005

Haas, K. T., Wightman, R., Meyerowitz, E. M., & Peaucelle, A. (2020). Pectin homogalacturonan nanofilament expansion drives morphogenesis in plant epidermal cells. *Science*, *367*(6481), 1003-1007. https://doi.org/10.1126/science.aaz5103

Hanke, D. E., & Northcote, D. H. (1975). Molecular visualization of pectin and DNA by ruthenium red. *Biopolymers*, *14*(1), 1-17. https://doi.org/10.1002/bip.1975.360140102

Harpaz-Saad, S., McFarlane, H. E., Xu, S., Divi, U. K., Forward, B., Western, T. L., & Kieber, J. J. (2011). Cellulose synthesis via the FEI2 RLK/SOS5 pathway and cellulose synthase 5 is required for the structure of seed coat mucilage in Arabidopsis. *The Plant Journal*, *68*(6), 941-953. https://doi.org/10.1111/j.1365-313X.2011.04760.x

Haughn, G., & Chaudhury, A. (2005). Genetic analysis of seed coat development in Arabidopsis. *Trends in Plant Science*, *10*(10), 472-477. https://doi.org/10.1016/j.tplants.2005.08.005

Haughn, G. W., & Western, T. L. (2012). Arabidopsis seed coat mucilage is a specialized cell wall that can be used as a model for genetic analysis of plant cell wall structure and function. *Frontiers in Plant Science*, *3*, 64. https://doi.org/10.3389/fpls.2012.00064

Hendry, G. A. F., Thompson, K., Moss, C. J., Edwards, E., & Thorpe, P. C. (1994). Seed persistence: a correlation between seed longevity in the soil and ortho-dihydroxyphenol concentration. *Functional Ecology*, *8*(5), 658-664. https://doi.org/10.2307/2389929

Hruz, T., Laule, O., Szabo, G., Wessendorp, F., Bleuler, S., Oertle, L., Widmayer, P., Gruissem, W., & Zimmermann, P. (2008). Genevestigator v3: a reference expression database for the meta-

analysis of transcriptomes. *Adv Bioinformatics*, *2008*, 420747. https://doi.org/10.1155/2008/420747

Huang, H., Ullah, F., Zhou, D. X., Yi, M., & Zhao, Y. (2019). Mechanisms of ROS regulation of plant development and stress responses. *Frontiers in Plant Science*, *10*, 800. https://doi.org/10.3389/fpls.2019.00800

Huang, Z., Boubriak, I., Osborne, D. J., Dong, M., & Gutterman, Y. (2008). Possible role of pectin-containing mucilage and dew in repairing embryo DNA of seeds adapted to desert conditions. *Annals of Botany*, *101*(2), 277-283. https://doi.org/10.1093/aob/mcm089

Huot, B., Yao, J., Montgomery, B. L., & He, S. Y. (2014). Growth-defense tradeoffs in plants: a balancing act to optimize fitness. *Molecular Plant*, *7*(8), 1267-1287. https://doi.org/10.1093/mp/ssu049 (NOT IN FILE)

Ikeuchi, M., Favero, D. S., Sakamoto, Y., Iwase, A., Coleman, D., Rymen, B., & Sugimoto, K. (2019). Molecular mechanisms of plant regeneration. *Annual Review of Plant Biology*, *70*, 377-406. https://doi.org/10.1146/annurev-arplant-050718-100434

Ikeuchi, M., Sugimoto, K., Iwase, A. (2013). Plant Callus: Mechanisms of Induction and Repression. *The Plant Cell*, *25*, 3159–3173.

Jefferson, R. A. (1987). Assaying chimeric genes in plants: the GUS gene fusion system. *Plant Molecular Biology Reporter*, *5*, 387-405. (IN FILE)

Jofuku, K. D., den Boer, B. G., Van Montagu, M., & Okamuro, J. K. (1994). Control of Arabidopsis flower and seed development by the homeotic gene APETALA2. *The Plant Cell*, *6*(9), 1211-1225. https://doi.org/10.1105/tpc.6.9.1211

Johnson, C. S., Kolevski, B., & Smyth, D. R. (2002). TRANSPARENT TESTA GLABRA2, a trichome and seed coat development gene of Arabidopsis, encodes a WRKY transcription factor. *The Plant Cell*, *14*(6), 1359-1375. https://doi.org/10.1105/tpc.001404

Johnson, J. M., Thurich, J., Petutschnig, E. K., Altschmied, L., Meichsner, D., Sherameti, I., Dindas, J., Mrozinska, A., Paetz, C., Scholz, S. S., Furch, A. C., Lipka, V., Hedrich, R., Schneider, B., Svatos, A., & Oelmuller, R. (2018a). A poly(A) ribonuclease controls the cellotriose-based interaction between Piriformospora indica and its host Arabidopsis. *Plant Physiology*. https://doi.org/10.1104/pp.17.01423

Johnson, J. M., Thurich, J., Petutschnig, E. K., Altschmied, L., Meichsner, D., Sherameti, I., Dindas, J., Mrozinska, A., Paetz, C., Scholz, S. S., Furch, A. C. U., Lipka, V., Hedrich, R., Schneider, B., Svatos, A., & Oelmuller, R. (2018b). A Poly(A) ribonuclease controls the cellotriose-based interaction between *Piriformospora indica* and its host Arabidopsis. *Plant Physiology*, *176*(3), 2496-2514. https://doi.org/10.1104/pp.17.01423

Jones, J. D. G., & Dangl, J. L. (2006). The plant immune system. *Nature*, *444*(7117), 323-329.

Kaku, H., Nishizawa, Y., Ishii-Minami, N., Akimoto-Tomiyama, C., Dohmae, N., Takio, K., Minami, E., & Shibuya, N. (2006). Plant cells recognize chitin fragments for defense signaling through a plasma membrane receptor. *Proceedings of the National Academy of Sciences, USA*, *103*(29), 11086-11091. (NOT IN FILE)

Kalunke, R. M., Tundo, S., Benedetti, M., Cervone, F., De Lorenzo, G., & D'Ovidio, R. (2015). An update on polygalacturonase-inhibiting protein (PGIP), a leucine-rich repeat protein that protects crop plants against pathogens. *Frontiers in Plant Science*, *6*, 146. https://doi.org/10.3389/fpls.2015.00146 (NOT IN FILE)

Karimi, M., Inze, D., & Depicker, A. (2002). GATEWAY vectors for Agrobacterium -mediated plant transformation. *Trends in Plant Science*, *7*(5), 193-195. (NOT IN FILE)

Klee, H. J., Horsch, R. B., Hinchee, M. A., Hein, M. B., & Hoffmann, N. L. (1987). The effects of overproduction of two Agrobacterium tumefaciens T-DNA auxin biosynthetic gene products in transgenic petunia plants. *Genes and Development*, *1*, 86-96. (NOT IN FILE)

Kliebenstein, D. J. (2016). False idolatry of the mythical growth versus immunity tradeoff in molecular systems plant pathology. In (Vol. 95, pp. 55-59). Physiological and Molecular Plant Pathology: Elsevier.

Kondo, Y., Hirakawa, Y., Kieber, J. J., & Fukuda, H. (2011). CLE peptides can negatively regulate protoxylem vessel formation via cytokinin signaling. *Plant & Cell Physiology*, *52*(1), 37-48. https://doi.org/10.1093/pcp/pcq129

Kondo, Y., Nurani, A. M., Saito, C., Ichihashi, Y., Saito, M., Yamazaki, K., Mitsuda, N., Ohme-Takagi, M., & Fukuda, H. (2016). Vascular Cell Induction Culture System Using Arabidopsis Leaves (VISUAL) Reveals the Sequential Differentiation of Sieve Element-Like Cells. *The Plant Cell*, *28*(6), 1250-1262. https://doi.org/10.1105/tpc.16.00027

Land, W. G. (2020). Use of DAMPs and SAMPs as therapeutic targets or therapeutics: a note of caution [OriginalPaper]. *Molecular Diagnosis & Therapy*, *24*(3), 251-262. https://doi.org/10.1007/s40291-020-00460-z

Lee, J., & Hollingsworth, R. (1997). Oligosaccharide β-glucans with unusual linkages from *Sarcina ventriculi*. *Carbohydrate Research*, *304*(2). https://doi.org/10.1016/s0008-6215(97)00204-8

Leon, J., Rojo, E., & Sanchez-Serrano, J. J. (2001). Wound signalling in plants. *J Exp.Bot.*, *52*(354), 1-9. (NOT IN FILE)

Levine, A., Tenhaken, R., Dixon, R., & Lamb, C. (1994). H 2 O 2 from the oxidative burst orchestrates the plant hypersensitive disease resistance response. *Cell*, *79*, 583-593. (IN FILE)

Li, P., Lu, Y. J., Chen, H., & Day, B. (2020). The lifecycle of the plant immune system. *CRC Crit Rev Plant Sci*, *39*(1), 72-100. https://doi.org/10.1080/07352689.2020.1757829

Liu, N., Yang, J., Fu, X., Zhang, L., Tang, K., Guy, K. M., Hu, Z., Guo, S., Xu, Y., & Zhang, M. (2016). Genome-wide identification and comparative analysis of grafting-responsive mRNA in watermelon grafted onto bottle gourd and squash rootstocks by high-throughput sequencing. *Molecular Genetics and Genomics*, *291*(2), 621-633. https://doi.org/10.1007/s00438-015-1132-5

Liu, T., Liu, Z., Song, C., Hu, Y., Han, Z., She, J., Fan, F., Wang, J., Jin, C., Chang, J., Zhou, J. M., & Chai, J. (2012). Chitin-induced dimerization activates a plant immune receptor. *Science*, *336*(6085), 1160-1164. (NOT IN FILE)

Locci, F., Benedetti, M., Pontiggia, D., Citterico, M., Caprari, C., Mattei, B., Cervone, F., & De Lorenzo, G. (2019). An Arabidopsis berberine bridge enzyme-like protein specifically oxidizes cellulose oligomers and plays a role in immunity. *The Plant Journal*, *98*(3), 540-554. https://doi.org/10.1111/tpj.14237

Macquet, A., Ralet, M. C., Kronenberger, J., Marion-Poll, A., & North, H. M. (2007). In situ, chemical and macromolecular study of the composition of *Arabidopsis thaliana* seed coat mucilage. *Plant & Cell Physiology*, *48*(7), 984-999. https://doi.org/10.1093/pcp/pcm068

Matsuoka, K., Sugawara, E., Aoki, R., Takuma, K., Terao-Morita, M., Satoh, S., & Asahina, M. (2016). Differential cellular control by cotyledon-derived phytohormones involved in graft reunion of Arabidopsis hypocotyls. *Plant & Cell Physiology*, *57*(12), 2620-2631. https://doi.org/10.1093/pcp/pcw177

Mattei, B., Spinelli, F., Pontiggia, D., & De Lorenzo, G. (2016). Comprehensive analysis of the membrane phosphoproteome regulated by oligogalacturonides in *Arabidopsis thaliana*. *Frontiers in Plant Science*, *7*, 1107. https://doi.org/10.3389/fpls.2016.01107

Melnyk, C. W. (2017a). Connecting the plant vasculature to friend or foe. *New Phytologist*, *213*(4), 1611-1617. https://doi.org/10.1111/nph.14218

Melnyk, C. W. (2017b). Grafting with *Arabidopsis thaliana*. *Methods in Molecular Biology*, *1497*, 9-18. https://doi.org/10.1007/978-1-4939-6469-7_2

Melnyk, C. W. (2017c). Monitoring vascular regeneration and xylem connectivity in *Arabidopsis thaliana*. *Methods in Molecular Biology*, *1544*, 91-102. https://doi.org/10.1007/978-1-4939-6722-3_9

Melnyk, C. W. (2017d). Plant grafting: insights into tissue regeneration. *Regeneration (Oxf)*, *4*(1), 3-14. https://doi.org/10.1002/reg2.71

Melnyk, C. W., Gabel, A., Hardcastle, T. J., Robinson, S., Miyashima, S., Grosse, I., & Meyerowitz, E. M. (2018). Transcriptome dynamics at Arabidopsis graft junctions reveal an intertissue

recognition mechanism that activates vascular regeneration. *Proceedings of the National Academy of Sciences, USA*, *115*(10), E2447-E2456. https://doi.org/10.1073/pnas.1718263115

Melnyk, C. W., & Meyerowitz, E. M. (2015). Plant grafting. *Current Biology*, *25*(5), R183-R188.

Melnyk, C. W., Molnar, A., Bassett, A., & Baulcombe, D. C. (2011). Mobile 24 nt small RNAs direct transcriptional gene silencing in the root meristems of Arabidopsis thaliana. *Current Biology*, *21*(19), 1678-1683. (NOT IN FILE)

Melnyk, C. W., Schuster, C., Leyser, O., & Meyerowitz, E. M. (2015). A developmental framework for graft formation and vascular reconnection in Arabidopsis thaliana. *Current Biology*, *25*(10), 1306-1318. (NOT IN FILE)

Mendu, V., Griffiths, J. S., Persson, S., Stork, J., Downie, A. B., Voiniciuc, C., Haughn, G. W., & DeBolt, S. (2011). Subfunctionalization of cellulose synthases in seed coat epidermal cells mediates secondary radial wall synthesis and mucilage attachment. *Plant Physiology*, *157*(1), 441-453. https://doi.org/10.1104/pp.111.179069

Messenlehner, J., Hetman, M., Tripp, A., Wallner, S., Macheroux, P., Gruber, K., & Daniel, B. (2021). The catalytic machinery of the FAD-dependent AtBBE-like protein 15 for alcohol oxidation: Y193 and Y479 form a catalytic base, Q438 and R292 an alkoxide binding site. *Arch Biochem Biophys*, *700*, 108766. https://doi.org/10.1016/j.abb.2021.108766

Mhamdi, A., & Van Breusegem, F. (2018). Reactive oxygen species in plant development. *Development*, *145*(15). https://doi.org/10.1242/dev.164376

Mudge, K., Janick, J., Scofield, S., & Goldschmidt, E. E. (2009). A history of grafting. In *Horticultural Reviews* (pp. 437-493). https://doi.org/https://doi.org/10.1002/9780470593776.ch9

Mélida, H., Bacete, L., Ruprecht, C., Rebaque, D., Del Hierro, I., Lopez, G., Brunner, F., Pfrengle, F., & Molina, A. (2020). Arabinoxylan-oligosaccharides act as damage associated molecular patterns in plants regulating disease resistance. *Frontiers in Plant Science*, *11*, 1210. https://doi.org/10.3389/fpls.2020.01210

Nakabayashi, K., Okamoto, M., Koshiba, T., Kamiya, Y., & Nambara, E. (2005). Genome-wide profiling of stored mRNA in *Arabidopsis thaliana* seed germination: epigenetic and genetic regulation of transcription in seed. *The Plant journal : for cell and molecular biology*, *41*(5). https://doi.org/10.1111/j.1365-313X.2005.02337.x

Nanda, A. K., & Melnyk, C. W. (2018). The role of plant hormones during grafting. *Journal of Plant Research*, *131*(1), 49-58. https://doi.org/10.1007/s10265-017-0994-5

Notaguchi, M., Higashiyama, T., & Suzuki, T. (2015). Identification of mRNAs that move over long distances using an RNA-Seq analysis of Arabidopsis/*Nicotiana benthamiana* heterografts. *Plant & Cell Physiology*, *56*(2), 311-321. https://doi.org/10.1093/pcp/pcu210

Notaguchi, M., Kurotani, K. I., Sato, Y., Tabata, R., Kawakatsu, Y., Okayasu, K., Sawai, Y., Okada, R., Asahina, M., Ichihashi, Y., Shirasu, K., Suzuki, T., Niwa, M., & Higashiyama, T. (2020). Cell-cell adhesion in plant grafting is facilitated by β-1,4-glucanases. *Science*, *369*(6504), 698-702. https://doi.org/10.1126/science.abc3710

Oka, T., Nemoto, T., & Jigami, Y. (2007). Functional analysis of *Arabidopsis thaliana* RHM2/MUM4, a multidomain protein involved in UDP-D-glucose to UDP-L-rhamnose conversion. *Journal of Biological Chemistry*, *282*(8), 5389-5403. https://doi.org/10.1074/jbc.M610196200

Palacio-Lopez, K., Sun, L., Reed, R., Kang, E., Sørensen, I., Rose, J. K. C., & Domozych, D. S. (2020). Experimental manipulation of pectin architecture in the cell wall of the unicellular charophyte, *Penium margaritaceum* [Original Research]. *Frontiers in Plant Science*, *11*(1032). https://doi.org/10.3389/fpls.2020.01032

Parkinson, M., & Yeoman, M. M. (1982). Graft formation in cultured, explanted internodes. *New Phytologist*, *91*(4), 711-719. https://doi.org/10.1111/j.1469-8137.1982.tb03350.x

Paultre, D. S. G., Gustin, M. P., Molnar, A., & Oparka, K. J. (2016). Lost in transit: long-distance trafficking and phloem unloading of protein signals in Arabidopsis homografts. *The Plant Cell*, *28*(9), 2016-2025. https://doi.org/10.1105/tpc.16.00249

Penfield, S., Meissner, R. C., Shoue, D. A., Carpita, N. C., & Bevan, M. W. (2001). MYB61 is required for mucilage deposition and extrusion in the Arabidopsis seed coat. *The Plant Cell*, *13*(12), 2777-2791. https://doi.org/10.1105/tpc.010265

Petersen, T. N., Brunak, S., von Heijne, G., & Nielsen, H. (2011). SignalP 4.0: discriminating signal peptides from transmembrane regions. *Nature Methods*, *8*(10), 785-786. https://doi.org/10.1038/nmeth.1701

Petrásek, J., & Friml, J. (2009). Auxin transport routes in plant development. *Development*, *136*(16), 2675-2688. https://doi.org/10.1242/dev.030353

Pettolino, F., Sasaki, I., Turbic, A., Wilson, S. M., Bacic, A., Hrmova, M., & Fincher, G. B. (2009). Hyphal cell walls from the plant pathogen Rhynchosporium secalis contain (1,3/1,6)-beta-D-glucans, galacto- and rhamnomannans, (1,3;1,4)-β-D-glucans and chitin. *FEBS Journal*, *276*(14), 3698-3709. https://doi.org/10.1111/j.1742-4658.2009.07086.x

Pfaffl, M. W. (2001). A new mathematical model for relative quantification in real-time RT-PCR. *Nucleic Acids Research*, *29*(9), e45. (NOT IN FILE)

Pontiggia, D., Benedetti, M., Costantini, S., De Lorenzo, G., & Cervone, F. (2020). Dampening the DAMPs: how plants maintain the homeostasis of cell wall molecular patterns and avoid hyper-immunity. *Frontiers in Plant Science*, *11*, 613259. https://doi.org/10.3389/fpls.2020.613259

Popper, Z. A., & Fry, S. C. (2003). Primary cell wall composition of bryophytes and charophytes. *Annals of Botany*, *91*(1), 1-12. https://doi.org/10.1093/aob/mcg013

Procko, C., Crenshaw, C. M., Ljung, K., Noel, J. P., & Chory, J. (2014). Cotyledon-generated auxin is required for shade-induced hypocotyl growth in *Brassica rapa*. *Plant Physiology*, *165*(3), 1285-1301. https://doi.org/10.1104/pp.114.241844

Pérez-Mendoza, D., Rodríguez-Carvajal, M., Romero-Jiménez, L., Farias, G. e. A., Lloret, J., Gallegos, M. T., & Sanjuán, J. (2015). Novel mixed-linkage β-glucan activated by c-di-GMP in Sinorhizobium meliloti. *Proc Natl Acad Sci U S A*, *112*(7), E757-765. https://doi.org/10.1073/pnas.1421748112

Ralet, M. C., Crepeau, M. J., Vigouroux, J., Tran, J., Berger, A., Salle, C., Granier, F., Botran, L., & North, H. M. (2016). Xylans provide the structural driving force for mucilage adhesion to the Arabidopsis seed cx\oat. *Plant Physiology*, *171*(1), 165-178. https://doi.org/10.1104/pp.16.00211

Rasul, S., Dubreuil-Maurizi, C., Lamotte, O., Koen, E., Poinssot, B., Alcaraz, G., Wendehenne, D., & Jeandroz, S. (2012). Nitric oxide production mediates oligogalacturonide-triggered immunity and resistance to *Botrytis cinerea* in *Arabidopsis thaliana*. *Plant, Cell & Environment*, *35*(8), 1483-1499. https://doi.org/10.1111/j.1365-3040.2012.02505.x. (NOT IN FILE)

Raviv, B., Aghajanyan, L., Granot, G., Makover, V., Frenkel, O., Gutterman, Y., & Grafi, G. (2017). The dead seed coat functions as a long-term storage for active hydrolytic enzymes. *PLoS One*, *12*(7), e0181102. https://doi.org/10.1371/journal.pone.0181102

Rebaque, D., Del Hierro, I., López, G., Bacete, L., Vilaplana, F., Dallabernardina, P., Pfrengle, F., Jordá, L., Sánchez-Vallet, A., Pérez, R., Brunner, F., Molina, A., & Mélida, H. (2021). Cell wall-derived mixed-linked β-1,3/1,4-glucans trigger immune responses and disease resistance in plants. *The Plant Journal*. https://doi.org/10.1111/tpj.15185

Romano, C. P., Hein, M. B., & Klee, H. J. (1991). Inactivation of auxin in tobacco transformed with the indoleacetic acid-lysine synthetase gene of Pseudomonas savastanoi. *Genes Dev*, *5*(3), 438-446. https://doi.org/10.1101/gad.5.3.438

Rose, T. L., Conceição, A. d. S., Xavier-Filho, J., Okorokov, L. A., Fernandes, K. V. S., Marty, F., Marty-Mazars, D., Carvalho, A. O., & Gomes, V. M. (2006). Defense proteins from *Vigna Unguiculata* seed exudates: characterization and inhibitory activity against *Fusarium oxysporum*. *Plant and Soil*, *286*(1), 181-191. https://doi.org/10.1007/s11104-006-9036-0

Sachs, T. (1991). Cell polarity and tissue patterning in plants. *Development*, *112 Suppl. 1*, 83-93. (IN FILE)

Saeman, J. F., Moore, W. E., Mitchell, R. L., & Millett, M. A. (1954). Techniques for the determination of pulp constituents by quantitiative paper chromatography. *TAPPI Journal*, *37*(8), 336-343.

Saez-Aguayo, S., Rondeau-Mouro, C., Macquet, A., Kronholm, I., Ralet, M. C., Berger, A., Sallé, C., Poulain, D., Granier, F., Botran, L., Loudet, O., de Meaux, J., Marion-Poll, A., & North, H. M. (2014). Local evolution of seed flotation in Arabidopsis. *PLoS Genetics*, *10*(3), e1004221. https://doi.org/10.1371/journal.pgen.1004221

Sala, K., Karcz, J., Rypien, A., & Kurczynska, E. U. (2019). Unmethyl-esterified homogalacturonan and extensins seal Arabidopsis graft union. *BMC Plant Biology*, *19*(1), 151. https://doi.org/10.1186/s12870-019-1748-4

Salmeán, A. A., Duffieux, D., Harholt, J., Qin, F., Michel, G., Czjzek, M., Willats, W. G. T., & Hervé, C. (2017). Insoluble (1 → 3), (1 → 4)-β-D-glucan is a component of cell walls in brown algae (Phaeophyceae) and is masked by alginates in tissues. *Sci Rep*, *7*(1), 2880. https://doi.org/10.1038/s41598-017-03081-5

Samar, D., Kieler, J. B., & Klutts, J. S. (2015). Identification and deletion of Tft1, a predicted glycosyltransferase necessary for cell wall β-1,3;1,4-glucan synthesis in Aspergillus fumigatus. *PLoS One*, *10*(2), e0117336. https://doi.org/10.1371/journal.pone.0117336

Savatin, D. V., Ferrari, S., Sicilia, F., & De Lorenzo, G. (2011). Oligogalacturonide-auxin antagonism does not require posttranscriptional gene silencing or stabilization of auxin response repressors in Arabidopsis. *Plant Physiology*, *157*(3), 1163-1174. https://doi.org/10.1104/pp.111.184663

Savatin, D. V., Gigli-Bisceglia, N., Marti, L., Fabbri, C., Cervone, F., & De Lorenzo, G. (2014). The Arabidopsis NUCLEUS- AND PHRAGMOPLAST-LOCALIZED KINASE1-related protein kinases are required for elicitor-induced oxidative burst and immunity. *Plant Physiology*, *165*(3), 1188-1202. https://doi.org/10.1104/pp.114.236901

Savatin, D. V., Gramegna, G., Modesti, V., & Cervone, F. (2014). Wounding in the plant tissue: the defense of a dangerous passage. *Frontiers in Plant Science*, *5*, 470. https://doi.org/10.3389/fpls.2014.00470 (NOT IN FILE)

Schall, P., Marutschke, L., & Grimm, B. (2020). The flavoproteome of the model plant *Arabidopsis thaliana*. *International Journal of Molecular Sciences*, *21*(15). https://doi.org/10.3390/ijms21155371

Schmid, M., Davison, T., Henz, S., Pape, U., Demar, M., Vingron, M., Schölkopf, B., Weigel, D., & Lohmann, J. (2005). A gene expression map of *Arabidopsis thaliana* development. *Nature Genetics*, *37*(5). https://doi.org/10.1038/ng1543

Schneider, C. A., Rasband, W. S., & Eliceiri, K. W. (2012). NIH Image to ImageJ: 25 years of image analysis. *Nature Methods*, *9*(7), 671-675. https://doi.org/10.1038/nmeth.2089

Seaman, M. N. J., Burd, C. G., & Emr, S. D. (1996). Receptor signalling and the regulation of endocytic membrane transport. *Current Opinion in Cell Biology*, *8*(4), 549-556. (ON REQUEST (08/29/96))

Sharma, A., & Zheng, B. (2019). Molecular responses during plant grafting and its regulation by auxins, cytokinins, and gibberellins. *Biomolecules*, *9*(9). https://doi.org/10.3390/biom9090397

Sieburth, L. E. (1999). Auxin is required for leaf vein pattern in Arabidopsis. *Plant Physiology*, *121*(4), 1179-1190. https://doi.org/10.1104/pp.121.4.1179

Sies, H., & Jones, D. P. (2020). Reactive oxygen species (ROS) as pleiotropic physiological signalling agents. *Nature Reviews: Molecular Cell Biology*, *21*(7), 363-383. https://doi.org/10.1038/s41580-020-0230-3

Souza, C. A., Li, S., Lin, A. Z., Boutrot, F., Grossmann, G., Zipfel, C., & Somerville, S. C. (2017). Cellulose-derived oligomers act as damage-associated molecular patterns and trigger defense-like responses. *Plant Physiology*, *173*(4), 2383-2398. https://doi.org/10.1104/pp.16.01680 (NOT IN FILE)

Spiegelman, Z., Ham, B. K., Zhang, Z., Toal, T. W., Brady, S. M., Zheng, Y., Fei, Z., Lucas, W. J., & Wolf, S. (2015). A tomato phloem-mobile protein regulates the shoot-to-root ratio by mediating

the auxin response in distant organs. *The Plant Journal*, *83*(5), 853-863. https://doi.org/10.1111/tpj.12932

Stegemann, S., & Bock, R. (2009). Exchange of genetic material between cells in plant tissue grafts. *Science*, *324*(5927), 649-651. https://doi.org/10.1126/science.1170397

Stegemann, S., Keuthe, M., Greiner, S., & Bock, R. (2012). Horizontal transfer of chloroplast genomes between plant species. *Proc Natl Acad Sci U S A*, *109*(7), 2434-2438. https://doi.org/10.1073/pnas.1114076109

Sullivan, S., Ralet, M. C., Berger, A., Diatloff, E., Bischoff, V., Gonneau, M., Marion-Poll, A., & North, H. M. (2011). CESA5 is required for the synthesis of cellulose with a role in structuring the adherent mucilage of Arabidopsis seeds. *Plant Physiology*, *156*(4), 1725-1739. https://doi.org/10.1104/pp.111.179077

Sørensen, I., Pettolino, F. A., Wilson, S. M., Doblin, M. S., Johansen, B., Bacic, A., & Willats, W. G. (2008). Mixed-linkage (1→3),(1→4)-β-D-glucan is not unique to the Poales and is an abundant component of Equisetum arvense cell walls. *The Plant Journal*, *54*(3), 510-521. https://doi.org/10.1111/j.1365-313X.2008.03453.x

Taller, J., Hirata, Y., Yagishita, N., Kita, M., & Ogata, S. (1998). Graft-induced genetic changes and the inheritance of several characteristics in pepper (Capsicum annuum L.). *Theoretical and Applied Genetics*, *97*(5), 705-713. https://doi.org/10.1007/s001220050946

Terras, F. R., Eggermont, K., Kovaleva, V., Raikhel, N. V., Osborn, R. W., Kester, A., Rees, S. B., Torrekens, S., Van Leuven, F., Vanderleyden, J., Cammue, B. P. A., & Broekaert, W. F. (1995). Small cysteine-rich antifungal proteins from radish: their role in host defense. *The Plant Cell*, *7*(5), 573-588. (NOT IN FILE)

Toplak, M., Wiedemann, G., Ulicevic, J., Daniel, B., Hoernstein, S. N. W., Kothe, J., Niederhauser, J., Reski, R., Winkler, A., & Macheroux, P. (2018). The single berberine bridge enzyme homolog of *Physcomitrella patens* is a cellobiose oxidase. *FEBS Journal*, *285*(10), 1923-1943. https://doi.org/10.1111/febs.14458

Trethewey, J. A., Campbell, L. M., & Harris, P. J. (2005). (1→3),(1→4)-β-D-glucans in the cell walls of the Poales (sensu lato): an immunogold labeling study using a monoclonal antibody. *American Journal of Botany*, *92*(10), 1660-1674. https://doi.org/10.3732/ajb.92.10.1660

Tucker, M. R., Lou, H., Aubert, M. K., Wilkinson, L. G., Little, A., Houston, K., Pinto, S. C., & Shirley, N. J. (2018). Exploring the role of cell wall-related genes and polysaccharides during plant development. *Plants (Basel)*, *7*(2), E42. https://doi.org/10.3390/plants7020042

Ulmasov, T., Murfett, J., Hagen, G., & Guilfoyle, T. J. (1997). Aux/IAA proteins repress expression of reporter genes containing natural and highly active synthetic auxin response elements. *The Plant Cell*, *9*(11), 1963-1971. (IN FILE)

Usadel, B., Kuschinsky, A. M., Rosso, M. G., Eckermann, N., & Pauly, M. (2004). RHM2 is involved in mucilage pectin synthesis and is required for the development of the seed coat in Arabidopsis. *Plant Physiology*, *134*(1), 286-295. (NOT IN FILE)

Voiniciuc, C., Schmidt, M. H., Berger, A., Yang, B., Ebert, B., Scheller, H. V., North, H. M., Usadel, B., & Gunl, M. (2015). MUCILAGE-RELATED10 produces galactoglucomannan that maintains pectin and cellulose architecture in Arabidopsis seed mucilage. *Plant Physiology*, *169*(1), 403-420. https://doi.org/10.1104/pp.15.00851

Voiniciuc, C., Yang, B., Schmidt, M. H., Gunl, M., & Usadel, B. (2015). Starting to gel: how Arabidopsis seed coat epidermal cells produce specialized secondary cell walls. *International Journal of Molecular Sciences*, *16*(2), 3452-3473. https://doi.org/10.3390/ijms16023452

Voxeur, A., Habrylo, O., Guenin, S., Miart, F., Soulie, M. C., Rihouey, C., Pau-Roblot, C., Domon, J. M., Gutierrez, L., Pelloux, J., Mouille, G., Fagard, M., Hofte, H., & Vernhettes, S. (2019). Oligogalacturonide production upon *Arabidopsis thaliana-Botrytis cinerea* interaction. *Proceedings of the National Academy of Sciences, USA*, *116*(39), 19743-19752. https://doi.org/10.1073/pnas.1900317116

Walker, M., Tehseen, M., Doblin, M. S., Pettolino, F. A., Wilson, S. M., Bacic, A., & Golz, J. F. (2011). The transcriptional regulator LEUNIG_HOMOLOG regulates mucilage release from the Arabidopsis testa. *Plant Physiol*, *156*(1), 46-60. https://doi.org/10.1104/pp.111.172692

Wang, J., Jin, Z., Yin, H., Yan, B., Ren, Z. Z., Xu, J., Mu, C. J., Zhang, Y., Wang, M. Q., & Liu, H. (2014). Auxin redistribution and shifts in PIN gene expression during Arabidopsis grafting. *Russian Journal of Plant Physiology*, *61*(5), 688-696. https://doi.org/10.1134/S102144371405015X

Wang, J., Li, D., Chen, N., Chen, J., Mu, C., Yin, K., He, Y., & Liu, H. (2020). Plant grafting relieves asymmetry of jasmonic acid response induced by wounding between scion and rootstock in tomato hypocotyl. *PLoS One*, *15*(11), e0241317. https://doi.org/10.1371/journal.pone.0241317

Wang, M., Xu, Z., Ahmed, R. I., Wang, Y., Hu, R., Zhou, G., & Kong, Y. (2019). Tubby-like Protein 2 regulates homogalacturonan biosynthesis in Arabidopsis seed coat mucilage. *Plant Molecular Biology*, *99*(4-5), 421-436. https://doi.org/10.1007/s11103-019-00827-9

Waterhouse, A., Bertoni, M., Bienert, S., Studer, G., Tauriello, G., Gumienny, R., Heer, F. T., de Beer, T. A. P., Rempfer, C., Bordoli, L., Lepore, R., & Schwede, T. (2018). SWISS-MODEL: homology modelling of protein structures and complexes. *Nucleic Acids Research*, *46*(W1), W296-W303. https://doi.org/10.1093/nar/gky427

Western, T., Burn, J., WL, T., DJ, S., L, M.-M., BA, M., & GW, H. (2001). Isolation and characterization of mutants defective in seed coat mucilage secretory cell development in Arabidopsis. *Plant Physiology*, *127*(3).

Western, T. L. (2012). The sticky tale of seed coat mucilages: production, genetics, and role in seed germination and dispersal. *Seed Science Research*, *22*(1), 1-25. https://doi.org/http://dx.doi.org/10.1017/S0960258511000249

Western, T. L., Skinner, D. J., & Haughn, G. W. (2000). Differentiation of mucilage secretory cells of the Arabidopsis seed coat. *Plant Physiology*, *122*(2), 345-356. https://doi.org/10.1104/pp.122.2.345

Western, T. L., Young, D. S., Dean, G. H., Tan, W. L., Samuels, A. L., & Haughn, G. W. (2004). MUCILAGE-MODIFIED4 encodes a putative pectin biosynthetic enzyme developmentally regulated by APETALA2, TRANSPARENT TESTA GLABRA1, and GLABRA2 in the Arabidopsis seed coat. *Plant Physiology*, *134*(1), 296-306. https://doi.org/10.1104/pp.103.035519

Willats, W. G., McCartney, L., & Knox, J. P. (2001). In-situ analysis of pectic polysaccharides in seed mucilage and at the root surface of Arabidopsis thaliana. *Planta*, *213*(1), 37-44. (NOT IN FILE)

Windsor, J. B., Symonds, V. V., Mendenhall, J., & Lloyd, A. M. (2000). Arabidopsis seed coat development: morphological differentiation of the outer integument. *The Plant Journal*, *22*(6), 483-493. https://doi.org/10.1046/j.1365-313x.2000.00756.x

Winter, D., Vinegar, B., Nahal, H., Ammar, R., Wilson, G. V., & Provart, N. J. (2007). An "Electronic Fluorescent Pictograph" browser for exploring and analyzing large-scale biological data sets. *PLoS One*, *2*(8), e718. https://doi.org/10.1371/journal.pone.0000718

Xoconostle-Cázares, B., Xiang, Y., Ruiz-Medrano, R., Wang, H. L., Monzer, J., Yoo, B. C., McFarland, K. C., Franceschi, V. R., & Lucas, W. J. (1999). Plant paralog to viral movement protein that potentiates transport of mRNA into the phloem. *Science*, *283*(5398), 94-98. https://doi.org/10.1126/science.283.5398.94

Yang, X., Baskin, C. C., Baskin, J. M., Gao, R., Yang, F., Wei, L., Li, L., He, H., & Huang, Z. (2013). Hydrated mucilage reduces post-dispersal seed removal of a sand desert shrub by ants in a semiarid ecosystem. *Oecologia*, *173*(4), 1451-1458. https://doi.org/10.1007/s00442-013-2735-3

Yang, X., Zhang, W., Dong, M., Boubriak, I., & Huang, Z. (2011). The achene mucilage hydrated in desert dew assists seed cells in maintaining DNA integrity: adaptive strategy of desert plant Artemisia sphaerocephala. *PLoS One*, *6*(9), e24346. https://doi.org/10.1371/journal.pone.0024346

Yang, Y., Mao, L., Jittayasothorn, Y., Kang, Y., Jiao, C., Fei, Z., & Zhong, G. Y. (2015). Messenger RNA exchange between scions and rootstocks in grafted grapevines. *BMC Plant Biology*, *15*, 251. https://doi.org/10.1186/s12870-015-0626-y

Yin, H., Yan, B., Sun, J., Jia, P., Zhang, Z., Yan, X., Chai, J., Ren, Z., Zheng, G., & Liu, H. (2012). Graft-union development: a delicate process that involves cell-cell communication between scion and stock for local auxin accumulation. *Journal of Experimental Botany*, *63*(11), 4219-4232. https://doi.org/10.1093/jxb/ers109

Yu, L., Shi, D., Li, J., Kong, Y., Yu, Y., Chai, G., Hu, R., Wang, J., Hahn, M. G., & Zhou, G. (2014). CELLULOSE SYNTHASE-LIKE A2, a glucomannan synthase, is involved in maintaining adherent mucilage structure in Arabidopsis seed. *Plant Physiology*, *164*(4), 1842-1856. https://doi.org/10.1104/pp.114.236596

Zablackis, E., Huang, J., Müller, B., Darvill, A. G., & Albersheim, P. (1995). Characterization of the cell-wall polysaccharides of *Arabidopsis thaliana* leaves. *Plant Physiology*, *107*(4), 1129-1138. https://doi.org/10.1104/pp.107.4.1129

Zang, H., Xie, S., Zhu, B., Yang, X., Gu, C., Hu, B., Gao, T., Chen, Y., & Gao, X. (2019). Mannan oligosaccharides trigger multiple defence responses in rice and tobacco as a novel danger-associated molecular pattern. *Molecular Plant Pathology*, *20*(8), 1067-1079. https://doi.org/10.1111/mpp.12811

Zhang, D., & Zhang, B. (2020). Pectin drives cell wall morphogenesis without turgor pressure. *Trends in Plant Science*. https://doi.org/10.1016/j.tplants.2020.05.007

Zipfel, C. (2014). Plant pattern-recognition receptors. *Trends in Immunology*, *35*(7), 345-351. https://doi.org/10.1016/j.it.2014.05.004

Zipfel, C., & Felix, G. (2005). Plants and animals: a different taste for microbes? *Current Opinion in Plant Biology*, *8*(4), 353-360. (NOT IN FILE)

Šola, K., Gilchrist, E. J., Ropartz, D., Wang, L., Feussner, I., Mansfield, S. D., Ralet, M. C., & Haughn, G. W. (2019). RUBY, a putative galactose oxidase, influences pectin properties and promotes cell-to-cell adhesion in the seed coat epidermis of Arabidopsis. *The Plant Cell*, *31*(4), 809-831. https://doi.org/10.1105/tpc.18.00954